

ALMA MATER STUDIORUM - UNIVERSITÀ DI BOLOGNA

FACOLTA' DI INGEGNERIA

Corso di Laurea Magistrale in Ingegneria Civile

Context sensitive design in transportation infrastructures

**RHEOLOGICAL AND ENERGETIC CHARACTERIZATION
OF WAX-MODIFIED ASPHALT BINDERS**

TESI DI:

Riccardo Lamperti

RELATORE:

Dott. Ing. **Cesare Sangiorgi**

CORRELATORI:

Prof. **Gordon Dan Airey**

Dott. Ing. **Claudio Lantieri**

Dott. Ing. **Matteo Pettinari**

Anno Accademico 2011/12

Sessione II

Ai miei cari

INDEX

<i>Introduction</i>	1
<i>1 Characteristics and Rheology of the Bitumen</i>	5
1.1 History	5
1.2 Origin and chemical composition of bitumen	6
1.3 Bitumen as colloidal model	10
1.4 Manufacture of bitumen	14
1.5 Types of bitumen	16
1.6 Rheology of bitumen	18
1.7 Viscoelastic behaviour of bitumen	21
<i>2 The Bitumen-Aggregate Affinity</i>	23
2.1 Introduction	23
2.2 Forces involved in adhesion	23
2.3 Theories on adhesion	26
2.3.1 Theory of (weak) boundary layers	26
2.3.2 Electrostatic theory	27
2.3.3 Chemical bonding theory	28
2.4 Bitumen Functional Groups	29
2.5 Aggregate Functional Groups	31
2.6 Surface energy and wettability	32
2.7 Theory for surface energy calculation from contact angle data	36
2.7.1 Geometric Mean Approach	36
2.7.2 Critical Surface Tension Approach	36
2.7.3 Acid-Base Approach	37
2.8 Thermodynamic theory	37

3 Reserch Project and Test Methods	47
3.1 Introduction	47
3.2 Ageing of bitumens	49
3.2.1 Rolling Thin Film Oven Test (RTFOT)	49
3.2.2 Pressure Aging Vessel (PAV)	52
3.3 Dynamic Shear Rheometer (DSR)	55
3.3.1 General concepts	55
3.3.2 Dynamic Mechanical Analysis	57
3.4 Bending Beam Rheometer	60
3.5 Dynamic Contact Angle	64
3.6 Dynamic Vapour Sorption-DVS Technique	66
4 The Rheology Reserch	71
4.1 Introduction	71
4.2 Dynamic Shear Rheometer test	72
4.2.1 Setting of the test and specimen preparation	72
4.2.2 Data analysis and representation	76
4.2.3 Mastercurves	76
4.2.4 Isochronal Plots	83
4.2.5 Black Diagram	87
4.2.6 Ageing Index	89
4.3 Bending Beam Rheometer test	90
4.3.1 Setting of the test and specimen preparation	90
4.3.2 Results	92
4.4 Performance Grade	93
5 The Affinity Reserch	103
5.1 Introduction	103
5.2 Dynamic Contact Angle tests	104

5.2.1 Setting of the test and specimen preparation	104
5.2.2 Surface energy of bitumens	117
5.3 Dynamic Sorption Device tests	120
5.3.1 Setting of the test and specimen preparation	121
5.3.2 Surface energy calculation of aggregates	129
5.4 Moisture damage parameters	132
6 Conclusions	139

INTRODUCTION

The first and more reliable technique to build up a road pavement is without any doubt the hot mix asphalt. It is produced by heating the asphalt binder to decrease its viscosity, and drying the aggregate to remove moisture from it prior to mixing, that is generally performed with the aggregate at nearly 160 °C. The quality of hot mixtures obtained by following the protocols, that are confirmed over the past is, in fact, an absolute reference. The recent tendency of reduce the exploitation of non-renewable resources and the need to ensure the environmental protection has moved the attention to find new ways of construction and maintenance. The asphalt paving industry is for this reason constantly exploring technological improvements. For instance, an excellent solution is achieved by lowering the production and placement temperatures of hot mix asphalt: these technologies are generically referred to as warm-mix asphalt (WMA). The benefits are multiple, starting from the energy savings ranged from 20 to 35 % at the plant depending on the system and the efficiency of the WMA plant. Data indicate plant emissions are significantly reduced: typical expected reductions are 30 to 40 percent for *Co*₂ and sulfur dioxide (*SO*₂), 50 percent for volatile organic compounds (*VOCs*), 10 to 30 percent for carbon monoxide (*Co*), 60 to 70 percent for nitrous oxides (*NO*_x), and 20 to 25 percent for dust. Furthermore, worker exposure is reduced: tests for asphalt aerosols/fumes and polycyclic aromatic hydrocarbons (*PAHs*) indicated significant reductions compared to HMA, with results showing a 30 to 50 percent reduction, providing healthier and safer work environment.

A Warm Mix Asphalt solution is obtained, for instance, by mixing the bitumen with a small quantity of waxes, with the intent of reduce the viscosity of the asphalt binder and hence the temperature needed to coat the aggregates and easily mix.

This techniques are something new: the scientific community focus on the development of WMA technologies may be traced back to two distinctive events: the 1992 United Nations' discussions on the environment and the 1996 Germany's consideration to

review asphalt fumes exposure limits. The United Nations' discussions resulted in the 1997 Kyoto Accord, which formalized a commitment by the signatory states to reduce greenhouse gas emission to the 1990 levels, while the Germany's review of asphalt fumes exposure limits lead to the formation of a partnership forum (The German Bitumen Forum) to discuss these considerations.

Is not surprising, consequently, that some aspects are still unclear. The uncertainty is essentially due to the fact that assessment data are still insufficient. In particular, the quantification of permanent deformation and the behaviour of the material at low temperatures still need to be investigated.

This work of thesis has the aim of study the effect of two different waxes on a 70/100 dmm bitumen. These waxes are the Adriamont, recently proposed, and the Sasobit®, a worldwide used, “environmentally friendly”, asphalt additive. Two aspects have been examined.

Firstly, rheological tests have been carried out. The Dynamic Shear Rheometer made it possible to plot the master curves, understanding the general behaviour of the three asphalt binders, and other important graphs like the Black Diagram, the Isochronal plot, the ageing index. The Bending Beam Rheometer allowed to comprehend the effect of the waxes on the asphalt binder at low temperatures, by measuring the stiffness of an asphalt binder beam subjected to a three point bending. In this part, Superpave procedures have been followed and, at last, the Performance Grade of the three asphalt binders has been determined. In order to prove it, tests have been made on three stage aged binders: unaged, short term aged asphalt (RTFOT) and long-term aged asphalt (PAV).

Secondly, an energetic characterization of the bitumens, and in parallel, of three aggregates for road use has been made. The mechanism of adhesion is, in fact, strictly related to the surface energy properties of the materials in contact. By measuring these properties with Wilhelmy Plate Device, for the bitumens, and with Dynamic Sorption Device, for the aggregates it was feasible to give an opinion of the affinity of all possible combinations. These technique are alternative to the common procedure to determine the bitumen-aggregate affinity, standardised in EN 12697-11, in which the materials are mixed together and then immersed in water, with the aim to visibly assess the quantity of bitumen displaced by water on the aggregate surface. On the contrary,

with the “energetic way” the materials are never mixed together, but studied separately, and the affinity opinion is expressed analytically by means of the work of adhesion.

Chapter 1 introduces the bitumen material, exposing its chemical properties, its structure, with nods on its rheology.

Chapter 2 deals with the affinity aggregate-bitumen, explains all the forces involved and possible mechanisms of adhesion. It further provides the basis for understanding the tests carried out.

In chapter 3 the tests for both the rheological and energetic research are described.

Chapter 4 and 5 shows, respectively, all the results for rheological and energetic research.

All the research has been carried out at the laboratories of NTEC, Nottingham Transportation Engineering Centre, U.K., a pioneering center for the study of the bitumens and their properties, also with the support of the Roads department of the faculty of Civil Engineering in Bologna. I am very grateful to all those that allowed me to be a part of NTEC.

CHAPTER 1

CHARACTERISTICS AND RHEOLOGY OF THE BITUMEN

1.1 History

As defined in European Standard EN 12597:2002, bitumen is intended as “those organic compounds consisting essentially of mixtures of organic hydrocarbons completely soluble in carbon disulfide and with binding capacity”.

It is a product used for millennia as a building material in a wide variety of applications. The earliest known use of bitumen was by Neanderthals, some 40,000 years ago. Natural bitumen, available in nature emerging in pools, was found adhering to stone tools used by Neanderthals at sites such as Hummal and Umm El Tlel in Syria. The use of bitumen for waterproofing and as an adhesive dates at least to the fifth millennium B.C. in the early Indus community of Mehrgarh, where it was used to line the baskets in which they gathered crops. In the ancient Middle East, the Sumerians used natural asphalt deposits for mortar between bricks and stones, to cement parts of carvings, such as eyes, into place, for ship caulking, and for waterproofing. In some versions of the Book of Genesis in the Bible, the name of the substance used to bind the bricks of the Tower of Babel is translated as bitumen.

But it's only after the industrial revolution that bitumen began to be used for paving. In fact, in the 1830s, there was a surge of interest, and asphalt became widely used "for pavements, flat roofs, and the lining of cisterns, and in England, some use of it had been made of it for similar purposes" [1]. Its rise in Europe was "a sudden phenomenon", after some natural deposits were found "in France although it could also be made artificially. One of the earliest uses in France was the laying of about 24,000 square yards of Seyssel asphalt at the Place de la Concorde in 1835.

On 25 November 1837, Richard Tappin Claridge patented the use of Seyssel asphalt for use in asphalte pavement, having seen it employed in France and Belgium, introducing firstly the use of bitumen for paving in United Kingdom. In the US, instead, roads have been paved with asphalt since at least 1870, when a street in front of the Newark, NJ

City Hall was paved. In 1876, asphalt was used to pave Pennsylvania Avenue in Washington, DC, in time for the celebration of the national centennial.

1.2 Origin and chemical composition of bitumen

Bitumen can be natural or artificial origin.

The natural one is usually impregnated in some sedimentary rocks (sandstones and limestones), or in the form of pockets in the soil or as outcrops of variable size (like the bitumen lake in Trinidad) . Natural bitumen deposits are found all over the world, in areas with suitable geological conditions in which the high permeability of the rock formations has enabled a process of natural fractionation of crude oil. Over time, the distribution of natural bitumens has been diminishing with the development and refinement of processing techniques, able to provide bitumen in large quantities at a price more and more competitive. In this way, although it exists also in natural state, nowadays it is mainly obtained as a residue of petroleum processing (artificial).

Bitumen is a complex mixture of organic compounds with high molecular weight, with a prevalence of hydrocarbons with a number of carbon atoms greater than C₂₅ and high valued of C/H, as well as small amounts of sulphur, nitrogen and oxygen, it also contains traces of metals such as nickel, iron and vanadium [2].

Despite physical and chemical compositions of petroleum can change with location, age and depth, bitumen elemental composition can be identified by the following scheme:

Element	% by weight
Carbon	82-88
Hydrogen	8-11
Sulfur	0-6
Oxygen	0-1.5
Nitrogen	0-1

Table 1.1 Mean composition of bitumens. (Read & Whiteoak, 2003)

Conversion (upgrading) of bitumen and heavy oils to distillate products requires reduction of the molecular weight and boiling point of the components of the feedstocks. The chemistry of this transformation to lighter products is extremely complex, partly because the petroleum feedstocks are complicated mixtures of hydrocarbons, consisting of 10^5 to 10^6 different molecules.

Any structural information regarding the chemical nature of these materials would help to understand the chemistry of the process and, hence, it would be possible to improve process yields and product quality. However, because of the complexity of the mixture, the characterization of entire petroleum feedstocks and products is difficult, if not impossible. One way to simplify this molecular variety is to separate the feedstocks and products into different fractions (classes of components) by distillation, solubility/insolubility, and adsorption/desorption techniques. For bitumen and heavy oils, there are a number of methods that have been developed based on solubility and adsorption.

The most common standard method used for separation of heavy oils into compound classes is SARA (saturates, aromatics, resins, and asphaltenes) analysis. This method divides crude oil components according to their polarizability and polarity. The saturate fraction consists of non polar material including linear, branched, and cyclic saturated hydrocarbons (paraffins). Aromatics, which contain one or more aromatic rings, are slightly more polarizable. The remaining two fractions have polar substituents, the distinction between the two is that asphaltenes are insoluble in an excess of heptane (or pentane) whereas resins are miscible with heptane (or pentane).

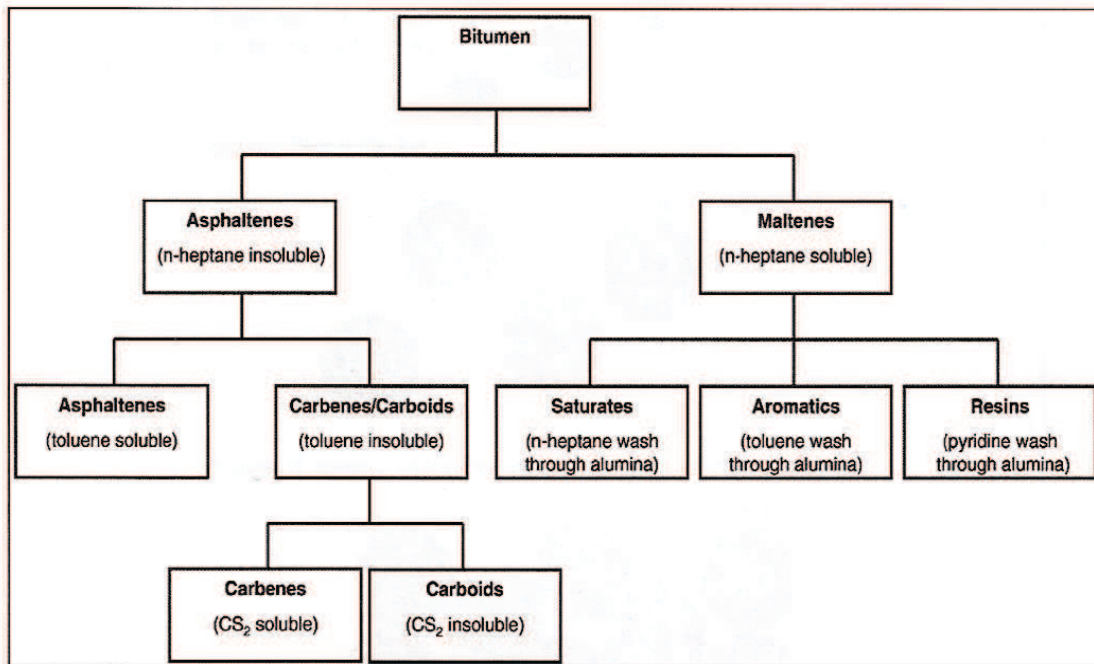


Figure 1.1 Parting of bitumen based on solubility class

A quick review of the characteristics of these four functional groups is presented below.

- *Saturates*

Saturated oils consist of straight and branch chain aliphatic hydrocarbons together with alkyl-naphthenes and some alkyl-aromatics. They are a viscous liquid fraction of yellowish-white colour with molecular weights ranging from 500 to 1000 *u*. At room temperature, they are in the liquid state and are chemically low reactive. Their C_{alif} / C_{arom} ratio is in favour of paraffins.

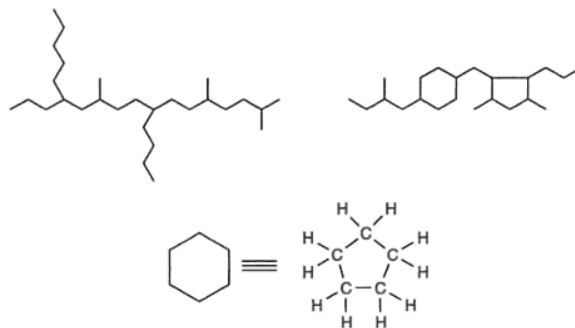


Figure 1.2 Saturated structure

- *Aromatics*

Aromatics comprise the lowest molecular weight naphthenic aromatic compounds in the bitumen and represent the major proportion of the dispersion medium for the peptised asphaltenes. They constitute 40 to 65 % of the total bitumen and are dark brown viscous liquids. The average molecular weight range is in the region of 300 to 2000. They consist of non-polar carbon chains in which the unsaturated ring systems (aromatics) dominate and they have a high dissolving ability for other high molecular weight hydrocarbons [3].

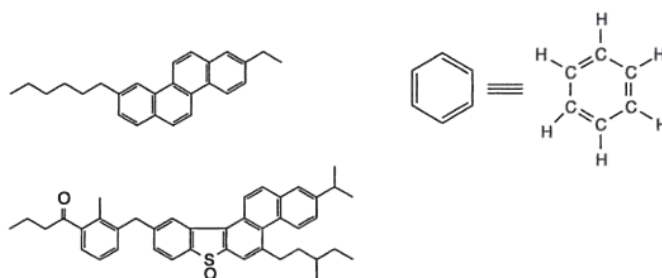


Figure 1.3 Aromatic structures

- *Asphaltenes*

Asphaltenes have manifestly adverse effects on the workability of petroleum and play a significant role in the physical properties of heavy oils and bitumen. For this reason they are probably the most studied fraction of petroleum and bitumen. It has been demonstrated that the viscosity of petroleum is significantly influenced by the presence and concentration of asphaltene. Their high molecular weight (generally higher than 2000 u), although difficult to measure, makes them the fraction richest in macromolecules. They have an aromatic type structural configuration and they are solid at room temperature, with grainy, black-brown aspect. Their mixture is very complex, formed of hydrocarbons, consisting mainly of condensed aromatic compounds (in which it is also found the presence of oxygen, nitrogen, sulphur and metal) and heteroaromatic compounds, containing sulphur and nitrogen in pyrrole rings.

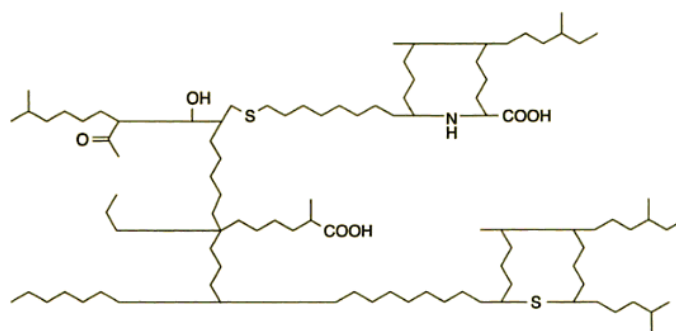


Figure 1.4 Possible structure of asphaltenes

- *Resins*

Resins are the most polar compounds. Structurally very similar to asphaltenes, they are very viscous at room temperature, dark brown in color and with remarkable adhesive properties. Within the bitumen, resins work as dispersing agents of the macromolecular structures of asphaltenes. Compared to these, resins have a smaller molecular weight, estimated between 500 and 100 u, but a much higher ratio of carbon aliphatic/aromatic carbon C_{alif} / C_{arom} due to the increased number of paraffinic chains. Some scientists assume that asphaltenes originated in nature by the oxidation of the resins.

1.3 Bitumen as colloidal model

Looking at the response to mechanical stresses have led to attribute the bitumen a colloidal structure (Nellensteyn hypothesis) consisting of a suspension of high molecular weight asphaltene micelles dispersed in a lower molecular weight oily medium identified as maltenes [2].

Indeed, very early in the study of crude oils, it was observed that mixing oils with several volumes of normal alkane solvents (propane, n-butane, n-pentane, n-hexane, n-heptane) resulted in the precipitation of black, friable solids called asphaltenes. These solids are relatively enriched in heteroatoms (nitrogen, oxygen, sulphur, metals) and are more aromatic than their parents oils. Asphaltenes are involatile, so they become concentrated in residual fractions. Deasphaltened oils (otherwise known as petrolenes or maltenes) differ in properties from whole crude oils; for example, maltenes are much

less viscous than whole crudes. Therefore asphaltenes, which normally make up a few mass percentage of crudes, are the principal viscosity-enhancing components, as they are with bitumens. Pointing out from these observations Nellensteyn, in 1924, introduced the concept that petroleum residua are colloidal dispersion of asphaltenes in maltenes (which in turn serve as a solvent phase) peptised by polar materials called resins, which may be isolated from maltenes. Mack, in 1932 studied rheological properties of asphalts confirmed this hypothesis. He proposed that asphaltenes are dispersed throughout the maltene phase as large agglomerations which are stabilised by association with aromatic components of the maltenes. Labout, in 1950, proposed that in asphalt having highly aromatic maltene fractions, asphaltenes are well dispersed (peptised) and do not form extensive association. Such asphalt were designated SOL-type asphalts. In asphalts with less aromatic maltene fractions, asphaltnes are not well dispersed and form large agglomerations with in extreme cases can form a continuous network throughout an asphalt. These bitumens were designated GEL-type asphalts. Figure 1.5 represent these two possible type of bitumens.

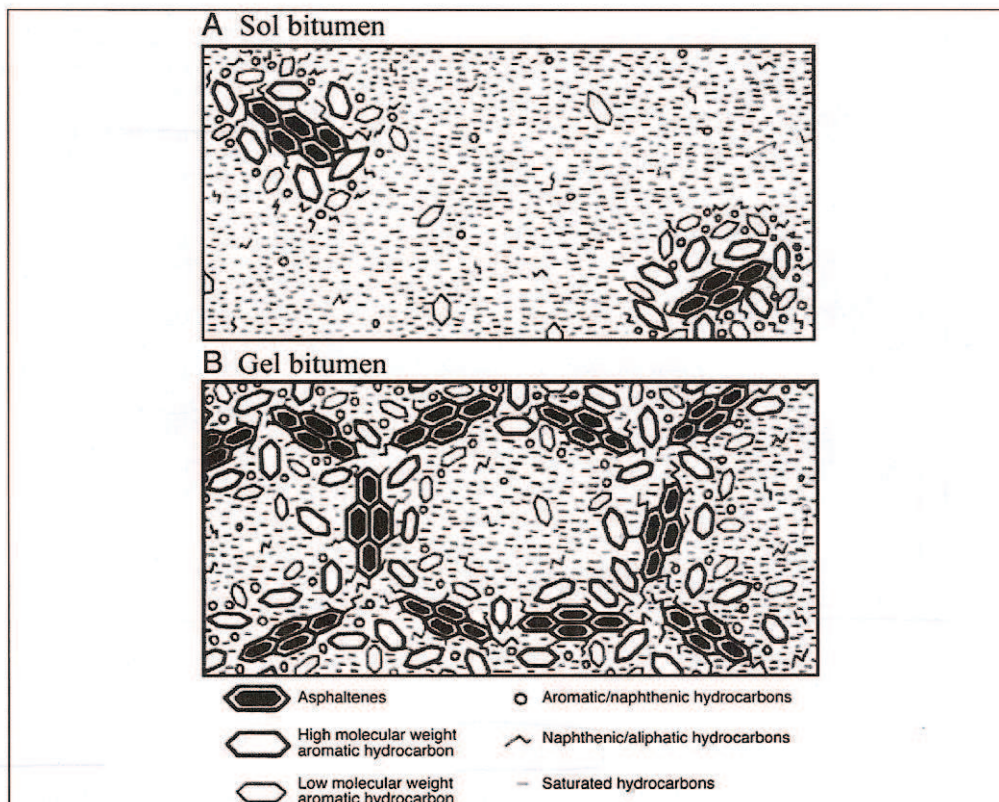


Figure 1.5 GEL and SOL structures

Pfeiffer and Saal gave an important contribute to the study of the colloidal system. They suggested that asphalt dispersed phases are composed of an aromatic core by layers of less aromatic molecules and dispersed in a relatively aliphatic solvent phase. They did not claim that there are distinct boundaries between asphalt dispersed and solvent phases, as in soap micelles, but there is in a continuum from low to high aromaticity from the solvent phase to the centers of the entities making up the dispersed phase.

Furthermore, they observed that asphaltenes, considered to be the core constituents of dispersed phases, have a marked tendency to adsorb aromatic hydrocarbon solvents, and they assumed that the same tendency would prevail in asphalt systems; that is, the asphaltenes would attract smaller aromatic components of maltenes, which would surround and peptise the asphaltenes. The smaller aromatic molecules would be compatible with naphthenic and aliphatic components of the remainder of the maltene phase. Therefore there is no contact between materials having greatly different surface tensions anywhere in the systems, although differences in surface tension between the aromatic asphaltene cores and the more naphthenic and aliphatic solvent may be fairly large.

Pfeiffer and Saal claimed that asphalt properties are function of the strength associations between fundamental components of dispersed phases and the extent to which dispersed phases are peptised by solvent phases. Peptisation is provided by a shell of resins that surrounds the asphaltene core with the thickness of the resin layer being temperature dependent. At low temperature and in case of high asphaltenes content the bitumen can show a compact structure. On the other hand, insufficient quantities of resins and aromatics (insufficient solvating power) may lead to an association of several micelles which may be simply expressed using the following thermal dependent equilibrium:



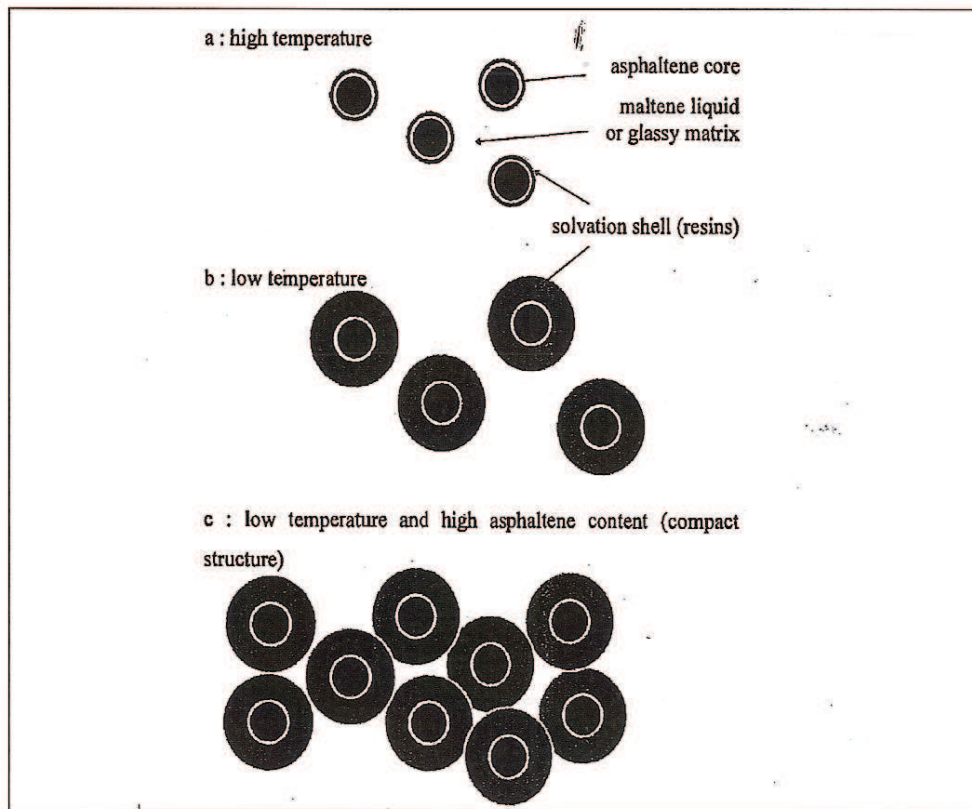


Figure 1.6 Temperature influence on asphaltenes aggregation

The system is therefore formed by liquid part (resins dissolved in a maltene matrix), in equilibrium with a solid part (resins peptizing the asphaltenes) and it is, of course, temperature dependent [2].

Depending on the origin of crude oil and the distillation process, the four above mentioned fractions take part in the bitumen approximately with this percentage:

- *Aromatics*: 40-70 %
- *Resins*: 10-25 %
- *Asphaltenes*: 5-25 %
- *Saturates*: 5-20 %

In order to evaluate the relationship between the chemical composition and the physical properties of bitumens, and to assess the stability of this system, few parameters need to

be controlled. When these ratios decrease, asphaltene micelles will coalesce and form larger aggregates.

- *Asphaltene Index I_A*

This is the changing rate of asphaltene content and it is calculated using n-heptane asphaltene precipitation

$$I_A = \frac{\text{Asphaltenes} + \text{Resins}}{\text{Aromatics} + \text{Saturates}}$$

A linear relationship between asphaltenes content and the index I_A is usually recorded, whilst the same index decreases with the increase of the resins content.

- *Colloidal Index I_C*

Many researchers believe this is the most suitable parameter to describe the stability of the colloidal system bitumen. Introduced by Gaestel and co-workers (1971) is the dispersing capability of maltenes to asphaltenes. It is also evaluated using n-heptane asphaltenes.

$$I_C = \frac{\text{Asphaltenes} + \text{Saturates}}{\text{Aromatics} + \text{Resins}}$$

The colloidal index I_C typically ranges from 0.5 to 2.7 for current road bitumens. A higher colloidal index means that the asphaltenes are more peptised by the resins in the oil based medium. The index value grows proportionally with the aging of the bitumen.

1.4 Manufacture of bitumen

Bitumen is sometimes called asphalt. These two words are interchangeable in the United States, in Europe and in the rest of the World, but to be clear asphalt denotes the impure form of generic material, whereas the bitumen, the basic mixture of heavy hydrocarbons free of inorganic impurities [4].

In this section a typical bitumen production process is shown. Asphalt is produced by fractional distillation of crude oil. Usually, distillation is done in two subsequent steps.

First the crude oil is heated up to 300-350°C and introduced into an atmospheric distillation column. Lighter fractions like naphtha, kerosene and gas oil are separated from the crude oil at different heights in the column. The heaviest fractions left at the bottom of the column are called heavy residue. The long residue is heated up to 350-400°C and introduced into a vacuum distillation column. By using reduced pressure it is possible to further distillate lighter products from the residue because the equivalent temperature (temperature under atmospheric conditions) is much higher. If second distillation were carried out under atmospheric conditions and by increasing the temperature above 400°C, thermal decomposition/cracking of the heavy residue would occur. The residue at the bottom of the column is called short residue and is the feedstock for the manufacture of asphalt.

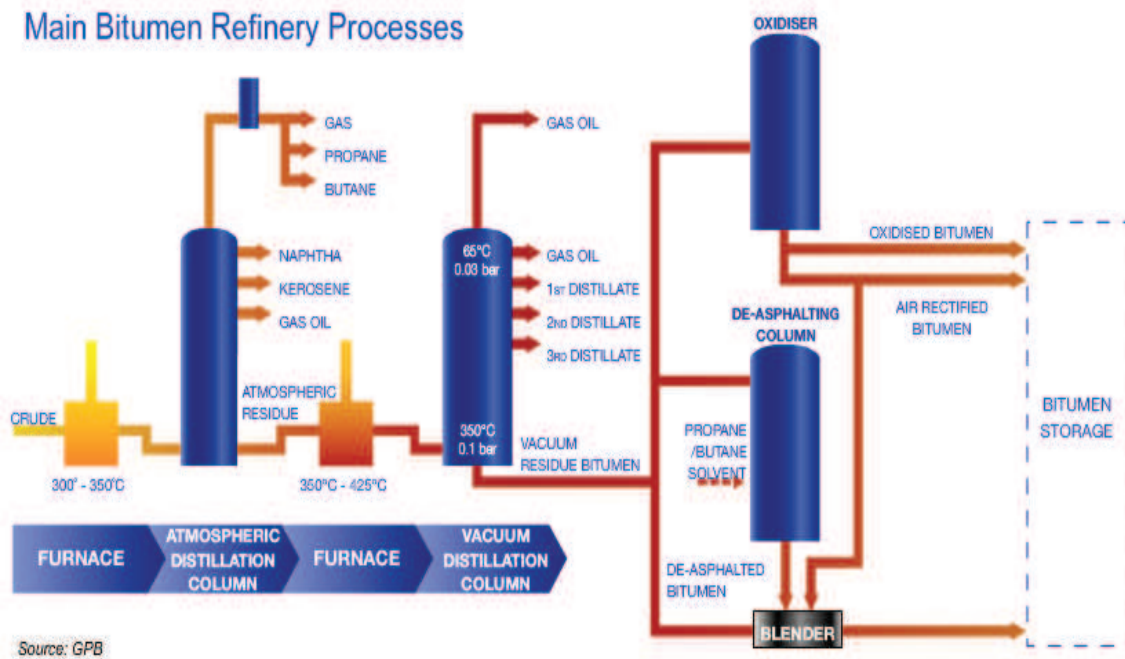


Figure 1.1 Main Bitumen Refinery Processes; www.eurobitume.eu

The viscosity of the short residue depends on the origin of the crude oil, the temperature of the long residue, the temperature and pressure in the vacuum column and the residence time. Usually, the conditions are such that short residue is produced with a Penetration between 100 and 300 dmm. The amount of short residue decreases and the relative amount of asphaltenes increases with increasing viscosity of the short residue. Asphalt manufactured from the short residue is called straight run asphalt. The

differences in properties between high and low penetration grade asphalt are mainly caused by different amounts of molecule structures with strong interactions. Low penetration grade asphalt contains more of these molecule structures. This is the main reason why their viscosity, Fraass breaking point, Softening point, etc., is so much higher than for high penetration grade asphalt. The fact that they contain less low viscosity products is of less significance.

1.5 Types of bitumen

As suggested by British Petroleum Company, there are six major classifications of petroleum bitumen produced by the refining and manufacturing process. [5]

- *Paving Grade Bitumen*

Paving grade bitumen (or asphalt cement in the USA) is the most widely used bitumen and is refined and blended to meet road engineering and industrial specifications that take into account different climatic conditions. Paving grade bitumen may also be considered as the parent bitumen from which the other forms are produced.

- *Cutback Bitumen*

Cutback bitumens consist of bitumen that has been diluted in solvent (cutter or flux) to make it more fluid for application; controlled amounts of petroleum distillates, such as kerosene, are normally used. This is done to reduce the viscosity of the bitumen temporarily so it can penetrate pavements more effectively or to allow spraying at temperatures that are too cold for successful sprayed sealing with neat bitumen. The fluidity of cutback bitumens (or cutbacks as they are known) depends on the degree of hardness of the bitumen and the proportion of diluent. The materials used to cutback bitumen will evaporate after application to leave the remaining material similar in hardness to the original bitumen. Cutbacks are classified according to the time it takes for them to cure, or become solid due to the evaporation of the diluent. Classifications are rapid curing (RC), medium curing (MC) or slow curing (SC). A cutback varies in behaviour according to the type of cutter or flux used as the diluent with white spirit commonly used for RC grades, kerosene for MC and diesel for SC.

- *Bitumen Emulsions*

Bitumen emulsions are dispersions of bitumen in water. Hot bitumen, water and emulsifier are processed in a high speed colloid mill that disperses the bitumen in the water in the form of small droplets. These droplets or particles of bitumen are normally in the 5-10 micrometre size range but may be even smaller. The emulsifier assists in forming and maintaining the dispersion of fine droplets of bitumen. Bitumen emulsions normally contain up to 70% asphalt and typically less than 1.5% chemical additives. If the bitumen starts to separate from the water solution in storage, the emulsion can usually be easily restored by gentle agitation to redisperse the droplets. Bitumen emulsions have a low viscosity compared to the bitumen from which they are produced and can be workable at ambient temperatures. Their application requires controlled breaking and setting. The emulsion must not break before it is laid on the road surface but, once in place, it should break quickly so that the road can be in service again without delay. Although the first emulsions were the anionic types, they are currently less favoured than the cationic types because the positively charged globules of bitumen in cationic emulsions better coat the majority of aggregate types and result in greater adhesion. Use of cationic emulsions is therefore preferred in most applications.

- *Modified Bitumens*

Modified bitumens are formulated with additives to produce enhanced performance characteristics by changing such properties as their durability, resistance to ageing, elasticity and/or plasticity. The most important modifiers are polymers. Polymer modified binders (PMB) are a major advancement in bituminous binder technology as these materials better satisfy the demands of increasing traffic volumes and loads on our road networks. As well as natural rubbers, polymers such as styrene butadiene styrene (SBS), polybutadiene (PBD) and ethylene vinyl acetate (EVA) are commonly used to modify bitumen. Nowadays, almost all bitumens used for paving are modified.

- *Multigrade Bitumen*

Multigrade bitumen is a chemically modified bitumen that has the properties of a hard paving grade bitumen at high service temperatures coupled with the properties

of a soft paving grade bitumen at low temperatures (i.e. it has properties that span multiple grades). Multigrade bitumens provide improved resistance to deformation and reduce the detrimental effects of high service temperatures, whilst providing reduced stiffness at low service temperatures than exhibited by a similar normal paving grade bitumen. For this reason, hard grade bitumens are normally used in the manufacture of high modulus asphalt.

- *Blown bitumen (oxidised)*

These kind of bitumen, also referred to as industrial bitumens (or oxidised bitumens) are made by blowing air through hot paving grade bitumen. The so-called blowing process results in harder bitumen that softens at a higher temperature than that at which paving grade bitumen softens. Industrial bitumens also have more rubber-like properties and their viscosities are much less affected by changes in temperature than is the case with paving grade bitumen. As suggested by their name, industrial bitumens are used in a wide variety of applications including roofing, flooring, pipe-coating etc...

- *Visbroken bitumen*

Visbreaking is a way to break heavy products (e.g. the residue from crude oil distillation or even very heavy crude oils) into lighter products. So far, the crude oil or residue is heated up to 450 °C and kept at that temperature for 1 to 20 minutes. During this period a large amount of molecular structures are broken into smaller structures. The product from the visbreaking process (VB) is further normally distilled. Asphalt produced from VB products age very fast. This is because these products contain very reactive constituents (olefins). Even blends of straight run asphalt with asphalt from VB products have the same ageing problems. This makes them unsuitable for most asphalt applications. The properties may be somewhat improved by blowing.

1.6 Rheology of bitumen

Rheology, is relatively recent name, proposed in 1928 by E. C. Bingham to indicate the science which studies the characteristics of deformation and sliding of the matter

(viscous, plastic) submitted to external forces [7]; these "rheological" characteristics depend in a substantial way by:

- macroscopic and microscopic structure of the matter
- arrangement and shape of the molecules in the compounds
- the entity of intramolecular actions
- the relative proportions and the degree of subdivision of the components in the mixtures
- the presence of substances still able to modify the actions of contact between the phases present

This dependence is so important that any variation of the structure, due both to the temperature, for the only different state of thermal agitation of molecules, both to reactions of the components with each other or with external agents (phenomena of setting, hardening, curing, etc.), both to alteration of proportions of the constituents or addition elements, either in the same action of external forces (orientation of the structure, states of constraint, etc.), can be accused by examining the behaviour of the body in the deformation.

All forms of shear behaviour, which can be described rheologically in a scientific way, can be viewed as lying in between two extremes: on one hand the flow of ideal viscous liquids and on the other the deformation of ideal elastic solids [8].

Bitumen is a thermoplastic material that, under most pavement operating conditions, shows a behaviour which is between these extremes and it is based on the combination of both the viscous and the elastic portion and therefore is called *viscoelastic*. Regardless of the field of use, bitumen performance is strictly related to its mechanical characteristics. Therefore these properties need to be studied in stress and temperature conditions representative of the future employ.

Elasticity is a physical property of materials which return to their original shape after the stress that caused their deformation is no longer applied [2]. This means that energy spent in deformation is preserved in the form of elastic potential energy and it is returned when the applied stress is removed. Robert Hooke in 1675, formulated a simple linear relationship for elasticity in which force is proportional to displacement

through a constant, known as *spring constant*. It can also be stated as a relationship between stress σ and strain ε and is valid for both normal and shear stresses.

$$\tau = G \cdot \gamma$$

Where:

τ = stress [Pa]

G = Shear Modulus [Pa]; it defines the resistance to the deformation of the solid

γ = strain []

Viscosity is a measure of the resistance of a fluid which is being deformed by either shear stress or tensile stress. In general, in any flow, layers move at different velocities and the fluid's viscosity arises from the shear stress between the layers that ultimately opposes any applied force. Newton's law describes the behaviour of purely viscous fluids, for which the stress is proportional to the strain rate and is independent of the strain level.

$$\tau = \eta \cdot \dot{\gamma}$$

Where:

τ = stress [Pa]

η = viscosity [$Pa \cdot s$]

$\dot{\gamma}$ = strain rate [s^{-1}]

Viscosity is a physical feature of the fluid and characterizes its behaviour against all the forces opposing the movement. Liquids that, for a given temperature and for any rate of shear strain, present a constant viscosity are called Newtonian fluids. Non-Newtonian fluids exhibit a more complicated relationship between shear stress and velocity gradient than simple linearity. Thus there exist a number of forms of viscosity.

Viscoelasticity is the property of materials that exhibit both viscous and elastic characteristics when undergoing deformation. In nature, several materials having intermediate behaviour between the above mentioned extremes are present. The extent of deviation from Newtonian or purely elastic behaviour is not an intrinsic characteristic

of a material, but depends on its physic-chemical state. Depending on the change of strain rate versus stress inside a material the viscosity can be categorized as having a linear, non-linear, or plastic response. In particular, the linear visco-elastic response happens when deformation and deformation rate are directly proportional to the stress; in this case the stress related to the strain and the strain rate are additives in such a way the stress-strain relationship is linear:

$$\tau = \tau_{\varepsilon} + \tau_{\eta} = G \cdot \gamma + \eta \cdot \dot{\gamma}$$

In most of the materials the linear behaviour is obtained with infinitesimal deformation or strain gradients. In case of finite strain the stress-strain relations are much more complex, because the material exceeds the region of linear viscoelasticity (LVE). This limit, is not well defined and vary both for different materials and for the same material due to its physical and chemical state (stress level, temperature, loading time). Furthermore some phenomena are characteristic of viscoelasticity:

- creep: if the stress is held constant, the strain increases with time;
- relaxation: if the strain is held constant, the stress decreases with time;
- the effective stiffness depends on the rate of application of the load;
- if cyclic loading is applied, hysteresis occurs, leading to a dissipation of mechanical energy;

1.7 Viscoelastic behaviour of bitumen

Bitumen is a viscoelastic material that behaves as a glass-like elastic solid at low temperatures and/or during rapid loading (short loading times = high loading frequencies) and as viscous fluid at low temperatures and/or during slow loading (long loading times = low loading frequencies). At normal pavement temperatures, the bitumen has properties that are in the visco-elastic region and it exhibits both elastic and viscous behaviour and displays a time-dependent response.

As mentioned before, the non-linear response of visco-elastic materials, is extremely difficult to characterise in the laboratory and to model in practical engineering problems. Fortunately, under normal pavement operating conditions, in terms of loads

and temperatures, bituminous binders can effectively be treated as LVE materials [9]. Linear behaviour is fulfilled at low temperatures and short loading times (high frequencies), where the material behaves as an elastic solid. The linearity is also comply at high temperatures and long loading times (low frequencies) where the materials behaves entirely as a Newtonian fluid. It is in the range of moderate temperatures and loading time (field conditions) that non-linearity is prominent. It is, therefore, in these conditions that is important, while testing, to ensure bituminous binders to remain within the LVE range by limiting the applied strain, or deformation, within certain boundaries.

The shape of the linear visco-elastic (LVE) response of a bitumen, including polymer modified bitumens, can be sub-divided into four zones:

- a terminal or flow zone,
- a plateau zone (only present in the case of a network),
- a transition zone
- a glassy zone.

The LVE response of bitumen and therefore the shape of the master curve can more generally be divided up or separated into three regions or zones of behaviour:

- At low temperatures or short loading times (high frequencies), bitumen behaves as glassy solid. The stiffness therefore approaches a limiting value of approximately 1 GPa in shear and 3 GPa in tension-compression or bending. In this region the stiffness is only slightly dependent on temperature and/or time of loading.
- At intermediate temperatures or loading times (frequencies), bitumen undergoes a gradual transition from glassy to fluid behaviour. This transition is characterized by large amounts of delayed elasticity. The stiffness modulus changes dramatically in this region as a function of temperature and/or loading time
- At high temperatures or long loading times (low frequencies), bitumen behaves as a viscous fluid. The bitumen is considered to behave as a Newtonian fluid and for low to moderate stresses and strains the shear rate is proportional to the shear stress. [2]

CHAPTER 2

THE BITUMEN-AGGREGATE AFFINITY

2.1 Introduction

Adhesion is the tendency of dissimilar particles or surfaces to cling to one another (cohesion instead refers to the tendency of similar or identical particles/surfaces to cling to one another). ASTM D907 defines it, in a scientific context, as “the state in which two surfaces are held together by valence forces or interlocking forces, or both” [10]. The adhesion bitumen-inert is a fundamental property for the durability of flexible pavements. The weakening or the detachment of bitumen film from the surface of the aggregate is, in fact, one of the main mechanisms of degradation of a superstructure. This chapter discusses primarily the main forces responsible for adhesion and the mechanisms of adhesion proposed to explain why one material sticks to another. We will focus on the thermodynamic theory, on which is based the key concept of *surface energy* (briefly, it is conventionally defined as the work that is required to build a unit area of a particular surface) . As we will see, this notion plays a central role in determining the wettability of an aggregate by a liquid. Usually, contact angle technique is used to determine the wettability characteristic of a solid surface, by measuring the angle of contact of a drop of pure liquid on that solid. Concluding, we will consider the theories for surface energy calculation from contact angle data.

2.2 Forces involved in adhesion

Several interaction forces are responsible for adhesion. According to classical text on surface science, treatises on adhesion, and general texts on adhesion science, it's possible to proceed with a fundamental understanding of the above mentioned forces [11]:

- ***Electrostatic Interactions between Ions***

The basis for understanding intermolecular forces is the Coulomb force, which is the electrostatic force between two separated charges. Electrostatic forces play a primary role in the formation of ionic bonds. An ideal ionic bond is formed when a positive ion (cation) and negative ion (anion), as charged particles, attract each other according to Coulomb's law, each acting as a nucleus surrounded by a rigid spherical distribution of electrons. In this process, each ion pair gains classical electrostatic stabilization energy. Electrostatic forces in an ionic bond are the strongest forces of interaction and the energy required to break a mole of these bonds are typically in the order of 140 to 250 kcal.

- ***Electrodynamic Interactions through van der Waals Forces***

The forces responsible for the deviation of behavior of a gas from an ideal gas are collectively known as van der Waals forces. J.D van der Waals first developed an equation of state to describe this deviation. Keesom, Debye, and London contributed much to the understanding of these forces, and for this reason, the three interactions are named for them. They include dipole-dipole interactions (Keesom orientation forces), dipole-induced dipole interactions (Debye induction forces), and induced dipole-induced dipole interactions (London dispersion forces). The van der Waals force is the sum of the three interactions. Usually, the London forces dominate. The bonds formed by electrodynamic forces are small when compared to ionic or covalent bonds and typically exhibit strengths less than 10 kcal/mol. The potential energy of interaction is inversely proportional to the sixth power of the distance between interacting entities. Even though individual interactions are short-range, these forces are additive through the instantaneous propagation of an electric field and its contribution may be of considerable importance in interactions where large organic molecules are involved.

- ***Interactions through Electron Pair Sharing***

While interactions facilitated by weak electrical forces resulting from oscillating charges is regarded as physical bonding, a union of two species through sharing of an electron pair is often referred to as chemical bonding. Chemical interactions take

place by rearrangement of bonding electrons within the interacting entities in order to establish balanced electron distributions between them. The latter are guided by the electronegativities of the atoms in the structure. Two broad categories of chemical bonding by electron pair sharing are discussed below.

○ *Interaction through Contributions of Electrons from Both Entities*

In this type of interaction, each atom contributes one of the shared electrons to form a new molecule. The bond formed in this way is called a covalent bond. A physical accumulation of electrons that occupy overlapping orbitals in space between nuclei takes place. Covalent bonds have directional character and interaction depends strongly on the exact position and orientation of the adsorbate with respect to the surface. Elements, which do not gain or lose electrons to form ions, will form covalent bonds. Covalent bonds and ionic bonds are the strongest type of bonds, with binding energies in the order of 170 kcal/mole. Values as low as 15 kcal/mol have, however, also been reported.

○ *Interaction through Donation of a Lone Pair of Electrons by a Single Entity*

These interactions are also known as donor-acceptor interactions. One of the molecules, the donor, must have at least one unshared or lone pair of electrons. The other molecule, or acceptor, must be electron deficient and will interact with the lone pair from the donor. Bonds formed in this way are called coordination bonds. Unlike ionic and covalent bonds that can be formed between two atoms, a coordinate bond is formed between two molecules or between two ions. They are similar to a covalent bond with partial ionic character and the difference between them is indistinguishable. Compounds formed by these interactions, coordination compounds, consequently represent a whole range of characteristics that lie between covalent and ionic compounds. Good describes this type of interaction as acid-base bonding and states that it can be considered weak-electron-sharing bonding. The Brønsted-Lowery and Lewis theories are the most widely accepted bases for describing acid-base concepts. The Brønsted-Lowery theory defines an acid as a substance capable of giving up a proton, and

a base as a substance with the tendency to accept a proton. Acids in this theory are limited to hydrogen-containing compounds. According to the Lewis theory, an acid is an electron pair acceptor, and a base is an electron pair donor. The Lewis definition encompasses the Brønsted definition, but does not limit acids to hydrogen-containing compounds. A Lewis acid-base system that forms a strong bond, in the order of 12 to 15 kcal/mole, can be regarded as an ordinary chemical bond. When a weak bond is formed, the system may dissociate readily even though the mechanism of electron sharing is the same as for a strong bond. These weak interactions may contribute significantly to adhesion forces across an interface or cohesion in a single phase. It is appropriate at this point to introduce hydrogen bonding. This unique type of bonding involves a molecule with a lone pair of electrons to bond with a hydrogen atom, already covalently bonded to another molecule. The hydrogen therefore acts as a bridging atom between two electronegative atoms, holding one by a covalent bond and the other by electrostatic forces. Hydrogen bonding can be described well by the Brønsted-Lowery theory. Naturally, as suggested by Good and van Oss in 1991, it is also possible to describe this bonding in terms of the more general Lewis acid-base theory [11].

2.3 Theories on adhesion

While the main forces have been analyzed, the following paragraph will show the main theories proposed by researchers to explain the adhesion [11]:

2.3.1 Theory of (weak) boundary layers

This theory is commonly known as the theory of weak boundary layers and states that adhesive bonds fail in either the adhesive or substrate, due to the presence of an interphase region of low cohesive strength. Pocius reports that adhesion scientists have used this theory as a fallback position for any adhesive bonding situation that cannot be explained by other rationalizations. Early promoters of this theory suggested that the cohesive strength of a weak boundary layer could always be considered the main factor influencing the level of adhesion. Low molecular weight (and therefore low cohesive

strength) contaminants on the surface, such as some organics and water, are a common cause of weak boundary layers. Although chemical and physical properties of certain bitumen-aggregate combinations produce compatible, high quality interfacial bonds, other properties should be considered which might lead to the formation of weak boundary layers. Jeon and Curtis, in 1990 stated that surfaces of aggregates exhibiting high porosity can act as molecular sieves, separating high and low molecular bitumen fractions. Phenomenological observation indicates that when absorption occurs, the bitumen remaining on the outside becomes hard and brittle. From the theory of weak boundary layers, it is postulated that a brittle inter-phase will form due to highly associated polar molecules left behind. This is similar to short term aging where volatiles evaporate during the manufacturing and construction process of hot mix asphalt. Curtis, in 1993 reported that no evidence of selective absorption could be found in separate research studies on this phenomenon [11].

2.3.2 Electrostatic theory

Solid surfaces can be characterized as electropositive or electronegative. This can be attributed to assemblies of atoms having an electronegative character and the consequent formation of molecular dipoles as previously discussed. Derjaguin, in 1955, proposed that essentially all adhesion phenomena could be explained by electrostatics. Essentially the electropositive material donates charge to the electronegative material thereby creating an electric double layer at the interface. Derjaguin analyzed the system as a capacitor. During interfacial failure of the system, separation of the two plates of the capacitor leads to an increasing potential difference up to a point where discharge occurs. The adhesive strength can therefore be attributed to the strength required to separate the charged surfaces in overcoming the Coulombic forces. The donor-acceptor interactions between aggregate and asphalt surfaces determine the extent of their adhesion in pavement. The effect of water on the aggregate-asphalt chemical bonding is expected to influence the water stripping performance. For solid surfaces such as aggregates, the donor-acceptor surface properties may be divided into proton and electron transfer contributions. Proton transfer surface properties are normally estimated from electrokinetic properties as a function of pH. Electron transfer properties are determined by measuring the zeta potential of the solid particles in

nonaqueous liquids of known donor or acceptor properties. For asphalts, instead, the proton transfer donor-acceptor surface properties can be determined from electrokinetic measurements of their emulsions as a function of pH.

Relying on Mertens and Wright work is possible to have a basic idea of the affinity between an aggregate and an inert. In fact, they classified the most common natural aggregates based on silica and alkaline content percentage as shown in figure 2.1, revealing that natural aggregate surfaces contain elements that cause both electropositive and electronegative features. Basalts, diorites and siliceous limestones are examples of intermediate aggregates.

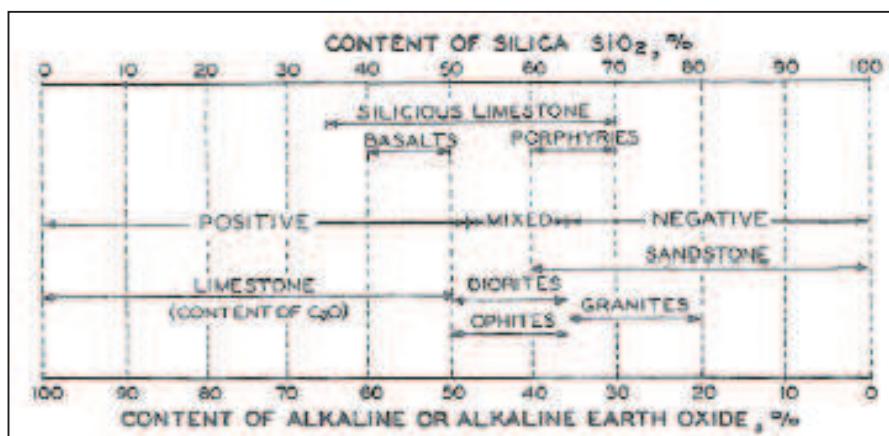


Figure 2.1

In bitumen, carboxylic acid for example ($R-COOH$, where R represents non-polar hydrocarbon alkane chains) is a chemical functional group that plays an important role in the adhesion process. In the presence of water, the molecule separates into a carboxylate anion ($R-COO^-$) and the proton (H^+) causing the bitumen surface to have a negative charge. The increase in the pH of the contacting water increases the extent of dissociation of the acid molecules [11].

2.3.3 Chemical bonding theory

Bitumen-aggregate interaction chemistry is highly complex and variable among different systems primarily due to the complex and variable composition of the materials involved. The polar molecules in bitumen exhibit specific points (sites), which interact with specific sites within the bitumen and on aggregate surfaces. “Active sites”, is a term used to describe reactivity of macromolecules and also the surfaces of

minerals, and implies a process wherein a surface chemical reaction of interest is promoted by a molecular-scale feature on the organic or mineral surface, i.e. surface functional groups. Bitumen and aggregate functional groups are discussed below, followed by a discussion of typical reactions that might take place during bitumen-aggregate bond formation [11].

2.4 Bitumen Functional Groups

Although bitumen is comprised of non-polar hydrocarbons; heteroatoms such as nitrogen (N), sulfur (S), and oxygen (O) may also exist as part of these molecules. These atoms introduce polarity into bitumen molecules and although only present in small amounts, have a controlling effect on the properties of the bitumen and its interaction with aggregate surfaces. Petersen, in 1986 has identified polar, strongly associated functional groups in bitumen. The figure below shows the chemical structures of important functional groups in natural bitumen including those formed during oxidation.

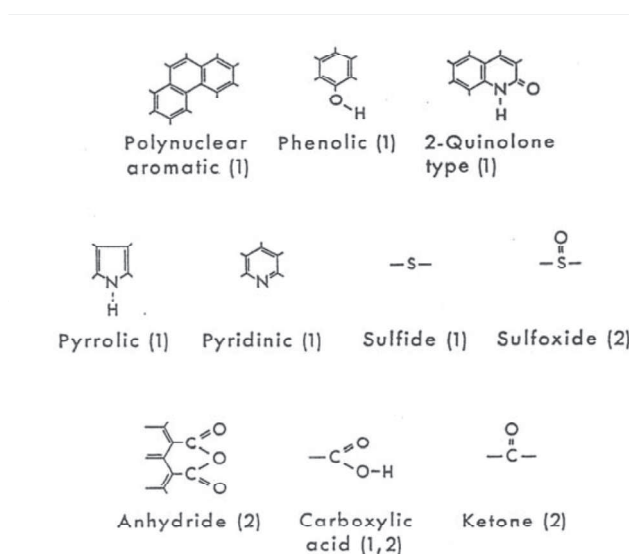


Figure 2.2

Benzene-like, unsaturated ring structures are common hydrocarbon compounds in crude oil, and along with alkanes, are typical constituents in the molecular make-up of bitumen. According to the historical micellar model, resins and ultimately asphaltenes represent the more polar fractions in bitumen.. An asphalt (bitumen) model based on

non-polar and polar species, derived from molecular size distribution has largely replaced the historic micellar model during Strategic Highway Research Program Research (SHRP). Many of the studies on bitumen-aggregate interaction focused on the affinity of different bitumen functional groups for aggregate surfaces. Adsorption of bitumen model compounds, representing specific functional groups in bitumen, has been conducted by researchers including Plancher, Petersen, Brannan and Park. Relative affinity of functional groups for aggregate surfaces and their relative displacement by water are generally presented in these studies. Although rankings differ depending on the type of aggregate, or sometimes model-aggregate, similar general trends are obtained. Table 2.1 summarizes selected findings for the average affinity of bitumen functional groups for aggregates, as well as their susceptibility for displacement by water. The importance of Table 2.1 is not the exact order, but rather the observation that these groups, which are most strongly adsorbed on aggregate surfaces, are also those displaced most easily by water. This observation emphasizes the fact that the influence of moisture on the durability of bitumen- aggregate bonds should be of primary concern from the starting point. Although minor components in bitumen, it is essentially the acidic components such as carboxylic acids, anhydrides, and 2-quinolone types that are the most highly concentrated in the adsorbed fraction. This is inline with the fact that bitumen generally exhibits an excess amount of acidic compounds compared to the amount of basic organic compounds [11].

Plancher et al. (1977)	Petersen et al. (1982)	SHRP
Most strongly adsorbed functional groups (decreasing order)		
Carboxylic acids	Carboxylic acids	Carboxylic acids
Anhydrides	Anhydrides	Sulfoxides
2-Quinolones	Phenols	Pyridine types
Sulfoxides	2-Quinolones	Phenolic
Pyridine types	Sulfoxides	Pyrrolic
Ketones	Ketones	Ketones

Table 2.1 Adsorbed functional groups

Plancher et al. (1977)	Petersen et al. (1982)	SHRP
Susceptibility of adsorbed functional groups for water displacement (decreasing order)		
Carboxylic acids	Anhydrides	Sulfoxides
Anhydrides	2-Quinolone types	Carboxylic acids
Sulfoxides	Carboxylic acids	Pyrrolic
Pyrridine types	Pyrridine types	Ketones
2-Quinolones	Sulfoxides	Pyrridine types
Ketones	Ketones	Phenolic

Table 2.2 General affinity of bitumen functional groups for aggregate surfaces

2.5 Aggregate Functional Groups

Aggregates are composed of an assemblage of one or more minerals, which have a definite chemical composition and an ordered atomic arrangement. In these arrangements, or atomic lattices, each atom is bound to neighboring atoms through electrostatic coordination bonds.

Strong electropositive Lewis acid bonding sites are typically formed on minerals where metals, such as magnesium, iron and calcium, are present. Oxygen in silica and other minerals can act as Lewis base sites. In general, it is reported that chemical sites on aggregate surfaces associated with high affinity for bitumen include elements such as aluminum, iron, magnesium and calcium while elements associated with low bonding affinity include sodium and potassium.

Noteworthy is the work of Jamieson, in which he has investigated the role of aggregate physical and chemical properties on net adsorption. A list of these parameters, linked to a correlation coefficient (which indicates the magnitude of their importance) is shown in table 2.2:

Variable influencing Net Adsorption	Correlation Coefficient
Potassium oxide	0.48
Surface Area	0.71
Calcium Oxide	0.75
Zeta Potential	0.87
Sodium Oxide	0.90

Table 2.3 Physical and chemical properties of aggregates on net adsorption (Jamieson, 1995)

The correlation coefficient of 0.9 indicates that the net adsorption is primarily a function of aggregate properties. This is in line with the common finding that adhesion is dominated by the properties of the aggregate. The increased order of impact is therefore, potassium oxide, surface area, calcium oxide, zeta potential, and sodium oxide. While these results corroborate the impact of alkali metals (K and Na) and calcium, it also shows that part of the adsorption-desorption action can be explained by zeta potential, as previously discussed. The contribution of surface area suggests availability of more active sites per unit mass of aggregate for interaction. In this regard, Petersen illustrated that surface site density on aggregates is also important [11].

2.6 Surface energy and wettability

Before proceed further with the thermodynamic theory we'd better introduce these notions. Surface tension is a contractive tendency of the surface of a liquid that allows it to resist an external force. It is easy to understand if we imagine, for instance, the floating of some objects on the surface of water (figure 2.3), even though they are denser than water, and in the ability of some insects not to sink when they are resting on the surface of a liquid.



Figure 2.3 A paperclip floats on water

The cohesive forces among liquid molecules are responsible for the phenomenon of surface tension. In the bulk of the liquid, each molecule is pulled equally in every direction by adjacent liquid molecules, resulting in a net force of zero. Since the molecules at the surface do not have other molecules on all sides of them, they are pulled inwards. The result of this is that the top surface of liquid behaves like an elastic stretched layer (figure 2.4).

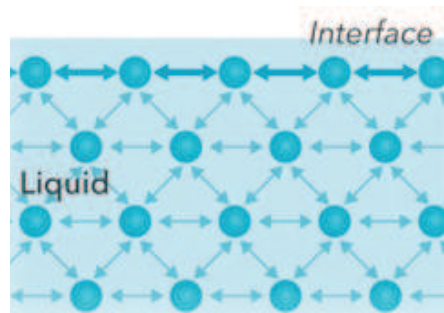


Figure 2.4 The elastic stretched layer

The example of a water droplet can help better understand. The drop of water falling from a tap takes the shape of a sphere (minimum surface area shape) as the molecules from the surface are attracted inside the bulk of the liquid until the minimum possible surface area is achieved. Therefore, the molecules at the surface are considered to possess excess energy because of this difference in intermolecular forces between the surface and bulk of the material, and this energy is referred to as surface free energy. Work is required to be done to bring these molecules on the surface and increase the surface area of the material.

Wetting is defined as the ability of a liquid to maintain contact with a solid surface, resulting from intermolecular interactions when the two are brought together. In 1805, Thomas Young, in the *Philosophical Transactions of the Royal Society of London*, was the first in state that wetting is determined by a force balance between adhesive and cohesive forces [12]. If complete wetting does not occur, then a bead of liquid will form, with a contact angle which is a function of the surface energies of the system.

Within this context is possible introduce the notion of contact angle: it is the angle, conventionally measured through the liquid, where a vapour-liquid interface meets a

solid surface. It is the simplest and fastest way to quantify the wettability of a solid surface by a liquid via the Young equation. A given system of solid, liquid, and vapor at a given temperature and pressure has a unique equilibrium contact angle. However, in practice contact angle hysteresis is observed, ranging from a maximal value (advancing contact angle) to a minimal value (receding contact angle). The equilibrium contact angle, reflecting the relative strength of the liquid-solid-vapour molecular interaction, is within those values, and can be calculated from them.

As explained above, dropping a drop of a liquid on a solid surface, we can observe a contact angle. A value less than 90° (low contact angle) usually indicates that wetting of the surface is very positive, and the fluid will spread over a large area of the surface. On the other hand, a value greater than 90° (high contact angle) generally means that wetting of the surface is unfavourable so the fluid will minimize contact with the surface and form a compact liquid droplet.

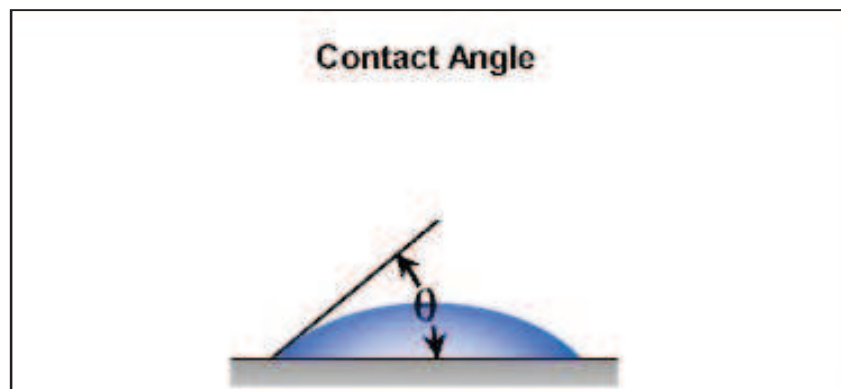


Figure 2.5 Contact Angle of a water droplet on a surface (ramé-hart instrument co.)

For water, a wettable surface may also be termed hydrophilic and a non-wettable surface hydrophobic. Super-hydrophobic surfaces have contact angles greater than 150° , showing almost no contact between the liquid drop and the surface. This is sometimes referred to as the "Lotus effect". On the contrary, for non-water liquids, the term lyophilic is used for low contact angle conditions and lyophobic is used when higher contact angles result. Similarly, the terms omniphobic and omniphilic apply to both polar and apolar liquids. Table 2.4 describes varying contact angles and their corresponding solid-liquid and liquid-liquid interactions [13].

<i>Contact Angle</i>	<i>Degree of wetting</i>	<i>Solid-liquid interactions</i>	<i>Liquid-liquid interactions</i>
$\theta = 0^\circ$	<i>Perfect Wetting</i>	<i>Strong</i>	<i>Weak</i>
$0^\circ < \theta < 90^\circ$	<i>High wettability</i>	<i>Strong</i>	<i>Strong</i>
		<i>Weak</i>	<i>Weak</i>
$90^\circ \leq \theta \leq 180^\circ$	<i>Low wettability</i>	<i>Weak</i>	<i>Strong</i>
$\theta = 180^\circ$	<i>Perfectly non-wetting</i>	<i>Weak</i>	<i>Strong</i>

Table 2.4 Contact Angles and corresponding degree of wetting

There are two main types of solid surfaces with which liquids can interact. Traditionally, solid surfaces have been divided into high-energy solids and low-energy types. The relative energy of a solid has to do with the bulk nature of the solid itself. Solids such as metals, glasses, and ceramics are known as 'hard solids' because the chemical bonds that hold them together (e.g., covalent, ionic, or metallic) are very strong. Consequently, it takes a large input of energy to break these solids so they are termed "high energy." Most molecular liquids achieve complete wetting with high-energy surfaces. The other type of solids is weak molecular crystals (e.g., fluorocarbons, hydrocarbons, etc.) where the molecules are held together essentially by physical forces (e.g., van der Waals and hydrogen bonds). Since these solids are held together by weak forces it would take a very low input of energy to break them, and, for this reason, they are termed "low energy." Depending on the type of liquid chosen, low-energy surfaces can permit either complete or partial wetting. [14]

The word "surface tension" is used for liquids in place of "surface energy". Surface energy quantifies the disruption of intermolecular bonds that occur when a surface is created. It is defined as the amount of work required to create a unit surface area of a material in vacuum.

2.7 Theory for surface energy calculation from contact angle data

Direct measurement of surface energy components of solids is rarely feasible.

Different techniques have been set up in the past, in order to measure reliable values for solid surface energy, from contact angle data. In the following section a quick review of them is proposed. [15]

2.7.1 Geometric Mean Approach

In this method, proposed by Fowkes, surface energy γ is the sum of several additive forces acting on the surface.

$$\gamma = \gamma_d + \gamma_p + \gamma_h + \gamma_i + \gamma_{ab}$$

Where:

γ_d = dispersion force

γ_p = polar force

γ_h = hydrogen bonding force

γ_i = induction force

γ_{ab} = acid-base force

Owens and Wendt, recovering the work of Fowkes, proposed that surface energy of a system consists of dispersive and polar interactions. This theory was based on the assumption that all the polar materials interact with each other as a function of their internal polar cohesive forces but later it was identified as incorrect by researchers because polar interactions are mostly electron acceptor (acid) and electron donor (base) type interactions and strong interaction can only occur when one material has an acidic character and the other has a basic character. [15]

2.7.2 Critical Surface Tension Approach

This method was proposed by William Zisman. He observed that $\cos\theta$, obtained by testing a smooth surface of a solid with a set of liquids, increases linearly as the surface tension γ_{lv} of the liquid decreased. Therefore, he was able to establish a rectilinear relation between $\cos\theta$ and the surface tension (γ_{LV}) for these liquids.

A surface is more wettable when γ_{LV} is low and when θ is low. He termed the intercept of these lines when the $\cos \theta = 1$, means zero contact angle (or complete wetting), as the critical surface tension (γ_c) of that surface. This critical surface tension is an important parameter because it is a characteristic of only the solid. Knowing the critical surface tension of a solid, it is possible to predict the wettability of the surface. [16]

2.7.3 Acid-Base Approach

Good, Van Oss and Chaudhury suggested that the surface energy components of a solid consists of two main interactions namely Lifshitz-van der Waals interactions and acid-base interactions. They divided the polar components into Lewis acid and base components, comprised of all the electron donor and electron acceptor type interactions. [15]

2.8 Thermodynamic theory

This theory is the most widely used to quantify adhesion between two materials as indicated by most comprehensive references on this subject. Thermodynamic theory is based on the concept that an adhesive will adhere to a substrate due to established intermolecular forces at the interface provided that intimate contact is achieved. The magnitude of these fundamental forces can generally be related to thermodynamic quantities, such as surface free energies of the materials involved in the adhesive bond. The orientation of polar molecules in bitumen as part of the process to minimize the free energy at the interface has been recognized and discussed in many previous reviews on stripping in bitumen-aggregate systems (Hicks, Kiggundu and Robberts, Little and Jones, to name a few). Some thermodynamic concepts need to be reviewed, in order to appreciate the material presented in this section. Thermodynamics is the branch of natural science concerned with heat and its relation to other forms of energy and work. A spontaneous process is one that occurs on its own, without external assistance. Such a process occurs due to an imbalance between two natural tendencies. The first tendency is the spontaneous conversion of potential energy into work and heat; the amount of heat given off or adsorbed during a process is called enthalpy H . On the other hand, the second tendency is the spontaneous increase in randomness of the

system, known as entropy S . In order to relate enthalpy and entropy, the Gibbs free energy (G) is defined so that, at constant temperature (Kelvin) and pressure (atm),

$$\Delta G = \Delta H + T\Delta S \quad (2.1)$$

Gibbs free energy thus represents the difference between initial and final energy state of a system and predicts whether a process, carried out at the defined constant temperature and pressure conditions, can occur or cannot occur. It measures the "useful" or process-initiating work obtainable from a isothermal and isobaric thermodynamic system. For $\Delta G < 0$, the energy will be released to perform work and the process will occur spontaneously. If, on the contrary $\Delta G > 0$, then energy will have to be absorbed from the environment and cannot occur on its own. For $\Delta G = 0$, the process is in equilibrium. Equation 2.1 indicates that the absolute temperature, T , must be specified due to temperature dependency of entropy. Fortunately, the magnitudes of H and S do not vary much over a limited temperature range. The free energy, however, may vary considerably with temperature unless S is very small. At relatively low temperatures, such as room temperature, ΔH usually dominates while ΔS become more important at high temperatures.

The Gibbs free energy is an important thermodynamic parameter in quantifying adhesive bonding. It should be pointed out that the Gibbs free energy in this context is the excess free energy of the system associated with the surface or interface. A detailed account of the derivation of thermodynamic parameters related to surfaces is presented by Adamson and Gast. *It is common to refer to the Gibbs free energy as the free energy of adhesion or, when applicable to the binding between similar phases, the free energy of cohesion.* In general, systems have a tendency to move towards the minimization of energy for stability. When two objects are strongly bonded to each other they tend to have lower energy (therefore lower free energy) and more energy is required to separate them.

The relationship between the Gibbs free energy, work of adhesion and surface energy are presented below. The surface energy, γ , in a thermodynamic sense is the reversible work required to create a unit area of new surface. While researchers such as Good and van Oss base their theory on the definition of the Gibbs free energy, the work of

adhesion (W_a) is more commonly used in the literature pertaining to the thermodynamic theory of adhesion. Although equal in magnitude, the work of adhesion and the Gibbs free energy of adhesion should be interpreted as follows,

$$W^a = -\Delta G^a \quad (2.2)$$

Consider a brittle material of unit cross sectional area subjected to a tensile force. Then, if the material is completely brittle, the work done on the sample is dissipated only through propagation of a crack, thereby creating two new surfaces. The total work expended per unit of surface area in forming the two surfaces (W^c), referred to as the total work of cohesion, is then equal to twice the surface energy per unit of surface area, of the material under consideration. Under these conditions,

$$W^c = 2\gamma \quad (2.3)$$

When two dissimilar materials form an interface by being in intimate contact, a tensile force can be applied to split the materials into dissimilar parts. For a completely brittle interface of unit cross sectional area, the energy expended should be the sum of the individual surface energies for the two materials involved. However, because the dissimilar materials are separated, some of the intermolecular forces present during intimate contact, are now missing. That is, an interfacial energy may have existed before separation, which should be accounted for by subtracting it from the energy done to create the two new surfaces. An interface may be defined as a special type of surface that forms a common boundary between two different materials. The molecules of both these materials at the interface are subjected to unequal forces compared to their respective bulk molecules. This creates a misbalance of forces at the interface and results in interfacial energy between the two materials, represented as γ_{12} . Analogous to the surface free energy in a vacuum, the interfacial energy between two materials is defined as the work required to create a unit area of the interface by separating the two materials in a vacuum.

Dupré, in 1867, postulated the following relationship, which plays a central role in the study of adhesion.

$$W^a = -\Delta G^a = \gamma_1 + \gamma_2 - \gamma_{12} \quad (2.4)$$

where γ_i is the surface energy of the i^{th} material and γ_{12} is the interfacial energy between the two materials in contact.

The terms wetting, spreading, and contact angle have become synonymous with adhesion. The shape of a liquid drop on a surface, usually described through the contact angle between them, provides information on the intermolecular forces of the individual phases involved as well as the interfacial forces between them. Although the great utility of contact angle measurements stems from their interpretations based on thermodynamic considerations, they can also be used to provide a measure of wetting and spreading on a macroscopic scale.

As previously stated, wetting of a surface (or spreading of the liquid over the surface) is the process where the adhesive comes into intimate molecular contact with the surface and establishes fundamental forces of adhesion. Wetting is a prerequisite for good adhesion. For complete spreading, the contact angle equals zero and the adhesive spreads spontaneously over the surface. Naturally, wetting and spreading depends also on the viscosity of the liquid, roughness and heterogeneity of the solid surface involved. From a thermodynamic point of view, wetting and spreading depends on the competition between adhesive forces and cohesive forces, which can be used to define a spreading coefficient, S .

$$S = W^a - W^c \quad (2.5)$$

Thus, the higher and more positive the value of S , the greater the work of adhesion is compared to the cohesive energy of the adhesive. A negative value of S represents a finite contact angle and zero corresponds to final equilibrium.

The properties of interfaces can normally be described as triple junctions, or a three-phase boundary. Young, in his “An essay on the cohesion of fluids” in 1805, proposed an equation to obtain surface tension from the contact angle formed when a drop of liquid is placed on a perfectly smooth, rigid solid. A schematic of the contact angle experiment is shown in figure 2.6, where θ is the contact angle between the solid-liquid (sl) interface and the tangent of the liquid-vapor (lv) interface.

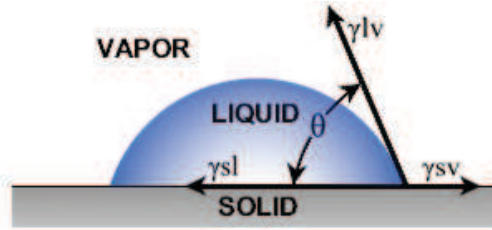


Figure 2.6 Three-phase boundary

To each interface, forming the triple line, a surface or interfacial free energy or tension can be attributed. Thus, γ_{sv} is the surface free energy of the solid in equilibrium with the saturated vapor of the liquid, γ_{lv} is the surface tension of the liquid in equilibrium with the solid, and γ_{sl} is the solid-liquid interfacial free energy. Young's equation is the result of the triple line in equilibrium (tension in force per unit length).

$$\gamma_{sv} = \gamma_{sl} + \gamma_{lv} \cos \theta \quad (2.6)$$

Pocius, with rigorous thermodynamic derivations based on minimizing the overall free energy, verified this equation, despite it was originally based on a mechanical definition. The solid-vapor interfacial energy in this equation, however, is not the true surface free energy of the solid. In fact, when vapor is adsorbed onto the surface of the solid, its free energy is reduced so that,

$$\gamma_{sv} = \gamma_s - \pi_e \quad (2.7)$$

where γ_s is the surface free energy of the solid only in contact with its own vapor, and π_e the equilibrium spreading pressure which is a measure of energy released during vapor adsorption. Although equilibrium spreading for the liquid phase should also be possible, this value has historically been assumed equal to zero. Good and van Oss have shown that π_e is negligible for high-energy liquids on low-energy solids, which is usually the case for contact angle measurements on polymeric surfaces.

By combining the Dupré equation (2.4) with Young one (2.6), the famous Young-Dupré equation is obtained:

$$W_a^{LS} = \gamma_{lv} (1 + \cos \theta) \quad (2.8)$$

The Young-Dupré equation is the starting point for any method that utilizes contact angles to obtain surface free energies by relating the contact angle to the work of adhesion. This is also the way to tie contact angles back to adhesion.

Fowkes, in 1964, suggested that surface energy is comprised of a polar and non-polar component. Since that time, several models were proposed for the calculation of the work of adhesion based on surface energy components. Several researchers and practitioners from different sectors of the adhesion science community report that the acid-base theory, developed by Van Oss et al. in 1988, is the best available at the time. Following the form suggested by Fowkes, the surface energy of a single phase is given by,

$$\gamma^{total} = \gamma^{LW} + \gamma^{AB} \quad [erg/cm^2] \quad (2.9)$$

where LW denotes Lifshitz-van der Waals, and AB denotes acid-base. The Lifshitz theory was introduced conceptually in the section addressing fundamental forces. The London, Keesom, and Debye components together form the apolar (LW) component of attraction. The Lifshitz theory has demonstrated that the contribution of the Keesom and Debye van der Waals forces are small relative to the London forces. The acid-base component represents polar, or specific, interactions primarily due to hydrogen bonding. The acid/base components are further separated into Lewis acid, γ^+ , and Lewis base γ^- components. [11]

$$\gamma^{AB} = 2\sqrt{\gamma^+\gamma^-} \quad (2.10)$$

The bond strength of a material (binder or aggregate; in our case) is the combination of these Lifshitz-van der Waals (non-polar) and Lewis acid/base forces and the total bond strength can be given as:

$$\Delta G = \Delta G^{AB} + \Delta G^{LW} \quad (2.11)$$

where:

$\Delta G = Total\ bond\ strength\ (Gibbs\ free\ energy\ of\ the\ material)$

$\Delta G^{AB} = Adhesive\ polar\ strength\ (Acid-Base\ component)$

$\Delta G^{LW} = Adhesive\ non-polar\ bond\ strength\ (Lifshitz - van\ der\ Waals\ component)$

The interfacial surface free energy can also be written as a sum of the Lifshitz-van der Waals and Lewis acid/base contributions.

$$\gamma_{BA} = \gamma_{BA}^{AB} + \gamma_{BA}^{LW} \quad (2.12)$$

The subscripts B and A stand for bitumen and aggregate.

The adhesive polar strength can be determined by using the following equation:

$$\Delta G^{AB} = -\gamma_{BA}^{AB} + \gamma_B^{AB} + \gamma_A^{AB} \quad (2.13)$$

In a similar way the adhesive non-polar bond strength is given as:

$$\Delta G^{LW} = -\gamma_{BA}^{LW} + \gamma_B^{LW} + \gamma_A^{LW} \quad (2.14)$$

Making use of Small's combining rule, Erbil proposed this equation for γ_{BA}^{AB} :

$$\gamma_{BA}^{AB} = 2(\sqrt{\gamma_B^+} - \sqrt{\gamma_A^+})(\sqrt{\gamma_B^-} - \sqrt{\gamma_A^-}) \quad (2.15)$$

Bhasin, by using geometric mean relationship, suggested for γ_{BA}^{LW} this equation:

$$\gamma_{BA}^{LW} = (\sqrt{\gamma_B^{LW}} - \sqrt{\gamma_A^{LW}})^2 \quad (2.16)$$

By inserting the (2.15) in (2.13), the (2.16) in (2.14), and finally substituting them in (2.11), the *ADHESIVE BOND STRENGTH IN DRY CONDITION* is obtained:

$$\Delta G_{AB}^a = 2\sqrt{\gamma_B^{LW}\gamma_A^{LW}} + 2\sqrt{\gamma_B^+\gamma_A^-} + 2\sqrt{\gamma_B^-\gamma_A^+} \quad (2.17)$$

Consider a three-phase system comprising asphalt binder, aggregate, and water (figure 2.7) where these components are represented by 'B,' 'A,' and 'W,' respectively. The following processes occur when water displaces the asphalt binder from the binder-aggregate interface. [15]

Water and aggregates are polar substances while bitumen is mostly a non-polar material. Thus water has greater attraction for aggregate surfaces than bitumen. This evidence increases the likelihood that water is in contact with the aggregate, moving the bitumen film. The following figure (2.7) shows the process in which the water acquires a surface portion of aggregate to the detriment of the bitumen.

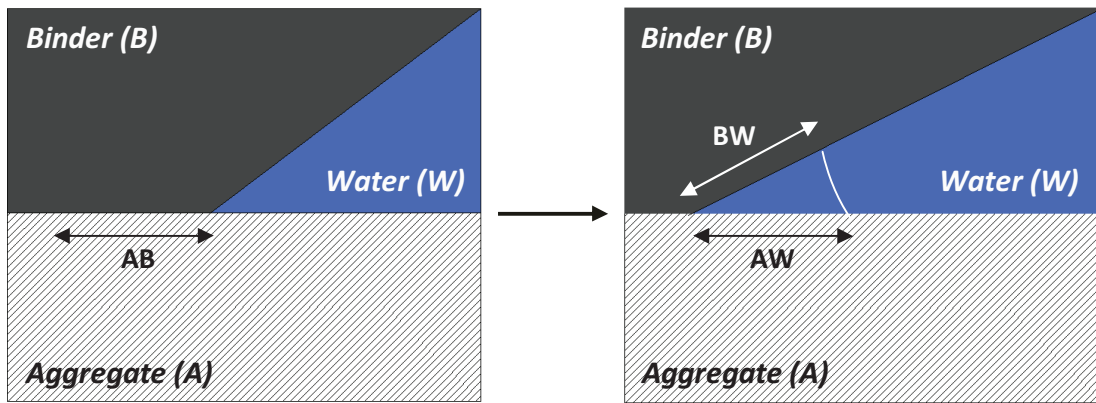


Figure 2.7 Displacement of bitumen on the aggregate surface by water

First, a part of the interface of the aggregate with the binder is eliminated (AB). Based on the definition of interfacial energy, the external work required for this is $-\gamma_{AB}$. Similarly, two new interfaces, between water and binder (BW), and between water and aggregate (AW), are created. The work done for the formation of these two new interfaces is $\gamma_{WB} + \gamma_{WA}$. Therefore, the total work done for water to displace binder from the surface of the aggregate is $\gamma_{WB} + \gamma_{WA} - \gamma_{AB}$. If the displacement process is thermodynamically favorable then it must be associated with an overall reduction in free energy of the system. In other words, the total work done on the system during the displacement process must be less than zero. Usually it is true for almost all asphalt binder-aggregate systems, suggesting that displacement of asphalt binder by water is a thermodynamically favoured phenomenon. [17]. In this context, the energy associated with the displacement of binder by water from the bitumen-aggregate interface, or debonding, is referred to as the work of debonding and is expressed as:

$$\Delta G_{BWA}^a = \gamma_{WB} + \gamma_{WA} - \gamma_{AB}$$

According to Cheng et al., in a similar way for the adhesive bond strength in dry condition, the equation for ADHESIVE BOND STRENGTH IN WET CONDITION is:

$$\begin{aligned} \Delta G_{BWA}^a &= \gamma_{WB} + \gamma_{WA} - \gamma_{AB} = \\ &= 2\gamma_W^{LW} + 2\sqrt{\gamma_B^{LW}\gamma_A^{LW}} - 2\sqrt{\gamma_B^{LW}\gamma_W^{LW}} - 2\sqrt{\gamma_A^{LW}\gamma_W^{LW}} + 4\sqrt{\gamma_W^+\gamma_W^-} + \\ &- 2\sqrt{\gamma_W^+}(\sqrt{\gamma_B^-} + \sqrt{\gamma_A^-}) - 2\sqrt{\gamma_W^-}(\sqrt{\gamma_B^+} + \sqrt{\gamma_A^+}) + 2\sqrt{\gamma_B^+\gamma_A^-} + 2\sqrt{\gamma_B^-\gamma_A^+} \end{aligned}$$

Thermodynamic concepts have been used by many researchers to elucidate adhesion between bitumen and aggregate materials. Ensley determined the heat of immersion using microcalorimetry. Curtis determined Gibbs free energies from adsorption isotherms. Lytton utilized surface energies measured on bitumen and aggregate surfaces to calculate free energies of adhesion and cohesion by applying modern surface energy theories as discussed in the forgoing paragraphs.

These concepts, especially surface energy, have played an important role in discoveries of the rules governing the microfracture and healing in bitumen-aggregate mixtures. Thermodynamic theory lends itself to quantifying the relationship between fundamental adhesion and practical adhesion. Since real materials are not completely brittle, especially polymer-like materials such as bitumen, energy dissipation can result from molecular chain disentanglement and stretching, and conformational changes (rotation about flexible intermolecular bonds) under applied loads, i.e. viscoelastic effects, as well as plastic deformation. Merrill report that the apparent or practical work of adhesion is much larger than the fundamental work of adhesion based on adhesive peel test experiments. However, the experiments showed that the practical work of adhesion is a multiplication of some dissipation factor with the fundamental work of adhesion. From fracture mechanics, the well-known Griffiths crack growth criterion suggests that for a completely brittle material, the energy necessary to break an adhesive (or cohesive) bond is equal to the fundamental work of adhesion, W^a . This energy can be considered the minimum amount of practical adhesion that one can expect from a bond. If other modes of dissipating energy exist, then this minimum value increases. Schapery extended this crack growth theory to viscoelastic materials based on the fundamental laws of fracture. Schapery and Lytton developed similar relationships for healing. Healing is the opposite of fracture and is pronounced when longer rest periods are introduced between applied loads, manifested in extended fatigue life. Lytton applied these fundamental relationships of fracture and healing to asphalt mixtures [11].

CHAPTER 3

RESEARCH PROJECT AND TEST METHODS

3.1 Introduction

This chapter has the aim of explain the research project and illustrate all the test used, pointing out the purpose, the specifications, and theory on the background.

The first and more reliable technique to build a road pavement is without any doubt the hot mix asphalt. It is produced by heating the asphalt binder to decrease its viscosity, and drying the aggregate to remove moisture from it prior to mixing, that is generally performed with the aggregate at nearly 160 °C. The quality of hot mixtures obtained by following the protocols, that are confirmed over the past is, in fact, an absolute reference. The recent tendency of reduce the exploitation of non-renewable resources and the need to ensure the environmental protection has moved the attention to find new ways of construction and maintenance. The main key is to reduce the laying temperature. This purpose can be achieved, for instance, by mixing the bitumen with a small quantity of waxes, with the intent of reduce the viscosity and hence the temperature needed to coat the aggregates and easily mixing. The benefits are many:

- lower plant mixing temperatures;
- lower mixing temperatures at the plant leads to a reduction in emissions;
- lower emissions during the paving operation provide a healthier and safer work environment;
- longer construction season become possible.

Several studies have been carried out on waxes but they are not yet confirmed by field performance. The aim of this research is to investigate the energetic and rheological effect of two waxes on a bitumen. The material analyzed are:

- a API neat bitumen 70 – 100 dmm (12360);
- the above bitumen modified with a 2% in weight with Adriamont wax (12361);
- the same neat bitumen 70 – 100 dmm modified with a 2% in weight with Sasobit wax (12362).

In order to have under control and easily recognize all the materials to be used in the laboratory, they all have been catalogued with a reference code (for example 12361 is the Adriamont modified binder).

The question is: do the waxes aggravate in some way the performance of the bitumen?

For this reason the three mixtures have been examined with various tests:

1. **Dynamic Shear Rheometer (DSR):** it is the basis for the study of the rheology of bitumens, especially at intermediate and high service temperature. The sample is subjected to a sinusoidal form stress. The system returns a series of rheological parameters such as the complex modulus, the phase angle, the rutting parameter and so on...The raw data can be plotted and elaborated in many ways as we will further see.
2. **Bending Beam Rheometer (BBR):** unlike the DSR, this rheometer performs flexural tests, providing a measure of low temperature stiffness and relaxation properties of asphalt binders. Because low temperature cracking is a phenomenon found mostly in older pavements, the test is run on the long-term aged residue from the PAV.
3. **Rollin Thin Film Oven Test (RTFOT):** provides simulated short term aged asphalt binder for physical property testing. The bitumen is exposed to elevated temperatures to simulate manufacturing and placement aging. The RTFOT also provides a quantitative measure of the volatiles lost during the aging process.
4. **Pressure Aging Vessel (PAV):** provides simulated long term aged asphalt binder for physical property testing. The bitumen is exposed to heat and pressure to simulate in-service aging over a 7 to 10 year period. By

subjecting the PAV-aged binder to rheological tests, we can figure out how the rheological properties change after aging.

5. **Dynamic Contact Angle (DCA):** This test, carried out on unaged asphalt binder, is used to determine the wettability property of a bitumen. A glass slide, coated by bitumen, is immersed in a probe liquid and the force applied is measured. Indirectly, the contact angle of the probe on the bitumen is calculated, and is used for find out the surface energy components of the bitumen.
6. **Dynamic Sorption Device (DVS):** like the DCA, this test is used to determine the surface energy components not of the bitumen but of the aggregates. Because a drop of liquid quickly spreads over the aggregate surface, the components are determined measuring the change in mass due to an applied pressure of probe liquid .In particular, it is interesting to investigate the behaviour of the mixtures as the temperature drop under zero Celsius degrees

3.2 Ageing of bitumens

In order to understand the properties on both unaged and short as well as long term aged binders, part of the binders were subjected to aging tests.

3.2.1 Rolling Thin Film Oven Test (RTFOT)

The Rolling Thin-Film Oven Test (RTFOT) provides simulated short term aged asphalt binder. One of the basic principle of the Superpave PG binder specification is that tests should be as closely tied with field performance as possible. Seeing as the constituent asphalt binder undergoes significant aging during the manufacturing and placement processes, a method to simulate the aging is important in investigating and predicting early age pavement behaviour and distresses. It can be now understand why the Superpave PG binder specification request short term aged bitumen to be tested at high temperatures to determine fatigue and rut resistance.

Although many different factors contribute to asphalt binder aging, the key component of concern for the RTFOT is the loss of volatiles. The loss of smaller molecules from

the asphalt binder, often termed “volatiles” increases an asphalt’s viscosity. Asphalt binders typically lose volatiles during the manufacturing and placement processes. The elevated temperature of these processes ages the asphalt binder by driving off a substantial amount of volatiles. Field tests have shown that in-place asphalt binder does not lose a significant amount of volatiles over its life.

The standards Rolling Thin-Film Oven test are AASHTO T 240 and ATSM D 2872: effect of heat and air on a moving film of asphalt (Rolling Thin-Film Oven Test). British Standard EN12607-1:2007 has been followed for this test, reducing the time test from 85 to 75 mins. [18]

A sample of asphalt binder is heated until it is fluid enough to pour. Then the sample is stirred to ensure homogeneity and remove air bubbles. In order to determine the mass, two of the eight jars are labelled and weighted empty; these are designated as the “mass change” bottles and the weight recorded as M_0 and M'_0 . The standard prescribe not to pour more than 35 grams per jar of asphalt. This restriction is due to the need to ensure that no binder will drain out the bottles during the test and that the binder form a thin film on the bottle. The “mass change” bottles are allowed to cool to room temperature in desiccators for 60 minutes; after this period, the mass is weighted and recorded as M_1 and M'_1 . The bottles are placed in the RTFOT oven carousel (figure 3.1) that is then closed and actuated.



Figure 3.1 Placing the RTFOT jars in the carousel

It is recommended that, once the bottles are placed in the carousel, the oven temperature reach the required 163°C in less than 15 minutes; for this reason the oven is preheated at least 30 minutes before the test is started. The test lasts 75 minutes from the time the temperature is 163°C. The carousel rotation continuously exposes new asphalt binder to the heat and air flow of 4000 ml/min and slowly mixes each sample. After the test the bottles are removed one at a time from the carousel, and the mass change bottles are placed in the dessiccator again.

Residue from the remaining bottles are transferred to a single container by pouring as much material as possible and in the quicker time possible. After 60 minutes of cooling, the two mass change bottles are weighted again and the mass is recorded as M_2 and M'_2 ; the residue is discarded. Samples are then stored for use on DSR tests or for the PAV-ageing.

The mass change of a sample as a percent of initial mass, is calculating as follow:

$$100 \cdot \frac{(M_2 - M_1)}{(M_1 - M_0)} \quad (3.1)$$

Where:

M_0 and M'_0 = Mass of glass containers nearest 1 mg;

M_1 and M'_1 = Mass of glass containers + cooled sample;

M_2 and M'_2 = Mass of glass container + sample after testing.

For the three asphalt binders, the following result have been obtained:

Binder	% Loss in mass jar 1	% Loss in mass jar 2	Mean % of change in mass
Base Binder	0.14	0.131	0.135
Adriamont	0.099	0.114	0.107
Sasobit	0.134	0.081	0.108

Table 3.1 Mass loss of the examined bitumen



Figure 3.2 RTFOT jars. The bottle at left is after the test, the bottle in the middle is before the test

3.2.2 Pressure Aging Vessel (PAV)

Pressure Aging Vessels (PAV's) use heated, pressurized air to simulate long-term oxidative aging of asphalt binders (in-service ageing over a 7 to 10 year period). Many HMA distresses either initiate or become more severe in older pavements. The Superpave PG binder specification calls for long term aged asphalt binder to be tested at intermediate and cold temperatures to determine fatigue and low temperature cracking resistance.



Figure 3.3 Pressure Aging Vessel

Therefore, a method to simulate aged asphalt binder is important in investigating and predicting these types of distresses.

The standard Pressure Aging Vessel procedure is AASHTO R 28: Accelerated Aging of Asphalt Binder Using a Pressurized Aging Vessel (PAV).

The key component of concern for the PAV, despite different factors contribute to aging, is oxidation. Oxidation increases the bitumen's viscosity with age up until a point when the asphalt is able to quench oxidation through immobilization of the most chemically reactive elements.

Oxidation can occur in the field during two distinct stages of a pavement's life (Bahia and Anderson, 1995):

1. During mixing and laying the elevated temperature lead to a quick ageing of the asphalt binder by volatilization while the large contact area with the heated aggregate lead to oxidation. The predominate aging mechanism during this stage is the loss of volatiles resulting from elevated mixing and placement temperatures. Hence, this stage is studied with RTFO test.
2. Over the life of an in-service pavement the constituent asphalt binder slowly ages as the oxygen from the surrounding environment percolates through the pavement and chemically reacts. This is the stage that PAV investigates.

In developing a procedure to simulate long term aging by oxidation, oven tests approach was initially considered. High temperatures applied to thin bitumen films were used to accelerate the oxidation process. However, this method resulted inappropriate because samples loosed significant amount of volatiles (this evidence is not found by field tests on older in-service pavements). Accordingly, the actual approach, by using high pressure, increase the diffusion rate of oxygen into the asphalt binder sample and limits the loss of volatiles. Furthermore, the aging can be carried out without using high temperatures, and field climate conditions can be approximated.

The PAV process is usually accomplished for 20 hours at either 90, 100 or 110°C, depending on the climate to be simulated. These details were chosen for practical, rather than theoretical reasons. In fact, the PAV time of 20 hours allow for one test plus the removal of completed samples and insertion of new samples within a 1 day.

The PAV process steps are listed below:

1. The RTFO aged asphalt binder is heated until it is fluid enough to pour, and then stirred. Preheated thin film oven pans are filled with 50 g each, placed into a pan holder that in turn is placed into the preheated PAV (figure 3.4);
2. PAV is sealed and allowed to return to the aging temperature;
3. Once the PAV has reached the desired temperature, PAV is pressurized to 2.07 MPa and the pressure is maintained for 20 hours;
4. At the end of the aging period, the pressure is gradually released and the pans are carefully removed from the PAV;
5. Pans are then placed in oven for roughly 15 minutes at 163°C in order to pour the asphalt aged binder in a unique container. The sample need to be placed in a vacuum open for 30 minutes for degas. This procedure is necessary for remove entrapped air that may affect the measures and the reliability of future tests;

PAV-aged binder is now ready to be used for further tests. In particular, it has been used for tests on the rheological properties, like DSR and BBR. The data on PAV-aged binder are needed to determine those parameters for SHRP specifications, that drive, as we will see, to the performance grade of the bitumens. [19]



Figure 3.4 Pour of RTFO binder into the pan

3.3 Dynamic Shear Rheometer (DSR)

3.3.1 General concepts

The dynamic shear rheometer (DSR) is used to characterize the viscous and elastic behaviour of asphalt binders at medium to high temperatures. The rheological tests are performed by subjecting a sample of bitumen, after thermal conditioning to stress or strain regimes known by reading the corresponding deformation response and stress. Measurements may be obtained at different temperatures, strain and stress levels, and test frequencies. The amplitude of the responding stress is measured by determining the torque transmitted through the sample in response to the applied strain. The stress and strain parameter are therefore calculated as

$$\sigma = \frac{2M}{\pi r^3} \quad (3.2)$$

Where:

σ = shear stress

M = torque

r = radius of parallel disks.

$$\gamma = \frac{\theta r}{h} \quad (3.3)$$

Where:

γ = shear strain

θ = deflection angle

h = gap between parallel disks.

The shear stress and strain in equation 3.2 and 3.3 are dependent on the radius of the parallel disks and vary in magnitude from the centre to the perimeter of the disk. The shear stress, shear strain and complex modulus G^* , which is a function of the radius to

the fourth power, are calculated for the maximum value of the radius. The phase angle, δ , is measured by the instrument by accurately determining the sin wave forms of the strain and torque.

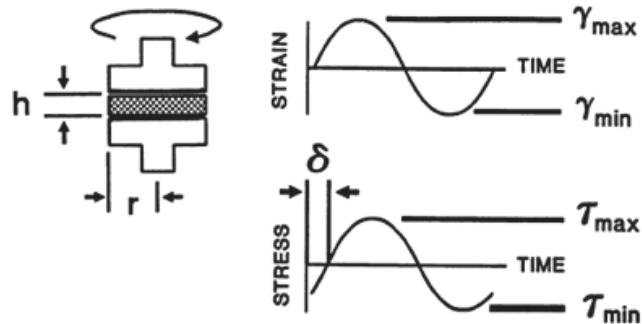


Figure 3.5 Sinusoidal stress and phase angle

Tests can be carried out with two different regimes: controlled-strain and controlled stress. Data obtained from the two types are interchangeable. Controlled-strain regime operates by applying a sinusoidal strain to the test specimen and measuring the magnitude and phase of the resulting stress. A controlled-stress regime, applies a sinusoidally varying stress and measures the magnitude and phase of the resulting strain.



Figure 3.6 8 mm plate configuration. The upper plate oscillates alternately clockwise and counterclockwise

The dynamic shear rheometer (DSR) is perhaps misnamed. Dynamic forces are not considered; the word “dynamic” refers to the manner in which the stresses or strain applied to the test specimen. In fact DSR could be used for viscosity measurement or tests in which stiffness and other viscoelastic characteristics of the samples are

measured. Viscosity measurements re rotational tests or creep tests, they are useful method to measure long time load behaviour of the binders. The latter are named dynamic tests because the stress/strain is applied in oscillatory regime; this allow significant extension to the range of material characterization by also considerably reducing test time. In fact, the tests carried out at a certain frequency ω are qualitatively equivalent to results obtained at a testing time

$$t = 1/\omega \quad (3.4)$$

Dynamic Shear Rheometer consist of three major parts: the rheometer, the controller and the computer. The rheometer normally includes a housing or frame, a motor for applying the strain or stress to the specimen, a transducer for measuring the response of the specimen, a temperature control and measurement system. The controller is simply an interface between the rheometer and the computer and contains the data acquisition and signal conditioning hardware for the motors and transducers used in the rheometer. The rheometer is usually operated and programmed by personal computer [9].

3.3.2 Dynamic Mechanical Analysis

The rheology of bitumen can be accurately measured by dynamic mechanical analysis using oscillatory type testing. Generally conducted within the region of linear visco-elastic response. DMA allow the visco-elastic nature of bitumen to be determined over a wide range of temperatures and loading times [20].

The importance of carrying out test with variable frequency (frequency sweeps) is that her the time-dependent shear behaviour is examined. The tests carried out at a certain frequency ω , are in fact qualitatively equivalent to results obtained at testing times

$$t = 1/\omega \quad (3.4)$$

Therefore, short term behaviour is simulated by rapid movements (at high frequencies) and long term behaviour by slow movements (at low frequencies). There are two options for specifications of the number oscillations per time unit: as frequency f with the unit [Hz] or as angular frequency with unit [$1/s$].

The followings holds:

$$\omega = 2\pi f \quad (3.5)$$

The principle visco-elastic parameters that are obtained from rheological measurement, mainly with the DSR, are the complex shear modulus, G^* , and the phase angle δ .

The complex shear modulus, G^* , is defined as:

$$G^*(\omega) = \frac{\tau(\omega)}{\gamma(\omega)} \quad (3.6)$$

Where:

$\tau(\omega)$ = sinusoidal function of shear stress

$\gamma(\omega)$ = sinusoidal function of shear strain

It provides a measure of the total resistance to deformation when the bitumen is subjected to shear loading. It contains elastic as well as viscous components which are designated as the storage modulus $G'(\omega)$, and loss modulus $G''(\omega)$, respectively.

These two components are related to the complex shear modulus and to each other through the phase (or loss) angle δ which is the phase or time lag between the applied shear stress and shear strain responses during a test. The larger the phase angle δ , and so the damping factor, the more viscous the material. For purely elastic materials, the phase angle will be zero whereas for purely viscous material it will be 90° .

The complex modulus G^* can be represented also by the vector sum of the storage portion, $G'(\omega)$, of the complex shear modulus and the loss modulus, $G''(\omega)$, or also as the difference between the real part, $G'(\omega)$, and the imaginary part $G''(\omega)$:

$$G^*(i\omega) = G'(\omega) - iG''(\omega) \quad (3.7)$$

The ratio of the loss to the storage is the $\tan\delta$ and is often called damping. It is a measure of the energy dissipation of the material under cyclic load. It is a measure of how well a material can get rid of energy and is reported as the tangent of the phase angle. It indicates how good a material will be at absorbing energy. It varies with the state of the material, its temperature, and with the frequency.

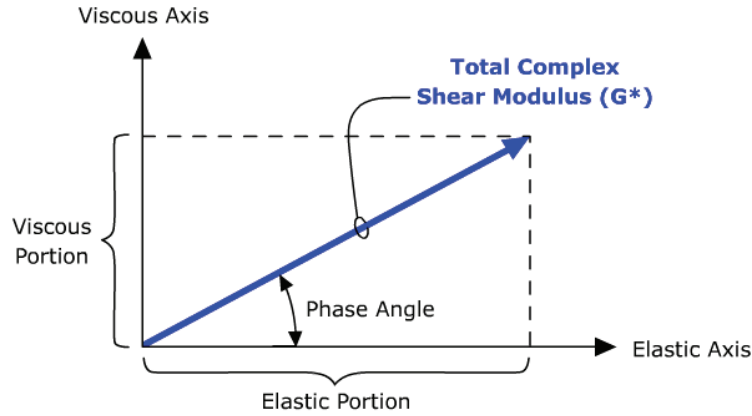


Figure 3.7 Vector form of Complex Modulus

Another function determined by performing a DMA, is the complex viscosity, η^* . Complex viscosity is frequency-dependent viscosity function and it represents the flow resistance of the sample subjected to oscillatory tests. It is defined, as a (normal) viscosity as the ratio between the shear stress and the deformation rate measure in oscillatory tests.

$$\eta^* = \frac{\tau(\omega)}{\dot{\gamma}(\omega)} \quad (3.8)$$

Also, the complex viscosity function is equal to the difference between a real part of the so-called dynamic viscosity η' , and the out-of-phase viscosity or imaginary part η'' .

The norm of the complex viscosity is related to the complex shear modulus as follows:

$$|G^*| = \omega \cdot \eta^* \quad (3.9)$$

G^* and δ are used as predictors of road pavements rutting and fatigue cracking. Early in pavement life rutting is the main concern, while later in pavement life fatigue cracking becomes the major concern.

In order to resist rutting, an asphalt binder should be stiff (it should not deform too much) and it should be elastic (it should be able to return to its original shape after load deformation). Therefore, the complex shear modulus elastic portion, $G^*/\sin\delta$ should be large. When rutting is of greatest concern (during a pavement's early and mid-life), a minimum value for the elastic component of the complex shear modulus is specified. Intuitively, the higher the G^* value, the stiffer the asphalt binder is (able to resist

deformation), and the lower the δ value, the greater the elastic portion of G^* is (able to recover its original shape after being deformed by a load). Hence the parameter $G^*/\sin\delta$ should be maximized. Therefore, minimum values for $G^*/\sin\delta$ for the DSR tests conducted on unaged binder and RTFO aged binder are specified.

In order to resist fatigue cracking, a bitumen should be elastic (able to dissipate energy by rebounding and not cracking) but not too stiff (excessively stiff substances will crack rather than deform-then-rebound). Therefore, the complex shear modulus viscous portion, $G^* \cdot \sin\delta$ should be a minimum. When fatigue cracking is of greatest concern (late in a pavement's life), a maximum value for the viscous component of the complex shear modulus is specified [2].

3.4 Bending Beam Rheometer

As surrounding temperatures drop, pavements contract and build up internal stresses. If this contraction occurs fast enough the pavement may crack because it does not have time to relax these stresses. This type of crack, typically called a “thermal crack”, or transverse crack (because of the direction of cracking in relation to the direction of traffic) can result from either of two related mechanisms:

1. *Single thermal cycle below the critical temperature.* A single severe drop in temperature that causes stress to quickly build up to a critical point that causes cracking. This is called “single-event low temperature cracking” and the particular temperature associated with these critical stresses is called the “critical temperature”.
2. *Thermal cycling above the critical temperature.* Repeated thermal contraction and expansion that occurs above the critical temperature can cause stresses to build up and eventually cause cracking [21].

The primary concern regarding this distress is the ingress of water to the pavement structure through the thermal cracks that increases the rate of stripping which leads to early deterioration of the asphalt concrete. Furthermore, water infiltration promotes pumping of unbound fines in the underlying material leading, in some cases, to a depression at the thermal crack. Finally, Fromm and Phang have postulated that an ice

lens could form beneath a thermal crack, which would cause an upward lipping or tenting of the crack edges. Additionally, there is mounting evidence that transverse cracks can act as stress focal points from which longitudinal cracks may form [22].

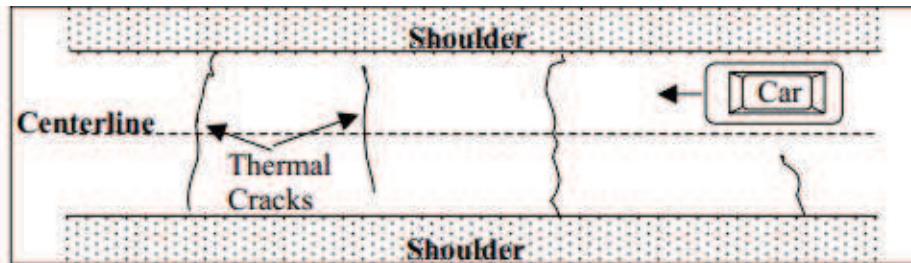


Figure 3.8 Direction of thermal cracks

The Bending Beam Rheometer (BBR) test is used to measure the low temperature stiffness and relaxation properties of asphalt binders. These parameters give an indication of an asphalt binder's ability to resist low temperature cracking. The BBR is used in combination with the DTT to determine an asphalt binder's low temperature PG grade. As with other Superpave binder tests, the actual temperatures anticipated in the area where the asphalt binder will be placed determine the test temperatures used.



Figure 3.9 Bending Beam Rheometer

Because low temperature cracking is a phenomenon found mostly in older pavements, the test is run on the long-term aged residue from the PAV.

The standard BBR test are AASHTO T 313 (Determining the Flexural Creep Stiffness of Asphalt Binder Using the Bending Beam Rheometer) and AASHTO PP 42 (Determination of Low-Temperature Performance Grade (PG) of Asphalt Binders) that is involved in the Superpave specification.

A sample of asphalt binder is heated, stirred to remove air bubbles and then poured into two aluminum BBR molds measuring 6.25 x 12.5 x 127 mm (Figure 3.8). Molds are allowed to cool for 45 to 60 minutes at room temperature, then by using a hot spatula the top of the sample is trimmed. To demold samples, they are immersed in an ice bath or freezer at -5°C for 5 to 10 minutes, just long enough that the beam can be easily removed from the mold without damaging it. Before the test, samples are conditioned for one hour into the testing fluid bath at the test temperature, in order that no gradient of heat are present in its inside. The sample is then simply place on supports at two points 102 mm apart in a controlled temperature fluid bath (suitable fluids are ethanol, methanol and glycol-methanol mixtures). A load of 100 g at the midpoint is applied that, under normal gravity conditions, produces 0.980 N of force.



Figure 3.10 BBR mould and demolded sample

The BBR test has been done on three beam samples. The reason is that sample preparations are not so easy and the risk to damage the sample before starting the test has to be taken into account. All testing should be completed within four hours and time restrictions need to be exactly followed, in order to ensure that the measured stiffness is the effective value at the test temperature.

Data, are measured at 8, 15, 30, 60, 120 and 240 seconds. These times were chosen because they are about equally spaced on a logarithmic time scale.

Two are the parameters of interest:

- the creep stiffness $S(t)$;
- the m-value: slope of the stiffness curve plotted versus the logarithm of time. It is a measure of the rate at which the asphalt binder relieves stress through plastic flow.

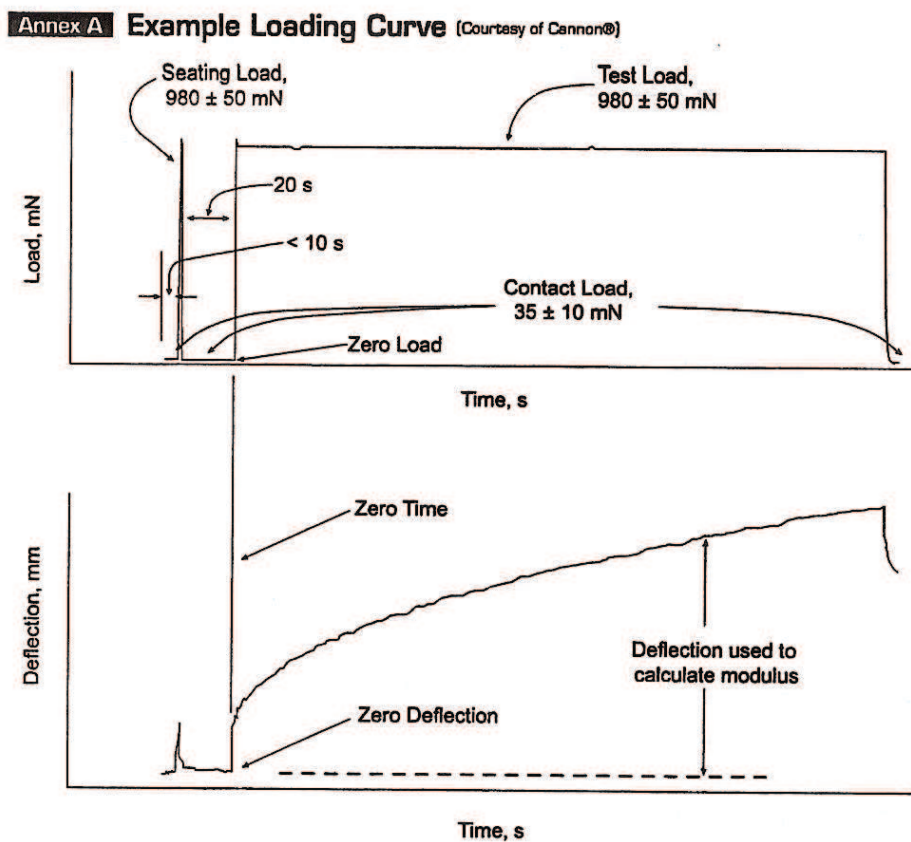


Figure 3.11 Graphs plotted during the test

The software provide in real time the graph of the load applied versus time and the plot of the deflection versus time. An example is shown in the figure above.

Creep stiffness is calculated using standard beam theory. The equation used is:

$$S(t) = A + B \log(t) + C [\log(t)]^2 \quad (3.10)$$

Where:

$S(t)$ = asphalt binder stiffness at a specific time

P = applied constant load (100 g or 0.98 N)

L = distance between beam supports (102 mm)

b = beam width (12.5 mm)

h = beam thickness (6.25 mm)

$\delta(t)$ = deflection at a specific time

A, B, C = empirically determined constants

This equation is the standard beam equation used for determining deflection with the stiffness and deflection terms switched. In a viscoelastic material such as bitumen the stiffness and resulting deflection are time dependent, thus they are both written as a function of time [21].

3.5 Dynamic Contact Angle (DCA)

A dynamic contact angle analyser (Wilhelmy plate device) is used to measure the contact angle of probe liquid with the bitumen under dynamic conditions. A clean glass slide is coated with the bitumen to be tested and hung from the balance of the equipment with the help of a crocodile clip. The thickness of the bitumen film must be uniform and thin. In fact, in this study, a correlation between the thickness and the contact angles obtained arose using some liquids.

A beaker containing the test liquid is placed under the glass slide. The bottom edge of the slide should be kept as parallel as possible with the surface of the probe liquid. The slide is immersed and then withdrawn from the liquid at a constant speed (figure 3.11) and the force involved is continuously measured (figure 3.12).

The value of the force applied during the immersion and withdrawal process is measured from the automatically controlled DCA analyzer balance.

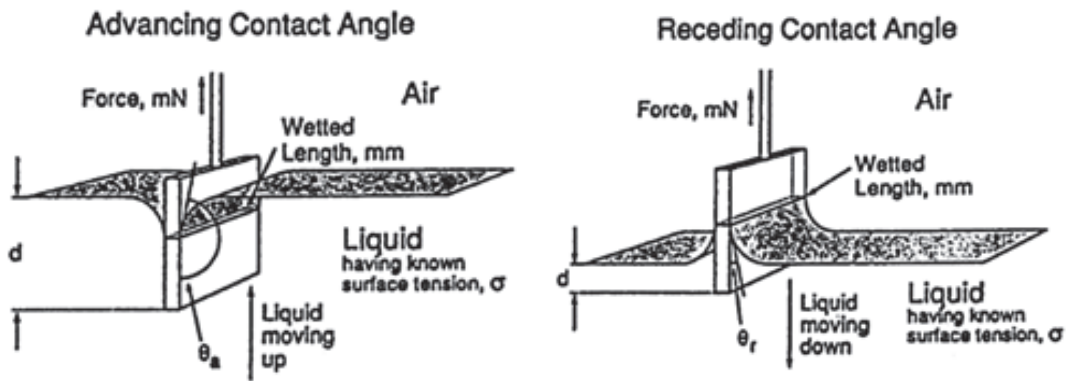


Figure 3.12 Immersion and withdrawn of the glass slide

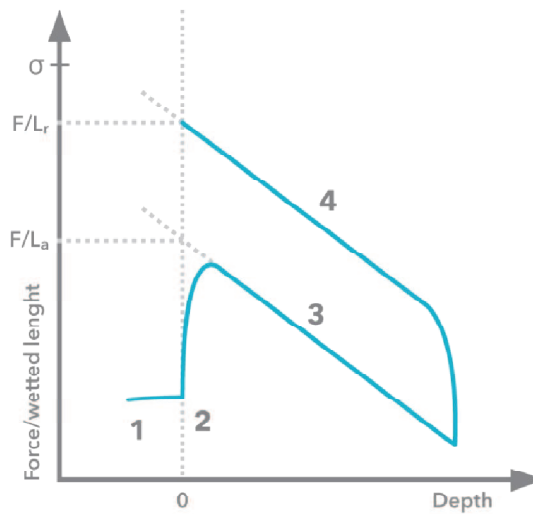


Figure 3.13 Force involved plotted versus depth of immersion

Therefore, unlike the goniometer that provide static and hence directly measure of the angle, the Wilhelmy plate device provides an indirect measure of the contact angle by using the following formula:

Where:

= difference between weight of plate in air an partially submerged in probe liquid

= volume of solid immersed in the liquid

ρ_L = density of the liquid

ρ_{air} = air density

g = gravitational force

P_t = perimeter of the bitumen coated slide

γ_L = total surface energy of the probe liquid

During dynamic contact angle analysis the advancing contact angle is measured when the bitumen coated slide is immersed in the probe liquid while the receding contact angle is measured when the slide is taken out from the liquid. The advancing contact angle values are always higher than the receding ones. The main reason for this hysteresis is the microscopic chemical heterogeneity of the solid (bitumen) surface. The other reason could be that the probe liquid has already wetted the surface of the bitumen during the advancing movement, hence resulting in reduction of the receding contact angle values. This is especially true when the binder samples are tested with a non polar (diiodomethane) liquid. It appears that diiodomethane starts dissolving the binder sample during the receding movement of the slide, as by that time the sample is in the liquid for quite a while. This means that receding contact angle values obtained with diiodomethane could be quite inaccurate. For the above mentioned reasons the advancing contact angle values are only used for the calculation of surface energy parameters of bitumen [15].

3.6 Dynamic Vapour Sorption-DVS Technique

This test is used in order to determine the surface energy parameters of aggregates. In chapter 2 we discussed about the the wettability and the contact angle technique for calculating the surface energy components of bitumens. Unfortunately, it is difficult to use the contact angle technique on high surface energy materials like aggregates (with surface energy values generally $> 60 \text{ mJ/m}^2$) as the liquids readily spread on high energy surfaces and it is difficult to obtain correct angle values. Vapour sorption

techniques are normally used for high surface energy materials. The DVS Advantage is designed to accurately measure a sample's change in mass as it sorbs precisely controlled concentrations of Probe vapours with known surface energy components with the help of an inert carrier gas (dry nitrogen is normally used). The sample is hung from a microbalance in a sample pan (an empty pan is usually hung on the other side of the balance as a 'reference'). Air carrying the test vapours is then passed over the sample at a well-defined flowrate and temperature. The sample mass readings from the microbalance then reveal the vapour adsorption/desorption behaviour of the sample.

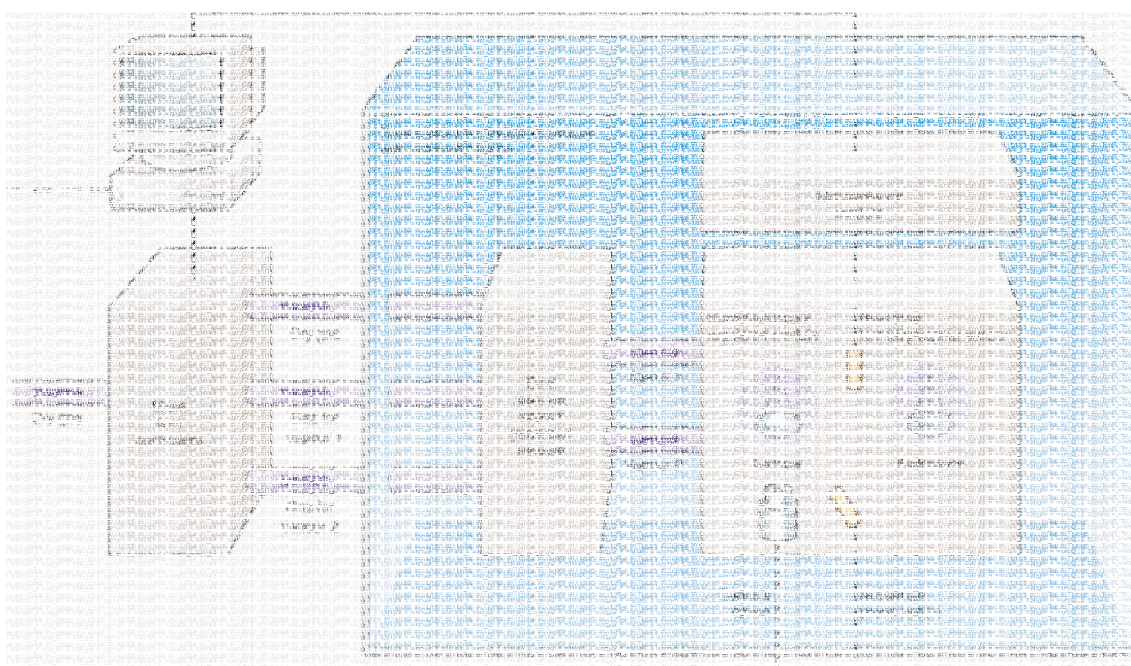


Figure 3.14 DVS-Advantage Schematic

On the basis of the surface characteristics of the aggregate, vapour probes get adsorbed at their surfaces which results in an increase in the mass of the aggregate sample. This technique is termed as gravimetric adsorption technique. The vapour mass adsorbed on the aggregate surface is measured for each solvent with the help of a sensitive balance. The probe liquids that have been used for the DVS testing are octane, ethyl acetate and chloroform.

The aggregates to be tested are first washed with deionised water and then dried in an oven. Aggregate fraction passing 5mm and retained on 2.36mm is generally used for the tests however, smaller size fraction can also be used. The upper limit on aggregate size

is because of the material holding capacity of the sample chamber. The probe liquid vapours are passed through the aggregate. The balance measures the quantity of solvent adsorbed onto the surface of the aggregates chamber. This method is comparatively suitable because it considers the irregularity in shape, and surface texture of the aggregates [23].

An adsorption isotherm is plotted between the partial vapour pressure of the probe vapour at x-axis and the adsorbed mass at y-axis, which is then used to calculate the spreading pressure and the specific surface area of the solid. Lots of graph can be plotted by analysing the data (for further specifications see chapter 5).

Here, the term adsorption means the adhesion of the vapour molecules on the surface of the aggregate and the specific surface area refers to the surface area per unit mass of the solid. The specific surface area of the solid is determined by using the Brunauer-Emmett-Teller (BET) approach and is given by equation (3.12)

$$A = \left(\frac{n_m N_0}{M} \right) \alpha \quad (3.12)$$

where:

A = specific surface area of solid, m^2

n_m = monolayer specific amount of vapour adsorbed on the surface of aggregate, mg
(monolayer capacity of the adsorbed solute on the adsorbent)

N_0 = Avogadro's number, $6.022 \times 10^{23} \text{ mol}^{-1}$

M = molecular weight of the vapour, g/mol

α = projected or cross-sectional area of the vapour single molecule, m^2

The number of vapour molecules adsorbed and required to form a monolayer on the solid surface is determined by using the Langmuir approach and is given by equation 3.13.

$$\frac{P}{n(P_0 - P)} = \left(\frac{c - 1}{n_m c} \right) \frac{P}{P_0} + \frac{1}{n_m c} \quad (3.13)$$

where:

P = partial vapour pressure, [Pa]

P_0 = saturated vapour pressure of solvent, [Pa]

n = specific amount adsorbed on the surface of the adsorbent, [mg]

c = BET constant (parameter theoretically related to the net molar enthalpy of the adsorption)

Adsorption of vapour molecules on the aggregate surface reduces its surface energy. So, spreading pressure as a result of adsorption of the vapour molecules can be expressed as:

$$\pi_e = \gamma_S - \gamma_{SV} \quad (3.14)$$

where:

π_e spreading pressure at maximum saturated vapour pressure or equilibrium spreading pressure, [ergs/cm²]

γ_S = aggregate surface energy in vacuum

γ_{SV} = aggregate surface energy after exposure to vapour

Spreading pressure at maximum saturation vapour pressure, π_e for each solvent, is calculated by using the following Gibbs free energy equation:

$$\pi_e = \frac{RT}{A} \int_0^{P_0} \frac{n}{P} dP \quad (3.15)$$

where:

R = universal gas constant, 83.14 cm³ bar/mol.K

T = absolute temperature, K

By introducing spreading pressure, π_e , in Young-Dupres's relation, Equation (2.8), the following relationship is obtained:

$$W_{SL} = \pi_e + \gamma_{LV}(1 + \cos \theta) \quad (3.16)$$

As mentioned earlier, the contact angle value for high energy solids is zero, Equation (3.16) can be re-written as:

$$W_{SL} = \pi_e + 2\gamma_{LV} \quad (3.17)$$

By substituting the above relation in Equation (2.17), the following equation is obtained;

$$2\gamma_L + \pi_e = 2\sqrt{\gamma_S^{LW}\gamma_L^{LW}} + 2\sqrt{\gamma_S^+\gamma_L^-} + 2\sqrt{\gamma_S^-\gamma_L^+} \quad (3.18)$$

Spreading pressures from three different probe vapours are measured in order to get the three surface energy components of the solid. It can be seen that irrespective of the test method, the basic principle of calculation of surface energy components is the same [15].

CHAPTER 4

THE RHEOLOGY RESEARCH

4.1 Introduction

In this chapter all the results of the performed rheological investigation will be shown. This research has the aim of understanding the mechanical properties of the three bitumens, fully characterizing them for use in Hot Mix Asphalts pavements.

In order to do undertake the research, Superpave procedures have been followed. These tests and specifications are specifically designed to address HMA pavement performance parameters such as rutting, fatigue cracking and thermal cracking. As well known, all tests need to be performed on both the unaged binders, as well as on the “RTFOT” aged and on the “PAV” aged. After having aged the bitumens, Dynamic Shear Rheometer (DSR) was used, in order to obtain fundamental characteristics (for example, the complex modulus and the phase angle to name a few), over frequencies ranging from 0.1 Hz to 10 Hz. Subsequently, using the time superposition template, mastercurves have been plotted. They serve to compare the above mentioned characteristics of the three binder over a frequency range bigger than that tested. Furthermore raw data have been used to plot many graphs, useful to compare the binders properties at constant temperature or frequency. By analysing some parameters from DSR tests, the temperatures at which carry out the BBR have been chosen. This last test has been very helpful in understanding the effect of the wax on the low temperature behaviour of the binder.

After having results from DSR and BBR it was possible to find out the performance grade of the three binder i.e. the range of temperatures at which this binder can be used ensuring the prescribed performance. The materials analyzed are:

- A API neat bitumen 70 – 100 dmm (12360)
- The above bitumen modified with a 2% in weight with Adriamont wax (12361)
- The same neat bitumen 70 – 100 dmm modified with a 2% in weight with Sasobit wax (12362)

4.2 Dynamic Shear Rheometer test

4.2.1 Setting of the test and specimen preparation

This test is able to provide an extremely accurate characterization of bituminous binders and their visco-elastic properties within the whole range of service temperatures.

A Bohlin CVO rheometer, produced by Malvern, has been used (figure 4.1).



Figure 4.1 Bohlin CVO rheometer

In chapter one we talked about the visco-elastic behaviour of the bitumen and we mentioned the simple linear stress-strain relationship. Normally, due to the extreme difficulties in characterizing the non-linear response, the bitumen is tested within the linearity range (LVE). Hence, linear methods of characterizations and analysis are considered more than adequate for engineering design problems [9], greatly simplifying the physical behaviour of bituminous binders.

Having said this, the first step has been to define the linear limit for each sample performing amplitude sweep tests. As suggested by the name, in these tests the shear strain has been increased from 0.1 % to 100 %, at the constant frequency of 1.59 Hz, measuring the parameters of interest 20 times during the test. SHRP program indicated the limit of linear viscoelastic behaviour as the point beyond which the measured value of the complex modulus decreases to 95 % of its zero-strain value (figure 4.2). The

corresponding value of strain will be imposed as a limit not to be exceeded in further frequency sweep tests.

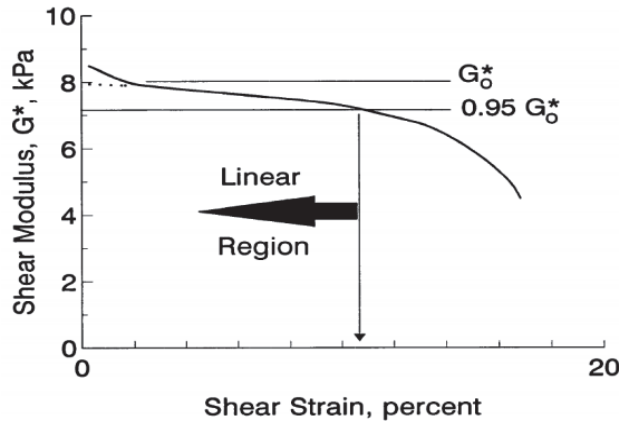


Figure 4.2 Criterion for the determination of the LVE

STRAIN LINEAR VISCOELASTIC LIMIT [%]									
Bitumen	10 °C			25 °C			50 °C		
	UNAGED	RTFOT	PAV	UNAGED	RTFOT	PAV	UNAGED	RTFOT	PAV
12-360 Base Binder	0.25	2.76	0.63	6.74			34.00	34.46	3.87
12-361 Adriamont	1.08	0.12	0.43	1.87			1.29		5.40
12-362 Sasobit	0.23	1.31	0.63	1.30			0.36	5.57	

Table 4.1 Amplitude sweep test. Strain corresponding to the LVE

LINEAR VISCOELASTIC LIMIT [Pa]									
Bitumen	10 °C			25 °C			50 °C		
	UNAGED	RTFOT	PAV	UNAGED	RTFOT	PAV	UNAGED	RTFOT	PAV
12-360 Base Binder	1.09E+07	1.52E+07	2.77E+07	4.82E+05			1.38E+04	2.56E+04	2.20E+05
12-361 Adriamont	1.42E+07	1.07E+07	3.49E+07	1.69E+06			2.89E+04		2.40E+05
12-362 Sasobit	1.85E+07	1.47E+07	3.71E+07	1.88E+06			4.92E+04	4.66E+04	

Table 4.2 Amplitude sweep test. Complex modulus corresponding to the 95% of the initial value

Conservatively, after amplitude sweeps tests, a limit of 0.10 % of strain for 8 mm plate tests and a limit of 0.50% of strain for the 25 mm have been imposed.

Once the linear viscoelastic limit was known, frequency sweeps were made.

Before testing a material it is good practice to prepare some vials; the reason is that as the binder need to be heated for pouring, using a vial at a time the ageing is reduced.

Samples have been prepared with two different methods:

- Hot-pour method for 25 mm plate: the binder is annealed until it is fluid enough to be poured directly on the lower plate of the DSR.
- Silicone mould method: hot binder is poured on 8 mm silicon mould of height approximately 1.5 times the testing gap. Once the binder is cooled , the disc is removed and centred on the lower plate of the DSR.. This method is the simplest way to prepare the 8 mm sample, but many researcher think the mould could affect the measure [2].

In both cases trimming is necessary to obtain the desirable sample dimension. Excessive or untrimmed material can cause errors in measurements so both under and over trimming are to be avoided.

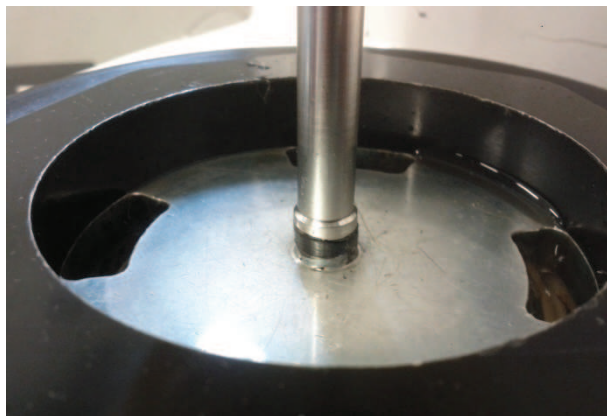


Figure 4.3 Sample ready to be tested with 8 mm plate after trimming operation

According to SHRP report 730, two plates have been used for tests: 8 mm diameter plate with a gap of 2 mm at intermediate pavement design temperatures, 0 to 40°C, and 25 mm diameter plate with a gap of 1 mm at the maximum pavement design

temperatures, ranging from 40°C to 80°C. It is recommended that there should be an overlap of rheological testing with two disk and gap configurations being used at the transition points [20].

After the sample has been poured, the Bohlin software is launched. Figure 4.3 shows the window of the program with parameters used: it is possible to choose the range of frequency at which to stress the sample, the number of frequencies (number of samples) and the degree of increase (linear or logarithmic). Furthermore it is possible to select the type of stress (stress proportional to frequency, controlled stress and auto-stress), its direction (from the lower to the upper or vice-versa) and the strain to apply to the sample (a value that must be lower than the linear viscoelastic limit). Using the auto-stress type, the stress is automatically calculated in such a way the strain is equal to the inserted value; obviously it will vary depending on the stiffness of the material under test.

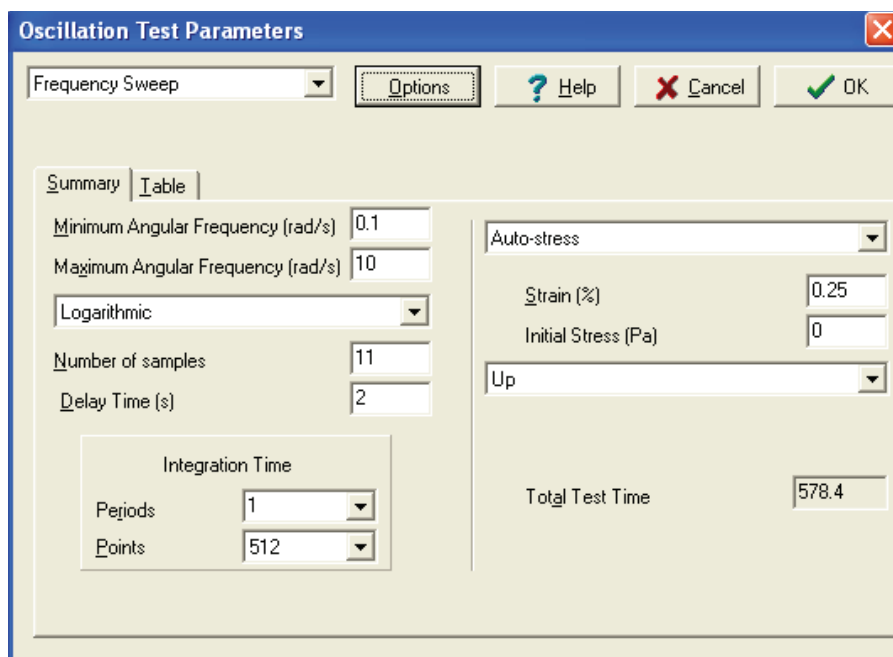


Figure 4.4 Oscillation Test Parameters window of Bohlin software

The last step before running the test is to decide the temperatures at which conduct the test and the thermal equilibrium time. All tests have been conducted within a range of temperatures from 10 °C to 80 °C with a progression of 5°C. With the intention of ensuring that the temperature of the binder be as uniform as possible (it should be

within ± 0.1 °C throughout the conditioning period and throughout the test) a thermal equilibrium time of 900 seconds has always been chosen. Hence, after having made a test at a defined temperature, the machine will increase the temperature and will condition the sample for 15 minutes, ensuring the bitumen is at the same temperature in all its parts.

4.2.2 Data analysis and representation

Dynamic Shear Rheometer returns a large number of parameters. They can be singularly used to satisfy SHRP requirements, or plotted to understand the tendency over a range of temperatures or frequencies.

4.2.3 Mastercurves

The results of the frequency sweeps at different temperatures are represented by a series of isothermal curves which show the variability of the parameter of interest with the frequency. Master curves are probably one of the primary analytical techniques to analyse cyclic mechanical data. They represent the viscoelastic behaviour of a bituminous binder at a given temperature for a large range of frequencies, bigger than that tested. This representation is based on the on the Time Temperature Superposition Principle (TTSP), which mathematically is an application of Boltzmann's superposition principle. TTSP (figure 4.5) states that the effects of time and temperature are related i.e. that response of the binders at high temperatures are related to their low frequency (time) behaviour and viceversa.

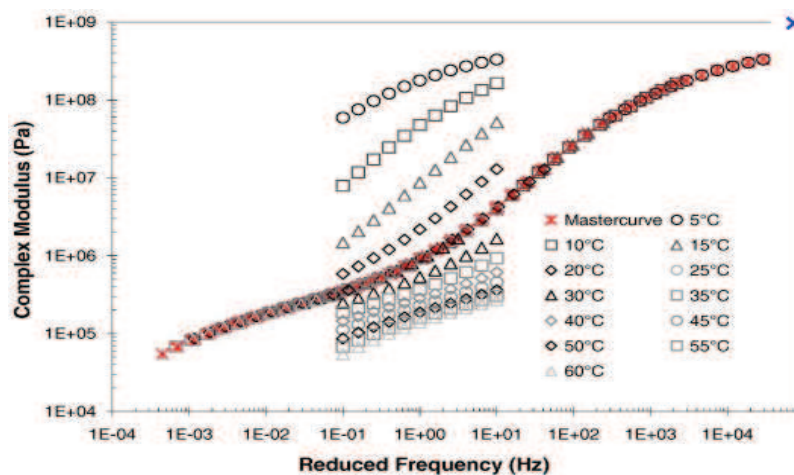


Figure 4.5 Time-Temperature Superposition Principle

Then subjecting to test a sample at high frequencies is somewhat equal to subject it to low temperatures. In this way a mastercurve is obtained by shifting each of the isotherms until they lie on the same plane as the curve at a reference temperature. Viscosity-temperature equations are used to characterise the temperature dependency of the binder, and therefore determine the shift factors needed.

Shift factors have been obtained regressing and forcing to fit two predetermined function. The first one is the William Landel and Ferry (WLF) equation, originally created for the free volume theory:

$$\log a_T = \log \frac{\eta(T)}{\eta(T_R)} = \frac{-C_1 \cdot (T - T_R)}{C_2 + (T - T_R)}$$

Where:

a_T = horizontal shift factor at temperature T

$\eta(T)$ = Newtonian viscosity at temperature T

$\eta(T_R)$ = Newtonian viscosity at temperature T_R

C_1, C_2 = empirical determined coefficients to fit the values of a_T

The second equation was formulated by Arrhenius, and as the above equation, provides a relation between the shift factors and the temperature.

$$\log a_T = \frac{\Delta H}{2.303 \cdot R} \cdot \left(\frac{1}{T} - \frac{1}{T_R} \right)$$

Where:

a_T = horizontal shift factor at temperature T

ΔH = activation energy, usually 250 kJ/mol

R = universal gas constant [8.314 J/°K-mol]

T, T_R = respectively temperature and reference temperature [°C]

The Arrhenius expression or function is useful for low viscosity liquids and polymer melts in the range $T > T_g + 100K$, where T_g is the glass-transition temperature i.e. the temperature at which a reversible transition from a hard and relatively brittle state into a molten or rubber-like state happens. Considering that T_g of bitumen is around -20°C and that the range of the isotherms to be shifted go from $10\text{-}80^\circ\text{C}$ in our case, WLF equation is probably the most suitable method. The software automatically fit the parameters in order to satisfy both the equations (figure 4.5) [2].

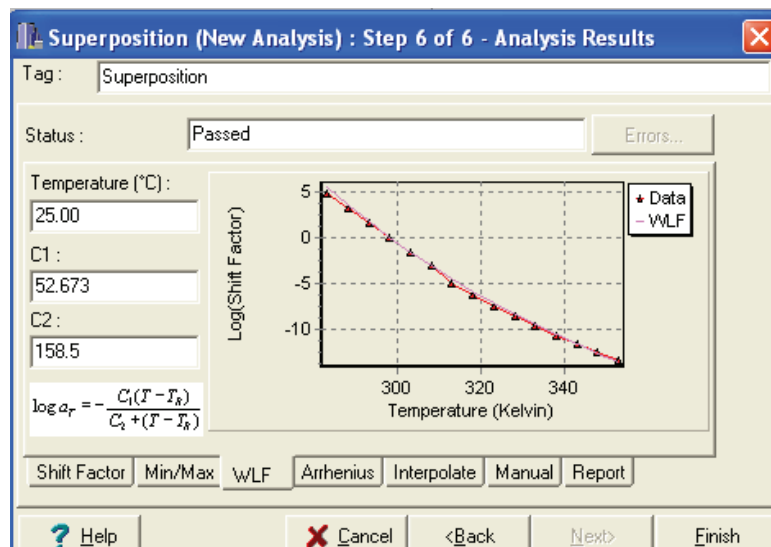


Figure 4.6 Williams Landel and Ferry interpolation

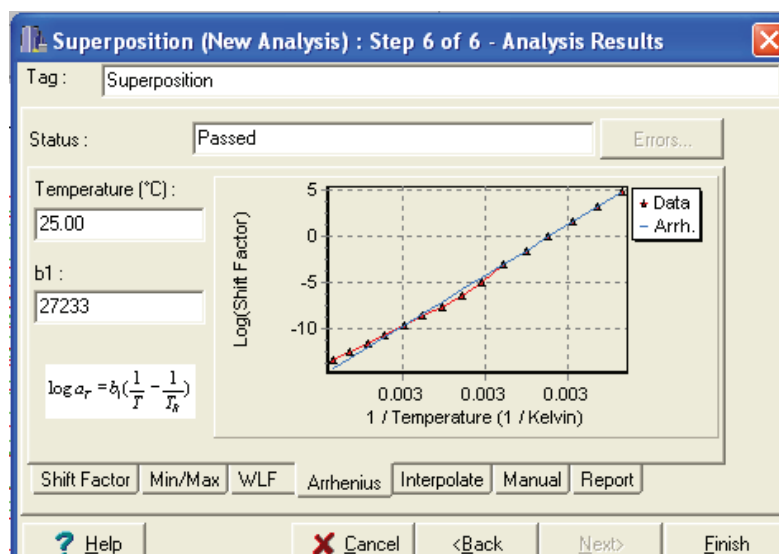


Figure 4.7 Arrhenius interpolation

Once shift factors have been determined, the software returns a table with the shifted frequencies and the corresponding parameters of interest. By exporting these values in Excel it was possible to build the mastercurves, starting from the Complex Modulus:

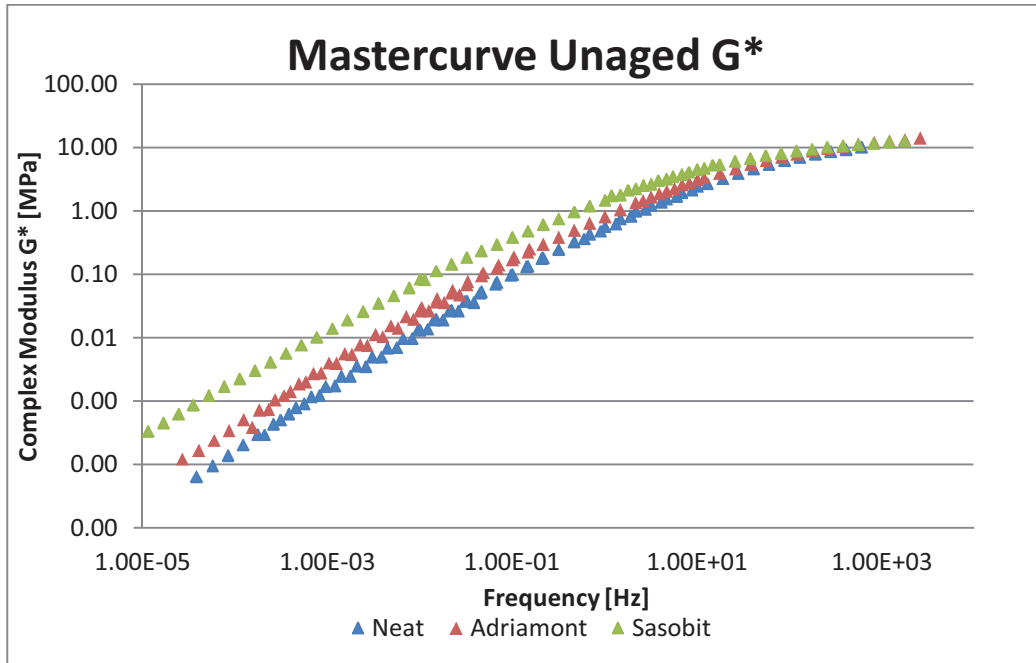


Figure 4.8 Comparison of Unaged Binder Mastercurves for Complex Modulus

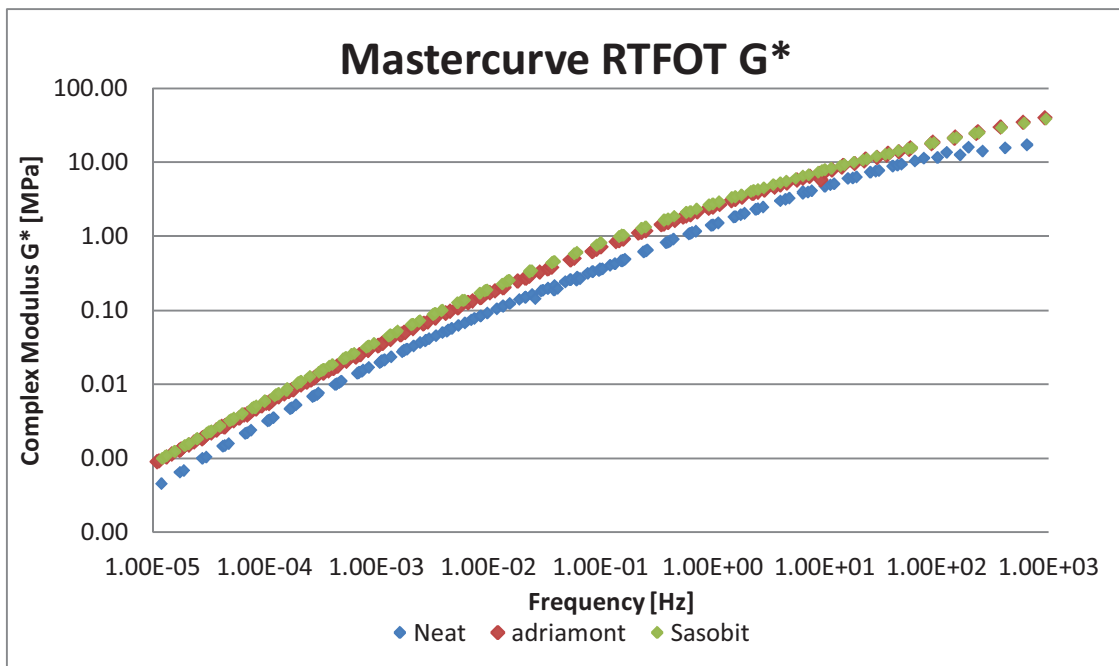


Figure 4.9 Comparison of RTFOT Binder Mastercurves for Complex Modulus

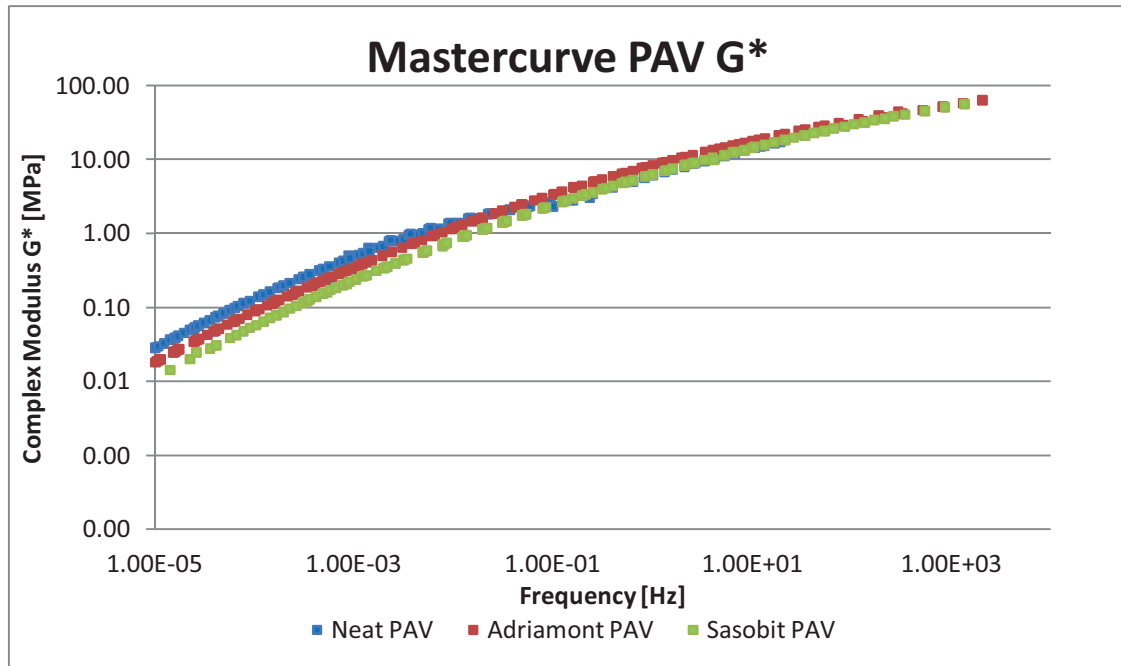


Figure 4.10 Comparison of PAV Binder Mastercurves for Complex Modulus

The unaged mastercurve highlights the effect of waxes that increase the complex modulus.

In the RTFOT graph, the curves are virtually parallel, with the curves of wax-modified asphalt binder slightly above that of base binder. However, many studies underline the inadequacy of the RTFOT methods with wax-modified binders. The researchers suspect that the wax, by lowering the viscosity, makes the bitumen more exposed to air flow, and hence it is subjected to a greater aging.

In the mastercurves obtained from testing the binder after PAV ageing, it is possible to observe that, particularly at low frequencies (high temperatures), the complex modulus of the base binder is greater than those of the wax-modified binders. The values are inverted compared to the unaged curves. This means that the base binder has undergone a greater aging compared to the wax-modified.

The three levels of Mastercurves (Unaged, after RTFOT, after PAV) are plotted in a single graph (figure 4.11) in order to have an idea of the differences of the Complex Modulus at each stage.

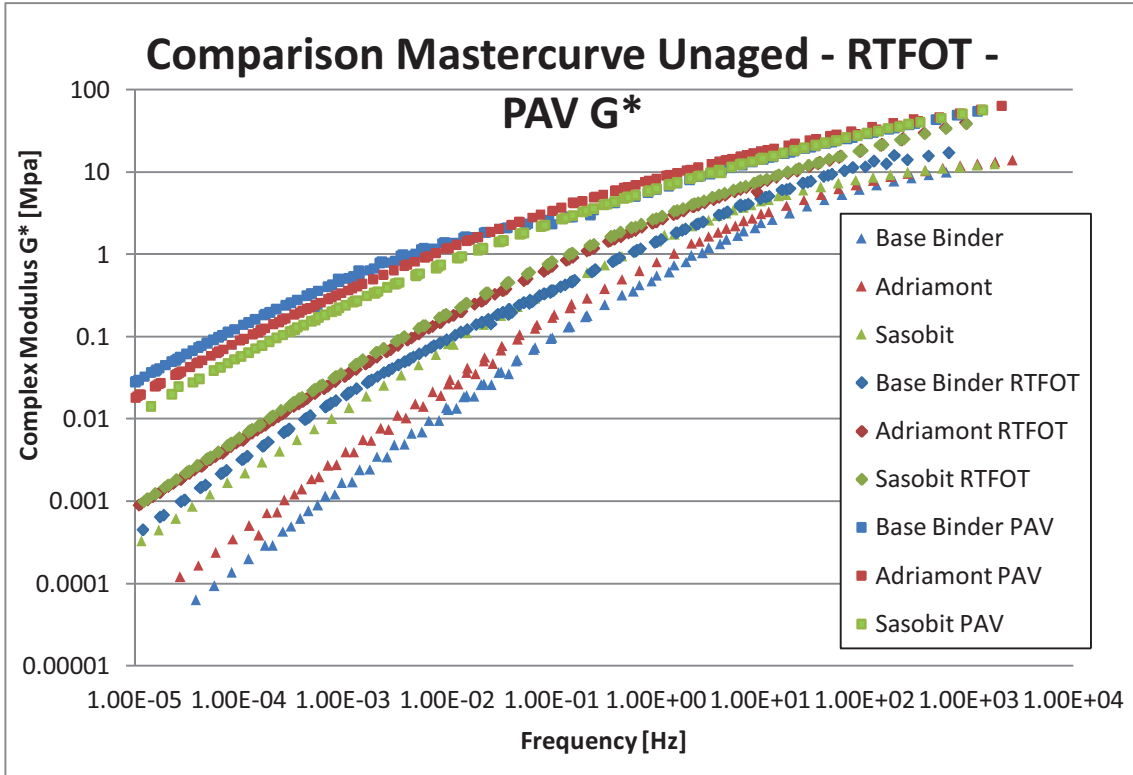


Figure 4.11 Comparison of the three level of aging Mastercurves for Complex Modulus

The next three pictures however, show the trend of phase angle δ , a measure of the degree of elasticity of the bitumen. The phase angle is determined from the time lag between the induced shear strain and the required shear stress in a controlled strain test.

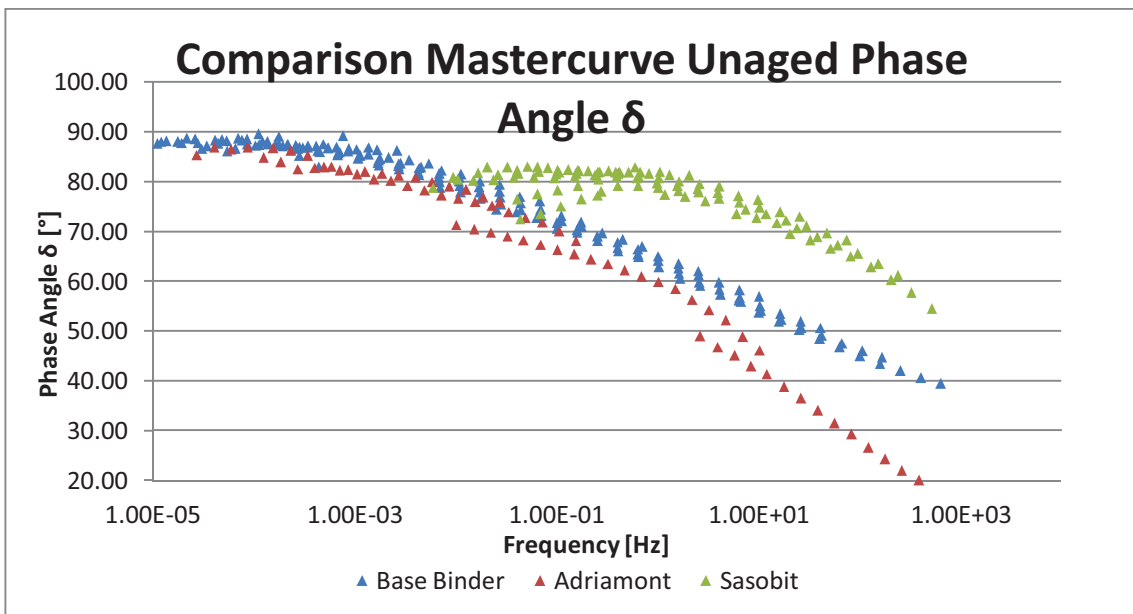


Figure 4.12 Comparison of Unaged Binder Mastercurves for Phase Angle

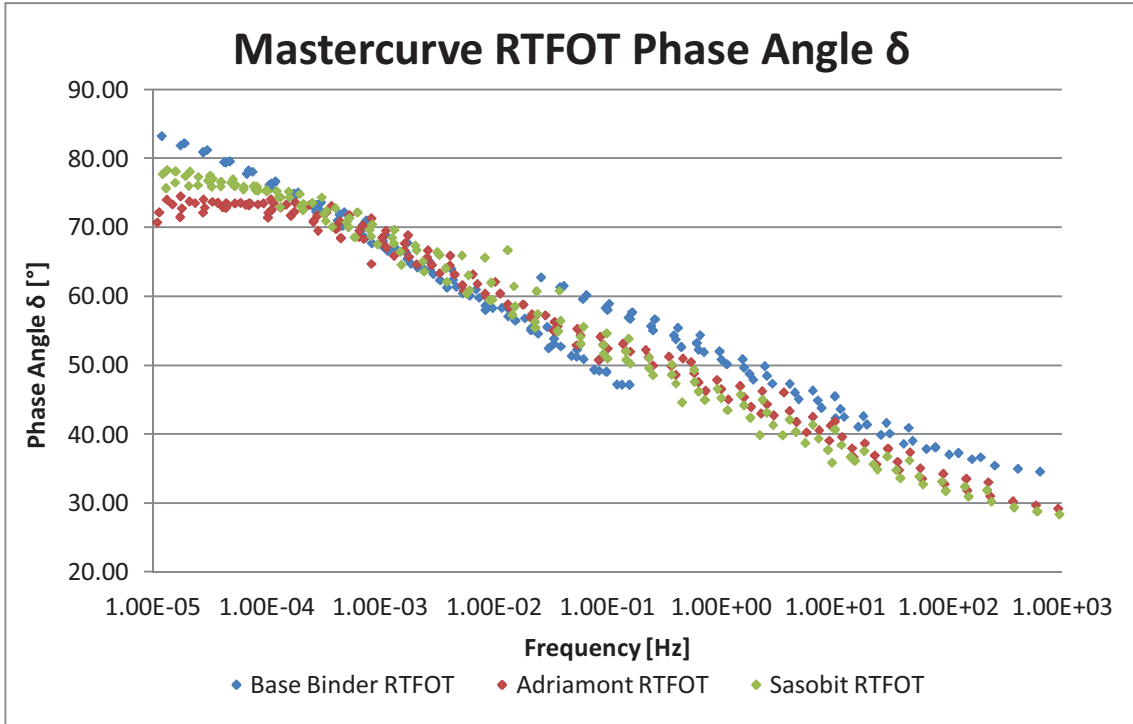


Figure 4.13 Comparison of RTFOT Binder Mastercurves for Phase Angle

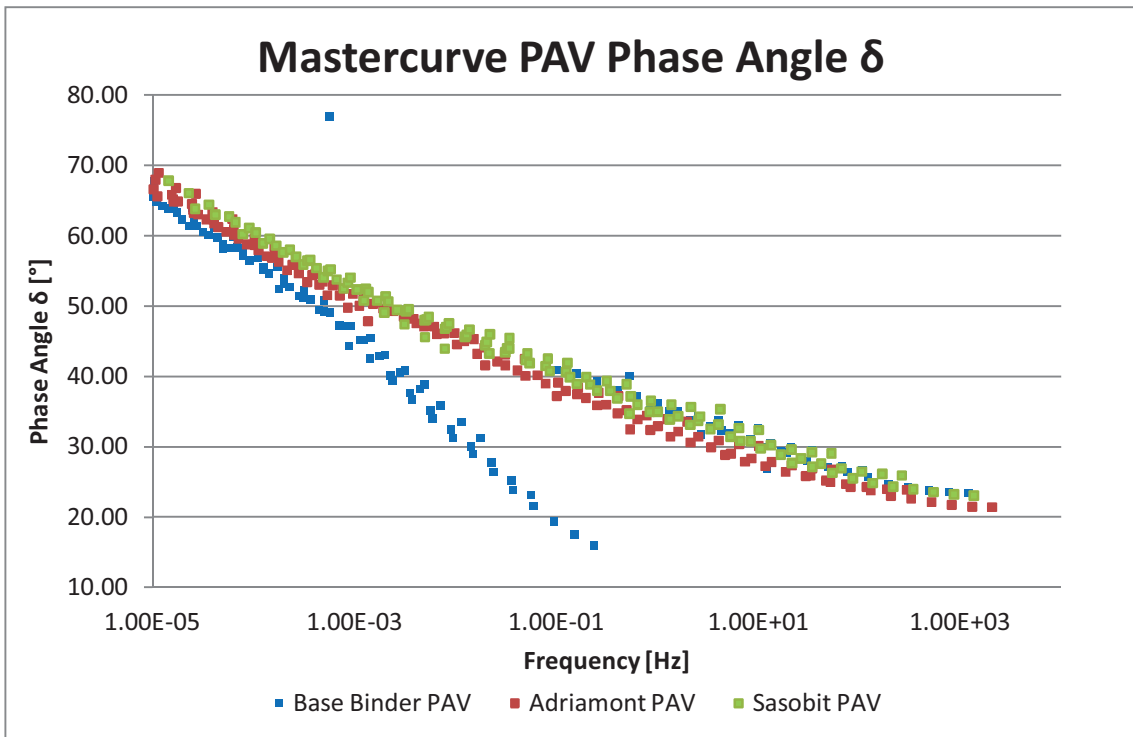


Figure 4.14 Comparison of PAV Binder Mastercurves for Phase Angle

4.2.4 Isochronal Plots

An isochronal plot is an equation, or a curve on a graph, which represents the relation of the viscoelastic parameters with temperatures at constant frequency. Isochronal plots are really useful to show the temperature susceptibility of a bituminous binder. For this analysis, the values are calculated at the frequency of 1,59 Hz, i.e. 10 rad/s. [2].

The following three figures represent a comparison of the Isochronal plot at each aging stage for a single binder.

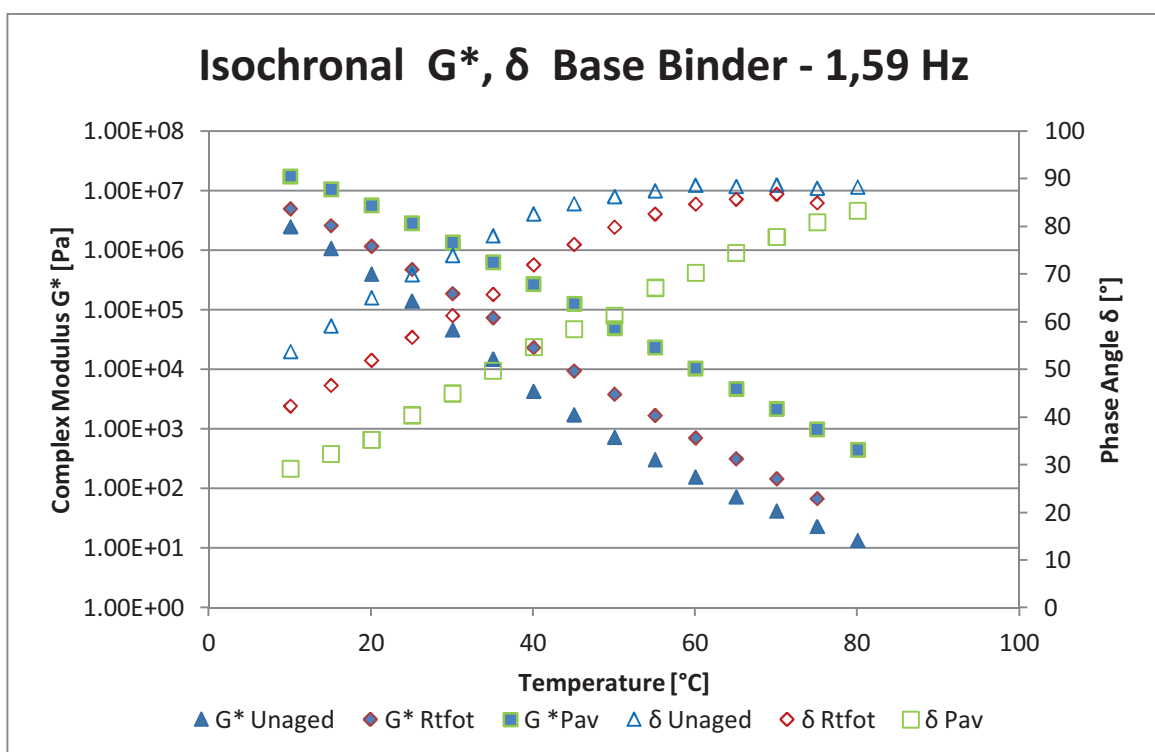


Figure 4.15 Base Binder Isochronal plot of G^* and δ at 10 rad/s

The effect of oxidative aging is seen as a constant increase in G^* and decrease in δ . Figure 4.15 shows that, for the base binder, the largest contribution to the increase of G^* is given by the PAV. The PAV phase angle trend is linear through the whole range of temperatures, while that of Unaged and of RTFOT decrease in slope at high temperature. Consequently the phase angle tends to the value of roughly 85 ° at the temperature of 80 °C at which the viscous behaviour is predominant.

The same trend can be observed in the Adriamont isochronal plot even though the RTFOT aging has led to a bigger increase in G^* compared to the previous case and the slope of the phase angle start to decrease earlier (figure 4.16)

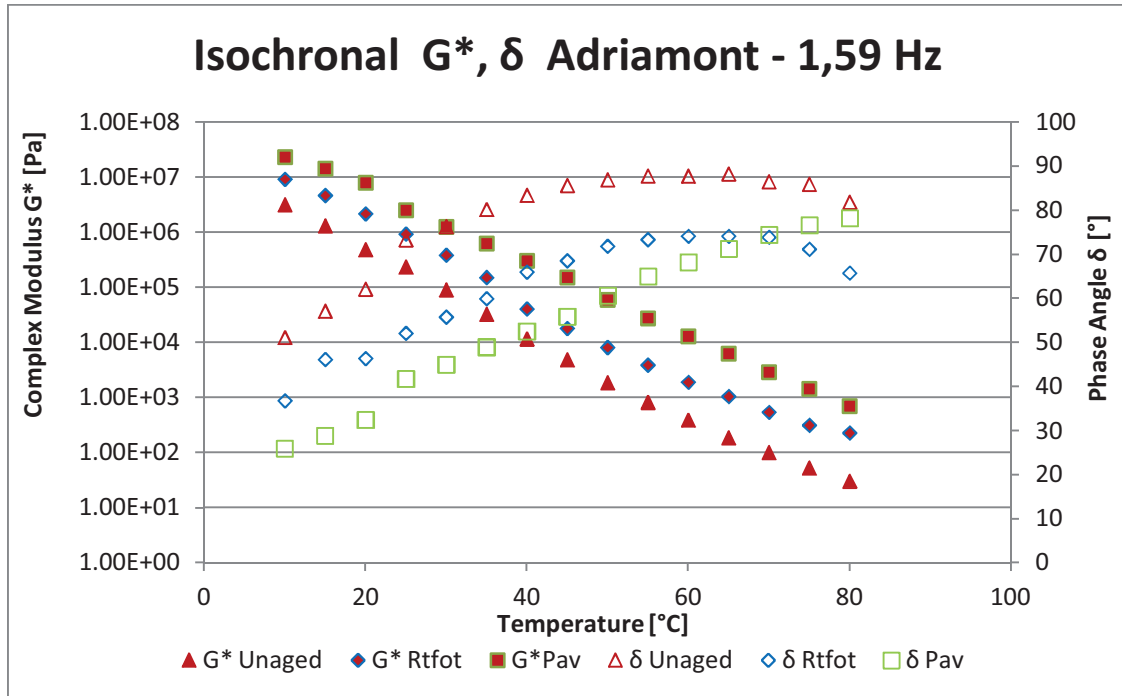


Figure 4.16 Adriamont Isochronal plot of G^* and δ at 10 rad/s

Sasobit isochronal shows the smallest increase in Complex Modulus. Compared to the other binders, the difference between the complex modulus before and after the RTFOT is minor. The phase angle tends to a unique value, less than that of base binder, at a temperature below the 80 Celsius degrees. Furthermore, by comparing figure 4.15 with figure 4.11, it can be confirmed that the base binder undergoes the highest aging.

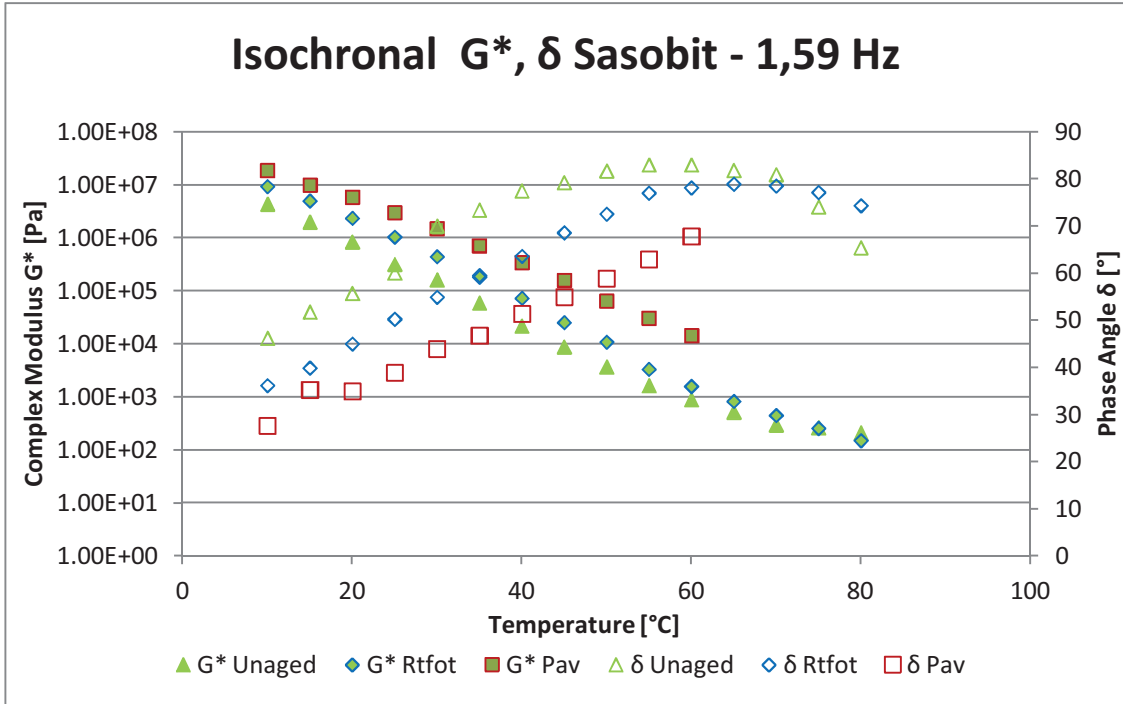


Figure 4.17 Sasobit Isochronal plot of G^* and δ at 10 rad/s

The following three figures offer a comparison of the Isochronal plot at the same aging stage for both the binders.

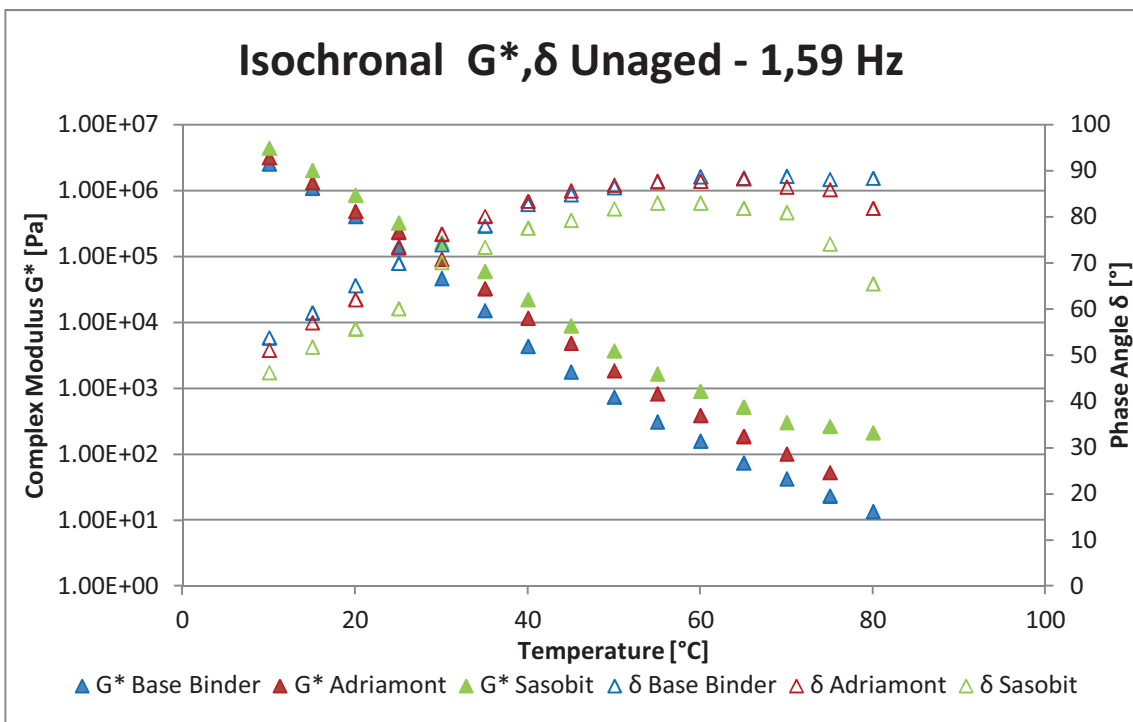


Figure 4.18 Unaged Isochronal plot of G^* and δ at 10 rad/s

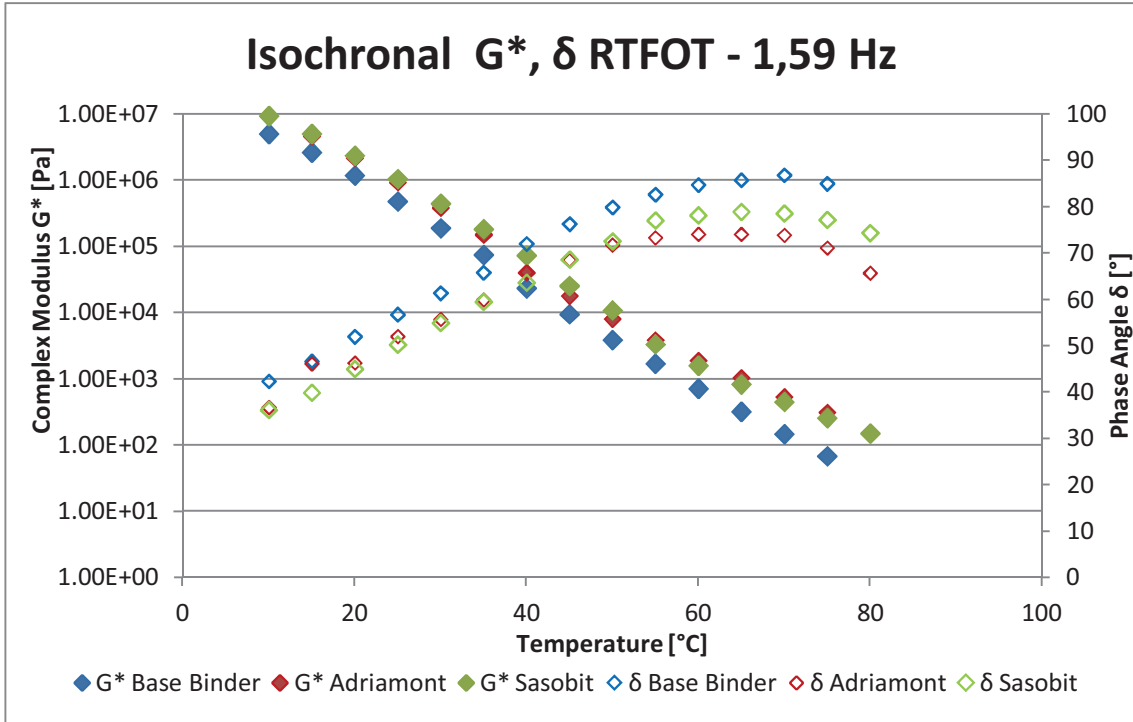


Figure 4.19 RTFOT Isochronal plot of G^* and δ at 10 rad/s

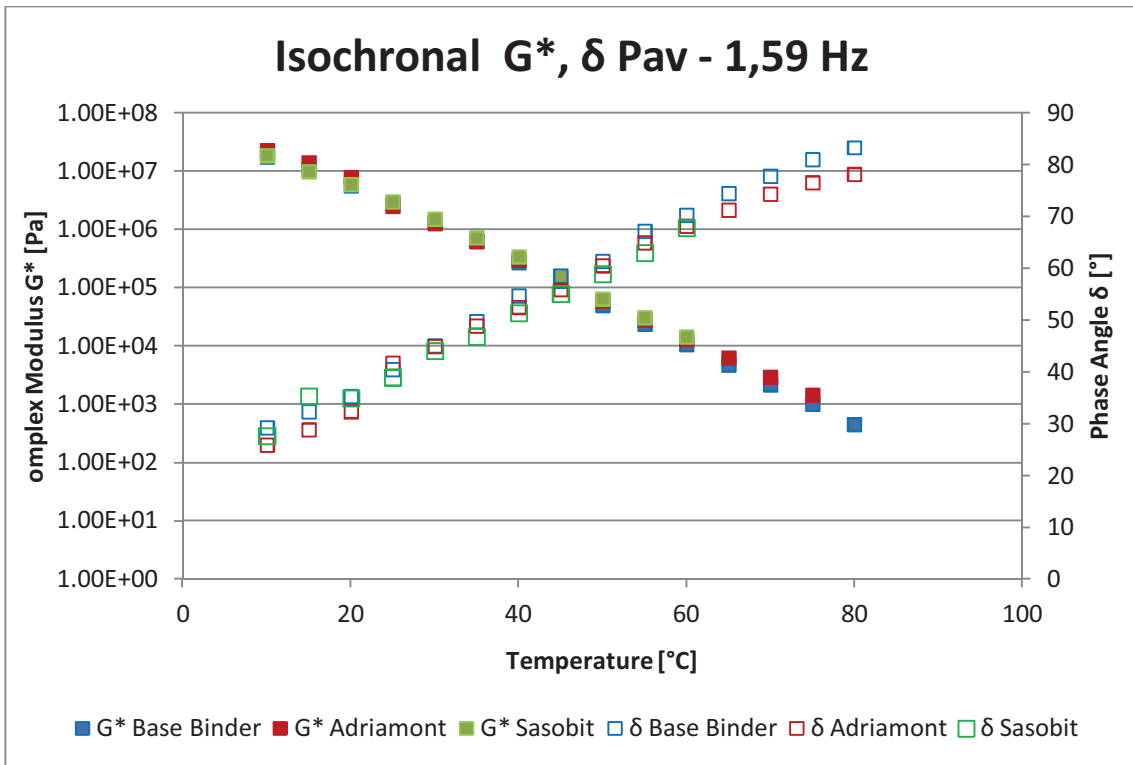


Figure 4.20 PAV Isochronal plot of G^* and δ at 10 rad/s

No big differences can be noted from the comparison. PAV-aged asphalt binders show an analogous behaviour. Hence, the waxes do not affect the performance of an in-service road pavement.

4.2.5 Black Diagram

Black diagram is a graph of the magnitude (norm) of the complex modulus G^* versus the phase angle δ . The frequency and the temperature are therefore eliminated from the plot, which allows all the dynamic data to be presented in one plot without the need to perform TTSP manipulations of the raw data.

A smooth curve in a black diagram is a useful indicator of time-temperature equivalency, while a disjointed curve indicates the breakdown of TTSP and the presence of either a high wax content bitumen, a highly asphaltene structured bitumen or a highly polymer modified bitumen. For this reason Black diagram is well known also as the fingerprint of the binder.

The following pictures show the black diagram for each binder.

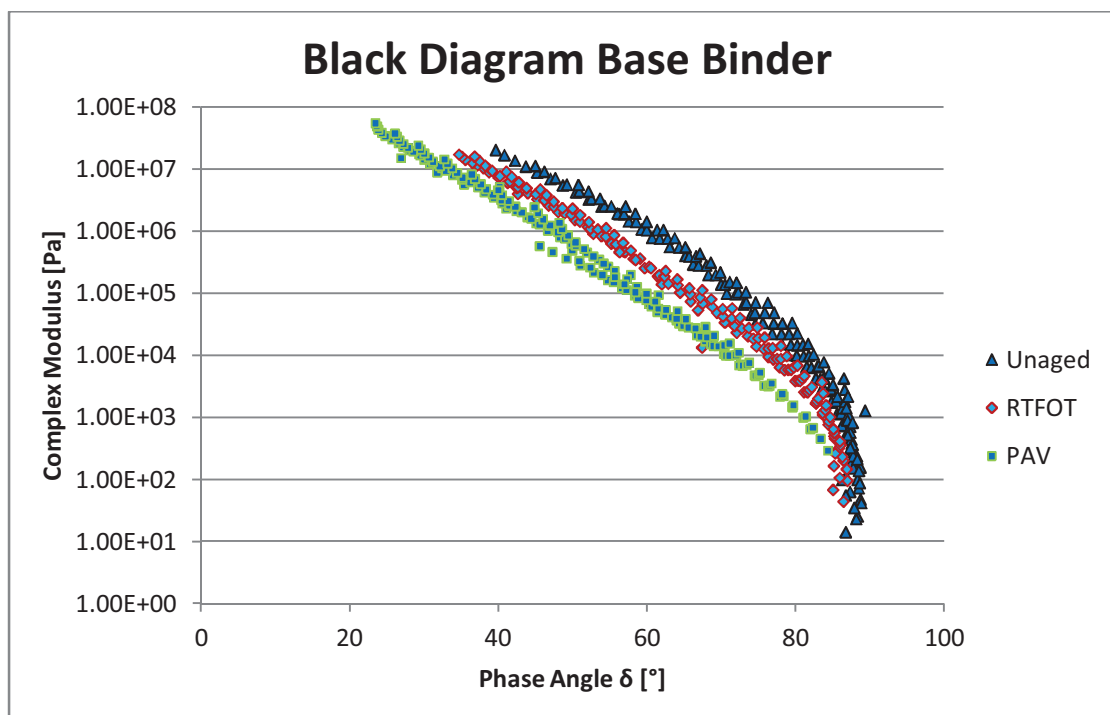


Figure 4.21 Black Diagram for Base Binder

The effect of oxidative ageing is seen a shift of the Black diagram curves towards lower phase angles. The rheological changes after ageing, therefore, consist of an increase in

stiffness and a greater proportion of elastic behaviour (minor phase angle) compared to the unaged binder [24]. These diagrams show that, for a same complex modulus, the behaviour of the binders after aging is less viscous. This aspect is more marked in wax-modified binders that in the base binder.

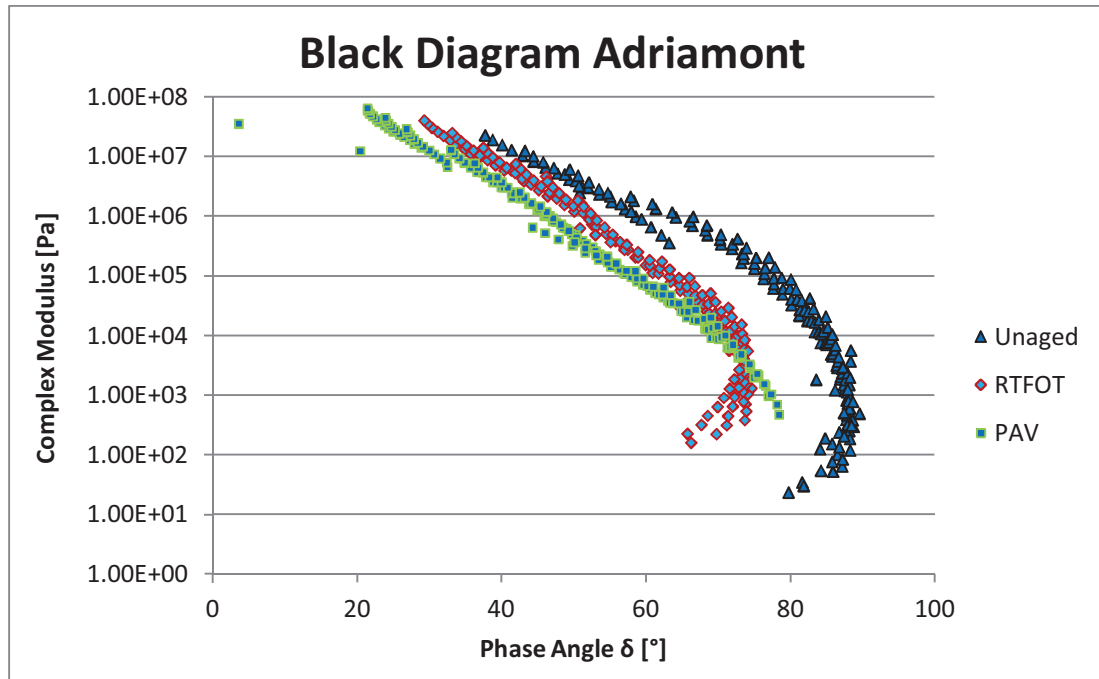


Figure 4.22 Black Diagram for Adriamont

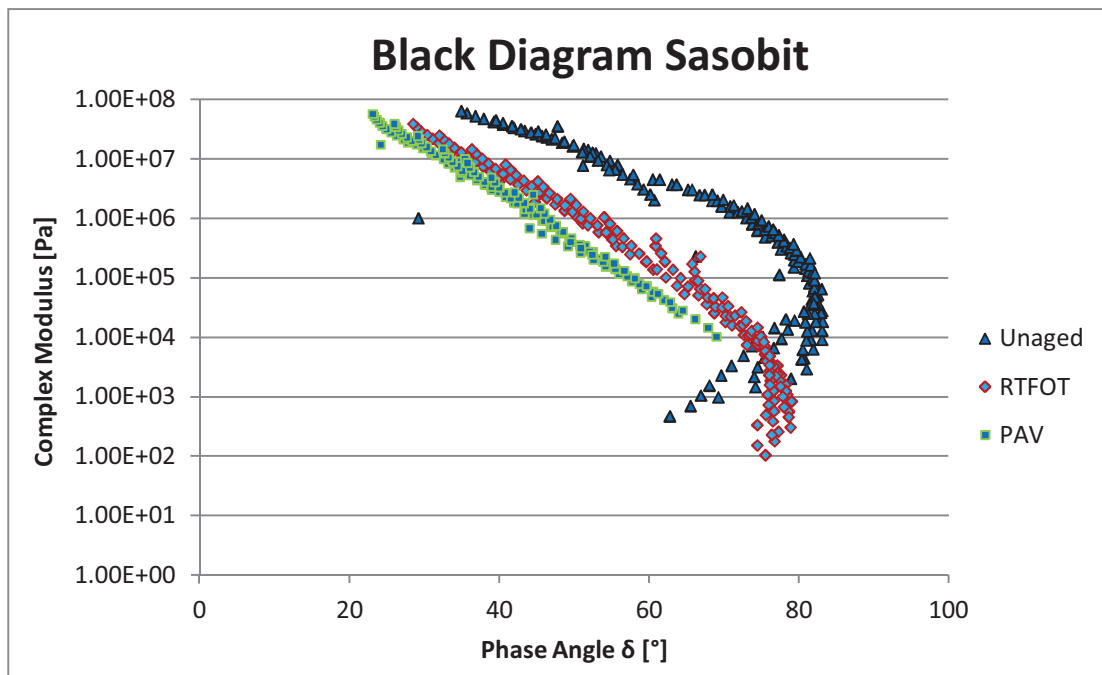


Figure 4.23 Black Diagram for Sasobit

Black diagrams indicate a different behaviour between non-modified and wax-modified binders. Base Binder exhibit especially uniform values: for a complex modulus higher than approximately 10^3 the curves are parallel, while for values lower than the mentioned limit curves tend to overlap and converge into a single curve.

The diagram of the modified bitumens could be explained as follows: as the bitumen loses his consistency (at low values of complex modulus, recorded at high temperatures) the wax forms a sort of grid which causes a greater springback. The Aging also affects the wax, whose lattice weakens after PAV.

4.2.6 Ageing Index

This index is the ratio of the Complex Modulus of a binder after RTFOT aging to the Complex Modulus after PAV aging. It provides a measure of the effect of long term aging (PAV) on the behaviour of the binder. The higher the ratio, the less the aging after the PAV. On the other hand, the lower the ratio, the more the bitumen has undergone an aging process. Figure 4.20 show the trend of the Ageing Index, calculated at a frequency of 1.59 Hz (10 rad/s) with the temperature; it confirms what has been observed with the mastercurves and the isochronal plots: the Sasobit modified binder is less affected by the aging compared to the others.

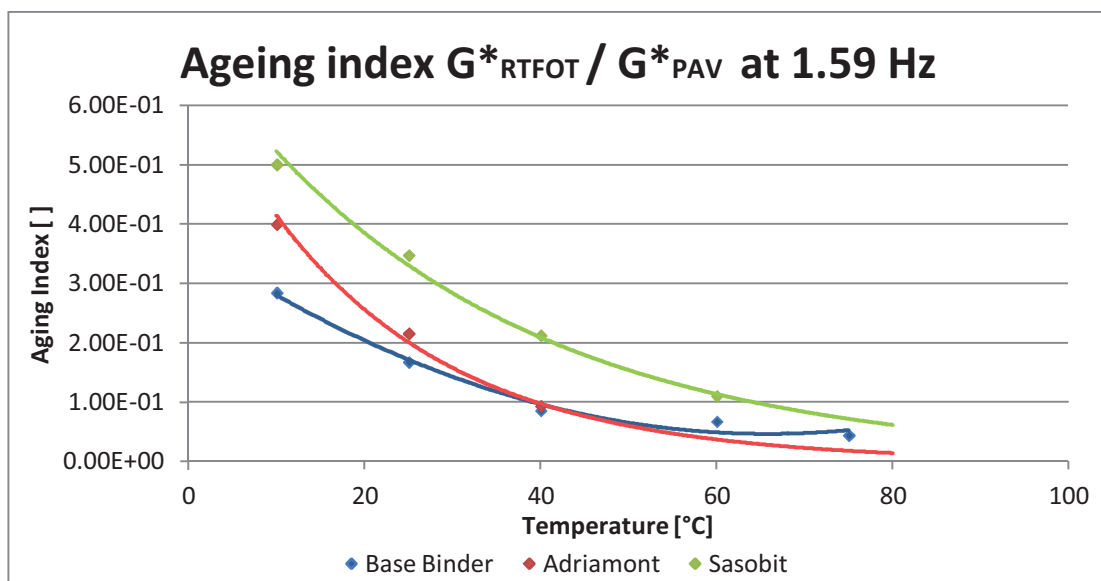


Figure 4.24 Ageing Index trend with temperature

4.3 Bending Beam Rheometer test

4.3.1 Setting of the test and specimen preparation

The Bending Beam Rheometer is a flexural rheometer. It provides a measure of low temperature stiffness and relaxation properties of asphalt binders. These parameters give an indication of an asphalt binder's ability to resist low temperature cracking. A TE-BBR Thermoelectric Bending Beam Rheometer of Cannon Instrumen Company has been used for tests.

Sample preparation is fundamental in this test. Hence all procedures must be followed with the maximum care, in order to obtain a reliable measure of the investigated properties. Poor specimens give poor test results.

The first thing to do is place the asphalt binder in oven, at a temperature of 150 °C, until it is sufficiently fluid to pour. Since a 500g tin has been used, the time needed was approximately 1 hour. During this time, aluminium BBR moulds are prepared (figure 4.22); their dimensions are specified in 6.25 mm thick by 12.70 mm wide by 127.0 mm long. It is recommended that no burrs are present on the moulds otherwise they must be removed.



Figure 4.25 Kit needed to prepare BBR moulds

Each mould is covered with a plastic strip adhered to it by applying petroleum jelly. The moulds are then assembled and held in place by a rubber band. It is highly important to check that the strips appear flat without any wrinkling: the internal surface of the

assembled moulds will affect the shape of the bitumen beam and hence the calculated Stiffness. When the bitumen is fluid enough, it is mixed and then poured in the mould. Pouring must be done carefully to ensure that no air voids are trapped, the corners are filled, and the surface of the asphalt binder is slightly above the top of the mould. Then the moulds are allowed to cool at room temperature for 45 to 60 minutes before they are trimmed of excess binder. Trimming is done by applying a hot spatula to the surface of asphalt binder; the contact must be momentary, only sufficient to soften the layer of asphalt binder that will be trimmed from the test specimen (figure 4.26).



Figure 4.26 Trimming operations

After that, the moulds are immersed in the liquid refrigerant of the test apparatus for 5 minutes immediately prior to demoulding (it is important not to exceed this time in order to minimize the development of physical hardening). This operation is accomplished with the aim to de-mould the sample without modifying its shape: bitumen must be sufficiently stiff during the demoulding process (figure 4.27). Careless demoulding can ruin an otherwise perfect test specimen.



Figure 4.27 Demolding before pre-conditioning at testing temperature

Once all these procedures have been followed, the specimens are rested on a support in the liquid refrigerant at the test temperature for 60 ± 5 minutes.

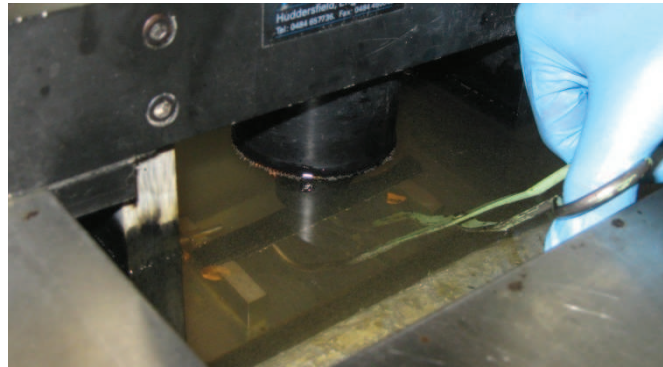


Figure 4.28 Bitumen beam placed on supports

A calibration procedure must be performed on the apparatus each time it is switched on. This is another important step because unless it is properly executed, an incorrect load will be displayed and used in the calculations.

Once 60 minutes have passed, the sample is placed on the beam supports and the test is started. A 980 mN test load is applied and maintained constant for 240 seconds. During this period, readings of deflection over time are recorded and Creep stiffness (S) and m -value at 8, 15, 30, 60, 120, and 240 seconds are calculated.

Although the test takes only 5 minutes to be finished, it is obvious that the test preparation is long and need particular attention in order to obtain fine samples and not damage them. Testing should be done as quickly as possible to minimize the effect of steric hardening that could occur. Steric hardening can increase asphalt binders' stiffness and hence cause unreliable measurement. Usually three beams are tested at each temperature, and a consistent result is achieved by calculating the average value of the two most similar results.

4.3.2 Results

In order to characterize the materials over a wide range of temperatures, tests have been accomplished at -24°C to 0°C with a step of 6°C .

A first way to analyze the results is to plot the logarithm of Stiffness versus the logarithm of time (figure 4.25)

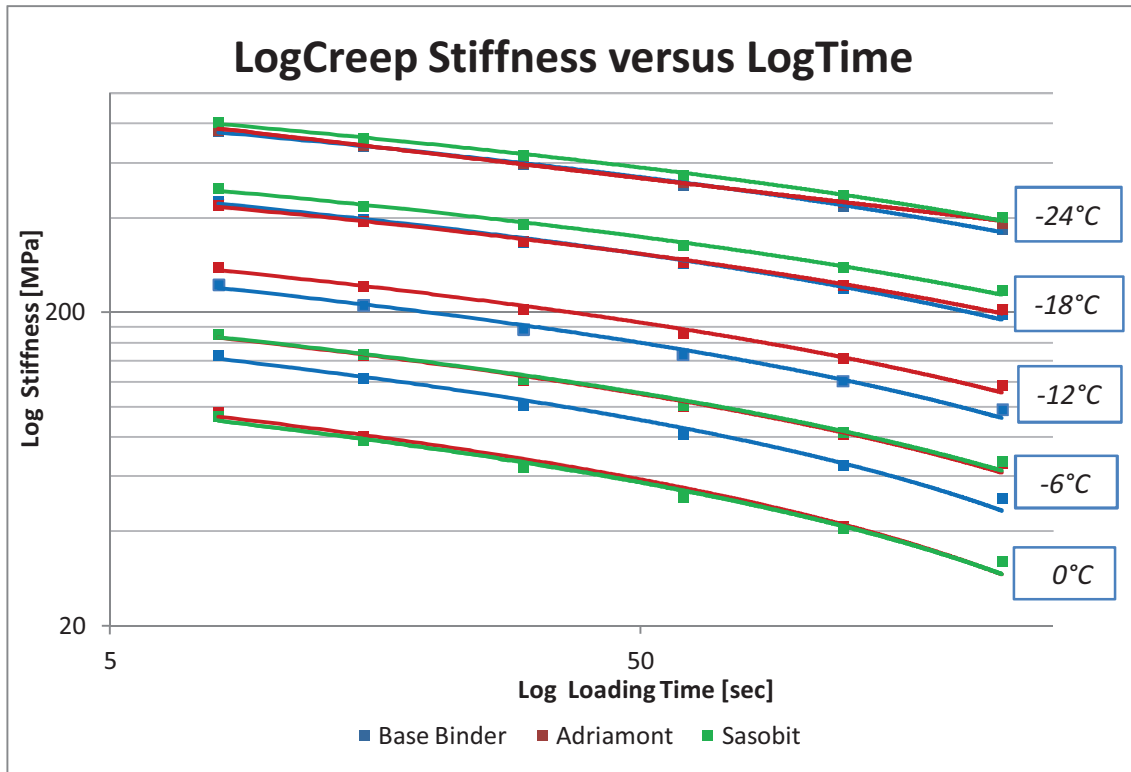


Figure 4.29 Logarithm of Creep Stiffness versus logarithm of Time

Figure 4.29 shows, as easily perceived, that the logarithm of Stiffness of the bitumen beams decrease with the logarithm of loading time. It is also obvious that the lower the temperature the higher the Stiffness. By carefully analysing the graph, it is possible to state that the Base Binder (blue curve), at a defined temperature, seems always to have a lower stiffness compared to the modified binders. This gap is greater at high loading time and tends to decrease as the testing temperature is lowered (it becomes insignificant for temperatures lower than -24°C).

Asphalt binders that are not too stiff at low temperatures and able to relax built up stresses are desirable. To better understand if, at low temperatures, the Base Binder performs better or not rather than the modified binders, further graphs need to be analyzed. The following two graphs show:

- the trend of the 60 seconds loading time creep Stiffness versus the temperature (it suggests how the stiffness of the binders changes with the temperature)
- the trend of the 60 seconds loading time creep Stiffness versus the temperature (it indicates the relaxation property of binders associated with low temperatures)

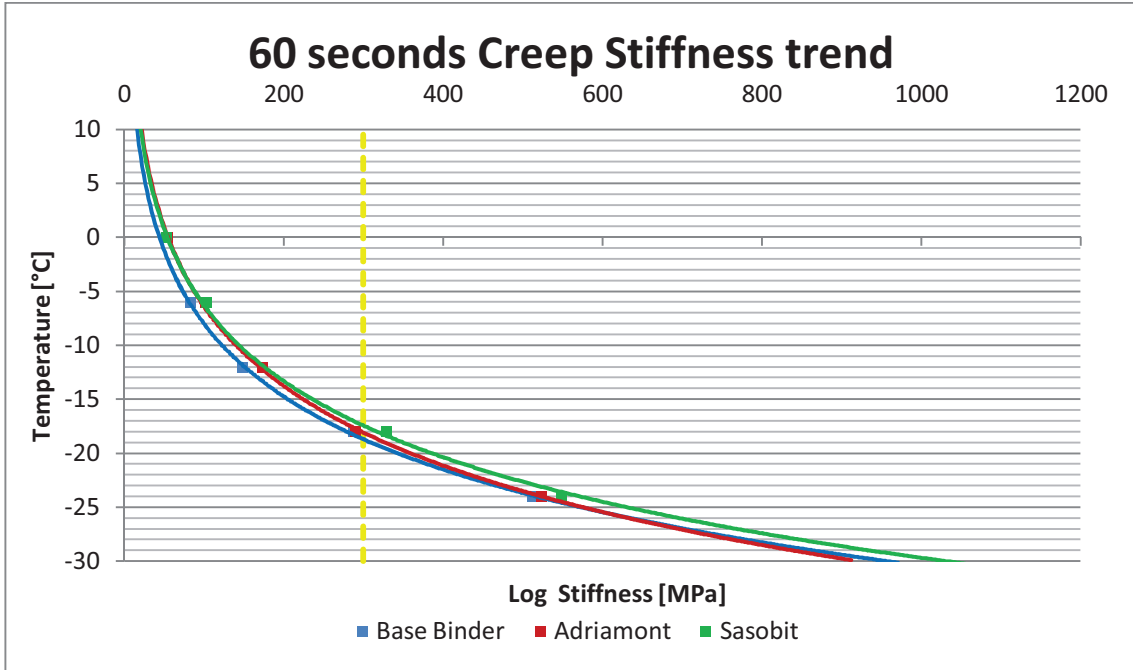


Figure 4.30 60 seconds creep stiffness trend

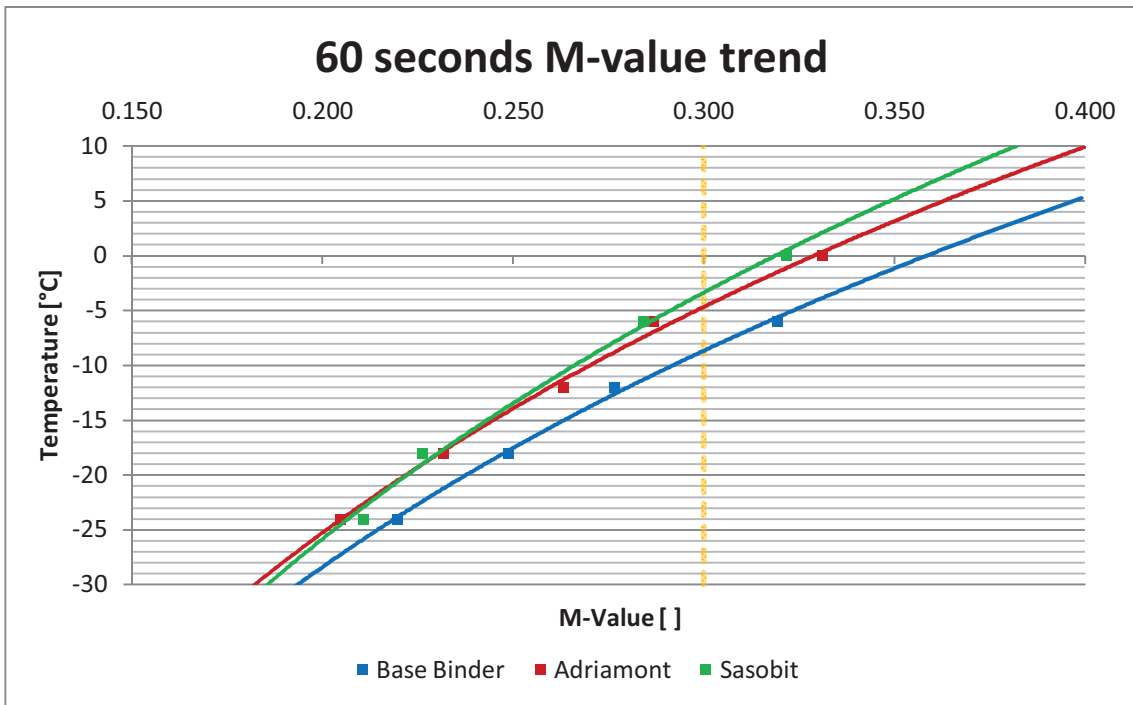


Figure 4.31 60 seconds M-value trend

Since all three curves are approximately parallel and overlapped, the creep stiffness trend does not give any information regarding the low temperature of the binders. The case of the m -value is different: it is possible to observe that the Base Binder curve stands below the two others and the higher the temperature the higher the gap.

Modified binders have the same trend until a temperature of approximately -10°C . For higher temperatures, Adriamont increases its m -value with time more than Sasobit modified binder and its curve seems to become parallel to that of Base Binder.

Hence, Adriamont and Sasobit waxes do not affect the Stiffness of the binder, but influence in a significant way the relaxation properties of the binder. Therefore, as the surrounding temperatures drop, both wax modified bitumens are less able than the Base Binder to relax the internal stresses that they contract and build up.

4.4 Performance Grade

With the aim of verifying the grade of an asphalt binder, it is necessary to conduct tests at three aging conditions and the data are used to calculate the specification parameters as follows [9]:

- Unaged binder: $G^*/\sin\delta$ at 10 rad/s must be greater than or equal to 1 kPa
- RTFOT-aged binder; $G^*/\sin\delta$ at 10 rad/s must be greater than or equal to 2.2 kPa
- PAV-aged binder; $G^* \cdot \sin\delta$ at 10 rad/s must be less than or equal to 5.0 MPa.

If any of the above requirements is not satisfied, the sample fails the specified grade.

For verification or acceptance purposes the test data are used to make a "go or no-go" decision. Table 4.3 shows the SHRP requirement obtained from frequency sweep tests.. The purpose is to determine the maximum temperature at which the first two requirements above are satisfied and the minimum temperature at which the third requirement is satisfied. Superpave program specifies that all binders must meet the same requirements, but each binder meet them in a different range of temperatures.

Hence, a binder PG 52-18 will ensure the above mentioned performance in a temperature ranging from -18°C to 52°C .

Binder	BASE BINDER		ADRIAMONT		SASOBIT	
Parameter	Value [KPa]	Temperature [Celsius]	Value [KPa]	Temperature [Celsius]	Value [KPa]	Temperature [Celsius]
UNAGED G* / SINdelta Min. 1.00 Kpa at 10 rad/s	1.77	45	1.85	50	1.66	55
	0.73	50	0.81	55	0.91	60
RTFOT G* / SINdelta Min. 2.20 Kpa at 10 rad/s	3.95	50	4.04	55	1.62	60
	1.72	55	1.96	60	0.84	65
PAV G* · SINdelta Max. 5000 Kpa at 10 rad/s	5675	15	6837	15	5754	15
	3286	20	4236	20	3400	20

Table 4.3 SHRP requirements for Binders

To be more accurate, an interpolation over the tested temperature has been made for each aging stage i.e. requirement (figure 4.22,4.23,4.24). An exponential law has been used for both nine cases, with a high R^2 value (table 4.4).

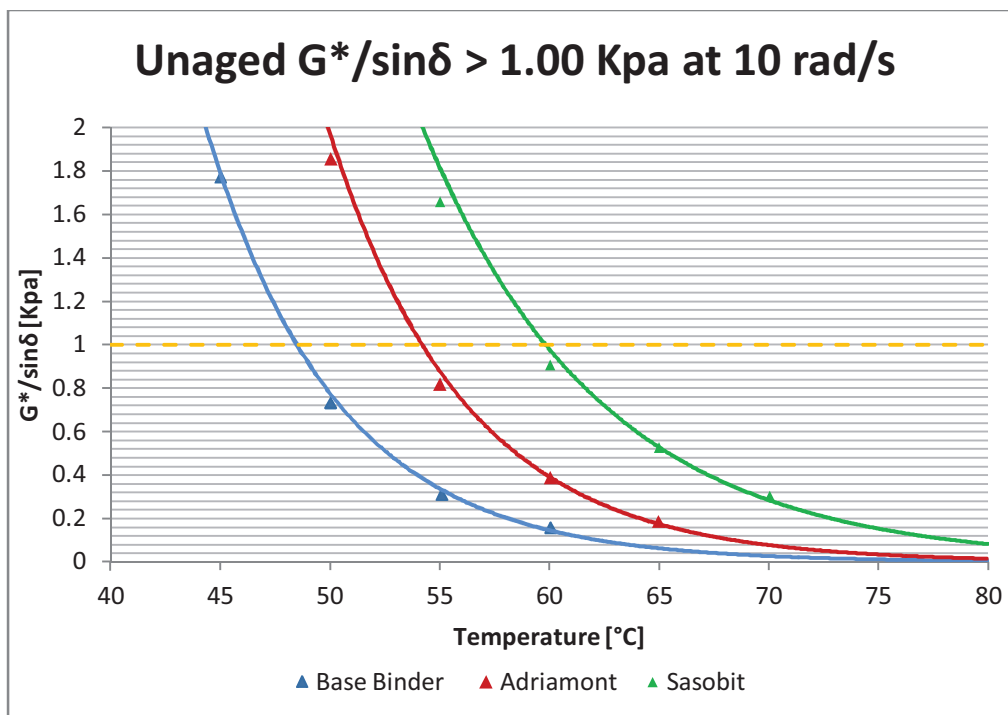


Figure 4.32 Interpolation of Unaged binder requirement

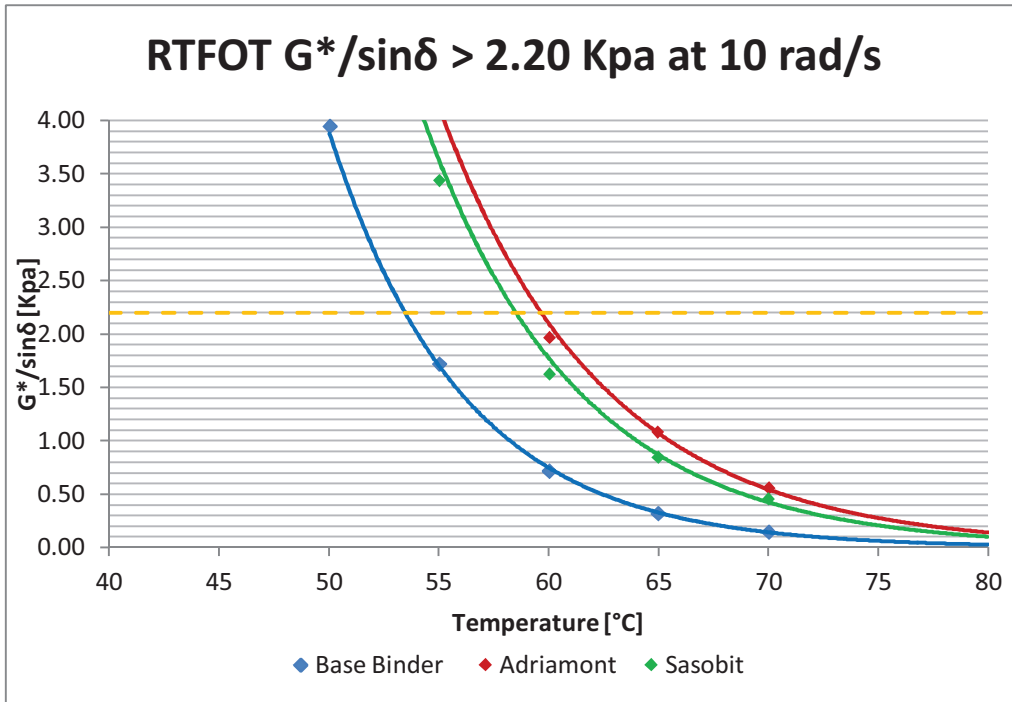


Figure 4.33 Interpolation of RTFOT-aged binder requirement

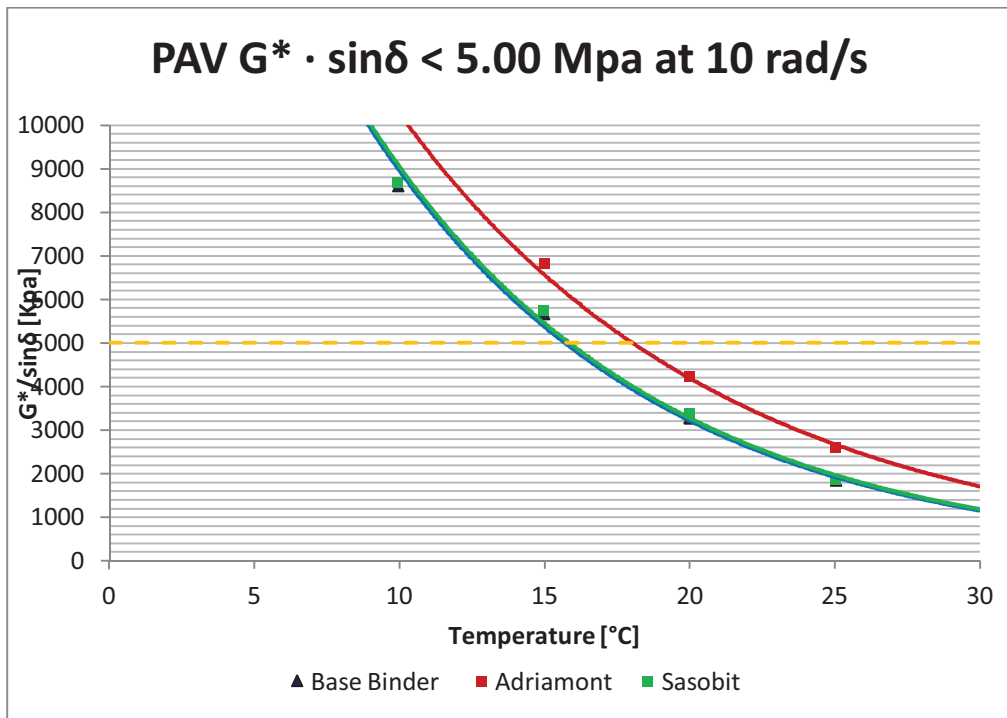


Figure 4.34 Interpolation of PAV-aged binder requirement

Binder	BASE BINDER		ADRIAMONT		SASOBIT	
Parameter	Temperature [Celsius]	R²	Temperature [Celsius]	R²	Temperature [Celsius]	R²
UNAGED G* / SINDelta Min. 1.00 Kpa at 10 rad/s	49	0.997	54	0.997	60	0.992
RTFOT G* / SINDelta Min. 2.20 Kpa at 10 rad/s	54	0.995	60	0.998	59	0.995
PAV G* · SINDelta Max. 5000 Kpa at 10 rad/s	16	0.995	18	0.994	16	0.997

Table 4.4 Summary of requirement interpolation

The grading temperature for the maximum pavement design temperature is determined in step one and two above. It corresponds to the maximum temperature at which the first two requirements above are satisfied. This temperature determines the first number in the performance grade (PG), as in PG 64-XX. The second number is determined by testing at the intermediate pavement design temperature.

From the data we can observe that the Base Binder satisfies the first two criteria at the temperature of 54 °C, while both the modified binders do at 60 °C. Hence, conservatively, it can be deduced that the base binder has got a upper PG of 52°C, while the modified binders have got a upper PG of 58°C. The pavement design temperatures and the associated test temperatures are summarized in table 4.5 for the different grades.

The results of the dynamic shear rheometer (DSR) test at the intermediate test temperature can be used as a guideline for the initial test temperature. Selecting the initial test temperature in accordance with the grade indicated on the basis of the DSR measurements on the tank and Rolling Thin Film Oven Test (RTFOT) residue

(measured at the maximum pavement temperature) and the Pressure Aging Vessel (PAV) aged material (measured at the intermediate pavement temperature).

Virtual Superpave Laboratory

Performance Graded Asphalt Binder Specification (from AASHTO MP 1)

Performance Grade	PG 46			PG 52						PG 58						PG 64						PG 70						PG 76						PG 82												
	34	40	46	10	16	22	28	34	40	46	16	22	28	34	40	46	10	16	22	28	34	40	10	16	22	28	34	40	10	16	22	28	34	40	10	16	22	28	34	40						
Average 7-day Maximum Pavement Design Temperature, °C ^a	< 46			< 52						< 58						< 64						< 70						< 76						< 82												
Minimum Pavement Design Temperature, °C ^a	-34	-40	-46	-10	-16	-22	-28	-34	-40	-46	-16	-22	-28	-34	-40	-46	-10	-16	-22	-28	-34	-40	-10	-16	-22	-28	-34	-40	-10	-16	-22	-28	-34	-40	-10	-16	-22	-28	-34	-40						
ORIGINAL BINDER																																														
Flash Point Temp, T 48, Minimum (°C)	230																																													
Viscosity, ASTM D 4402: ^b Maximum, 3 Pa·s, Test Temp, °C	135																																													
Dynamic Shear, TP 5: ^c G' / sin ² , Minimum, 1.00 kPa Test Temp @ 10 rad/s, °C	46			52						58						64						70						76						82												
ROLLING THIN FILM OVEN RESIDUE (T 240)																																														
Mass Loss, Maximum, percent	1.00																																													
Dynamic Shear, TP 5: G' / sin ² , Minimum, 2.20 kPa Test Temp @ 10 rad/s, °C	46			52						58						64						70						76						82												
PRESSURE AGING VESSEL RESIDUE (PP 1)																																														
PAV Aging Temperature, °C ^d	90			90						100						100						100 (110)						100 (110)						100 (110)												
Dynamic Shear, TP 5: G' / sin ² , Maximum, 5000 kPa Test Temp @ 10 rad/s, °C	10	7	4	25	22	19	16	13	10	7	25	22	19	16	13	10	7	25	22	19	16	13	10	7	25	22	19	16	13	10	7	25	22	19	16	13	10	7	25	22	19	16	13	10	7	
Physical Hardening ^e	Report																																													
Creep Stiffness, TP 1 Determine the critical cracking temperature as described in PP 42	-24	-30	-36	0	-6	-12	-18	-24	-30	-36	-6	-12	-18	-24	-30	-36	0	-6	-12	-18	-24	-30	0	-6	-12	-18	-24	-30	0	-6	-12	-18	-24	-30	0	-6	-12	-18	-24	-30	0	-6	-12	-18	-24	-30
Direct Tension, TP 3 Determine the critical cracking temperature as described in PP 42	-24	-30	-36	0	-6	-12	-18	-24	-30	-36	-6	-12	-18	-24	-30	-36	0	-6	-12	-18	-24	-30	0	-6	-12	-18	-24	-30	0	-6	-12	-18	-24	-30	0	-6	-12	-18	-24	-30	0	-6	-12	-18	-24	-30

Table 4.5 Superpave Performance Grade Asphalt Binder Specification

In such a way, the Bending Beam Rheometer test would have been carried out at the temperatures of -12°C, -6°C, 0°C but, in order to better characterize the materials, further temperatures of -24°C and -18°C have been investigated.

Two are the criteria that need to be satisfied:

- Creep stiffness S(t) at 60 seconds must be < 300 MPa
- M-value (slope of the curve Log *Stiffness* – Log *Time*) at 60 seconds must be > 0.300

There is a specific reason for measuring the deflection at 60 seconds. When the BBR test was originally developed, most data that correlated thermal cracking of in-service HMA pavements with asphalt binder stiffness used loading times of 1 to 5.5 hours. From this, a limiting stiffness based on 2 hours of loading was selected as the specification target. Unfortunately, 2 hours was considered too long for a standard laboratory test so the time-temperature superposition principle was used to shorten test time. This principle basically allows test results from a shorter loading time using one or more temperatures to be used to estimate the test results at a longer loading time. Testing showed that for most asphalt binders, if the test temperature were increased by 10°C the BBR stiffness at 60 seconds loading time could be equated to the asphalt binder stiffness at 2 hours in the field at the low temperature specification. Therefore, the BBR test takes 60 seconds and is conducted at a temperature 10°C higher than the low temperature specification. Thus, for a PG 64-22 asphalt binder, the test temperature would be -12°C, which is 10°C higher than the low temperature specification of -22°C [21].

By interpolating trends at 60 seconds of creep stiffness and m-value, the following values have been obtained:

Specification for Low Performance Grade			
Specification	Base Binder	Adriamont	Sasobit
Temp [°C] when S < 300 Mpa	-18.7	-18.1	-17.5
Temp [°C] when m > 0.3	-8.7	-4.6	-3.4

Table 4.6 Low Performance Grade Specification

Both criteria need to be satisfied. Although the stiffness criterion is satisfied at roughly -18°C for all bitumens, the m-values become greater than 0.300 at a far higher temperature. Keeping in mind the above reasoning, the Base Binder has a low

performance grade of -18°C , while both the wax-modified binders have a low performance grade of -12°C .

Summarizing the Base Binder has a performance grade 54-18 while both the wax-modified have a performance grade shifted above of 6 degree (PG 60-12).

<i>Performance Grade</i>			
Binder	Base Binder	Adriamont	Sasobit
LowGrade	-18	-12	-12
Upper Grade	54	60	60

Table 4.7 Performance grade of the asphalt binders

Concluding, the effect of waxes on the asphalt binders can be summarized as a shift of the performance grade temperatures above by 6°C .

Wax-modified binders are then more suitable for slightly higher temperatures. This is mainly due to the poor ability of those binders to relax thermal stresses. As can be seen in table 4.6, Adriamont modified asphalt binder satisfies the superpave criteria at -4.6°C while Sasobit modified binder at the temperature of -3.4°C . Compared to the the temperature of -8.7°C , at which the base binder assumes an m-value greater than 0.300 and then satisfies the superpave criterions, the difference is great.

CHAPTER 5

THE AFFINITY RESEARCH

5.1 Introduction

The main goal of this research is to measure the surface energy components of three bitumens and combine them with that of three different aggregates, in order to determine the work of adhesion of nine combinations arising therefrom and the susceptibility of asphalt to water damage. The materials analyzed are:

- A API neat bitumen 70 – 100 dmm (12360)
- The above bitumen modified with a 2% in weight with Adriamont wax (12361)
- The same neat bitumen 70 – 100 dmm modified with a 2% in weight with Sasobit wax (12362)

- Porphyry passing to 4,75 mm and retained at 2 mm (12364)
- Diorite passing to 4,75 mm and retained at 2 mm (12365)
- Basalt passing to 4,75 mm and retained at 2 mm (12366)

In order to control and easily recognize all the materials used in the laboratory, they have been catalogued with a reference code (for example 12361 is the Adriamont modified binder).

The following section will include an explanation of the work done, starting from the surface energy components of the bitumens calculated with the Dynamic Contact Angle (DCA) technique. Later, the surface energy components of the aggregates will be looked at, calculated with the Dynamic Sorption Device (DVS). To conclude, these energy parameters of both bitumens and aggregates will be combined through four parameters suggested by Bhasin (2006). These parameters allow us to quantify the

adhesive bond strength of the mixture, both in the presence and in the absence of water, and thus the susceptibility of the mixture to the water damage.

5.2 Dynamic Contact Angle tests

5.2.1 Setting of the test and specimen preparation

The first step is the sample preparation. Microscope glass slides are used (24 mm x 40 mm) for the preparation of bitumen films. A tin filled with bitumen is placed in oven at a temperature and for a time such that the sample is fluid enough to form a thin film of the desired thickness. The glass slides are first cleaned with acetone and then rinsed with distilled water. In order to remove any moisture or organic matter from the slide that may possibly affect the measure, both sides of the slides are passed through a blue flame. Thus, the clean glass slide are dipped into and out of the molten sample, of approximately 15 mm depth, and are left out to drain for a few seconds. Then the prepared slides are placed one by one onto a slide holder and kept in a desiccator for 24 hours. The preparation of glass slides is an important requirement for the successful measurement of the surface energy, and, as we will see, can largely affect the values obtained with some probe liquids.



Figure 5.1 Glass slides prepared ready to be stored in desiccator

After 24 hours of storage, glass slides are ready to be tested.

The equipment and the computer system are turned on. A 100 ml beaker with the required probe liquid is filled up to a depth of 50 ml and then placed on the stage of the equipment. The supporting software, through which the test is controlled, prompts you to enter some input data such as:

- Speed of the motor (speed with which the stage is moved i.e. the sample slide is immersed in the probe liquid). A speed of 40 microns/sec was selected
- Depth of immersion. 5 mm has been chosen
- Surface tension of the probe liquid. This is a known value for each probe liquid
- Slide thickness and width. These sizes have been measured with the help of a calliper. For some probe liquids, like diiodomethane, the thickness must be as uniform as possible along the surface of the slide and the same for each slide.

The slides are then attached with the provided copper clip and hanged on the sample stirrup with the help of forceps, and the front cover of the equipment is closed.

Before starting it is good practice to wait until the slide stops swinging and becomes stable. By clicking on “acquire data” the stage containing the beaker is raised and lowered at the pre-entered speed, immersing the slide (figure 5.2) and depth and the force involved is continuously measured [15].



Figure 5.2 A sample starts to be immersed in the probe liquid

After roughly 10 minutes, the test is complete and the software draws a graph between the mass of slide (as its ordinate) and depth of immersion (as its abscissa), displaying the advancing and receding contact angles, calculated through this equation:

$$\cos\theta = \frac{\Delta F + V_m (\rho_L - \rho_{air} \cdot g)}{P_t \cdot \gamma_L} \quad (5.1)$$

Where:

ΔF = difference between weight of plate in air and partially submerged in probe liquid

V_m = volume of solid immersed in the liquid

ρ_L = density of the liquid

ρ_{air} = air density

g = gravitational force

P_t = perimeter of the bitumen coated slide

γ_L = total surface energy of the probe liquid

Due to intermolecular forces of adhesion between the sample and the probe, this graph is different, dependent on the probe liquid used (water, glycerol, diiodomethane) as shown in the following three pictures.

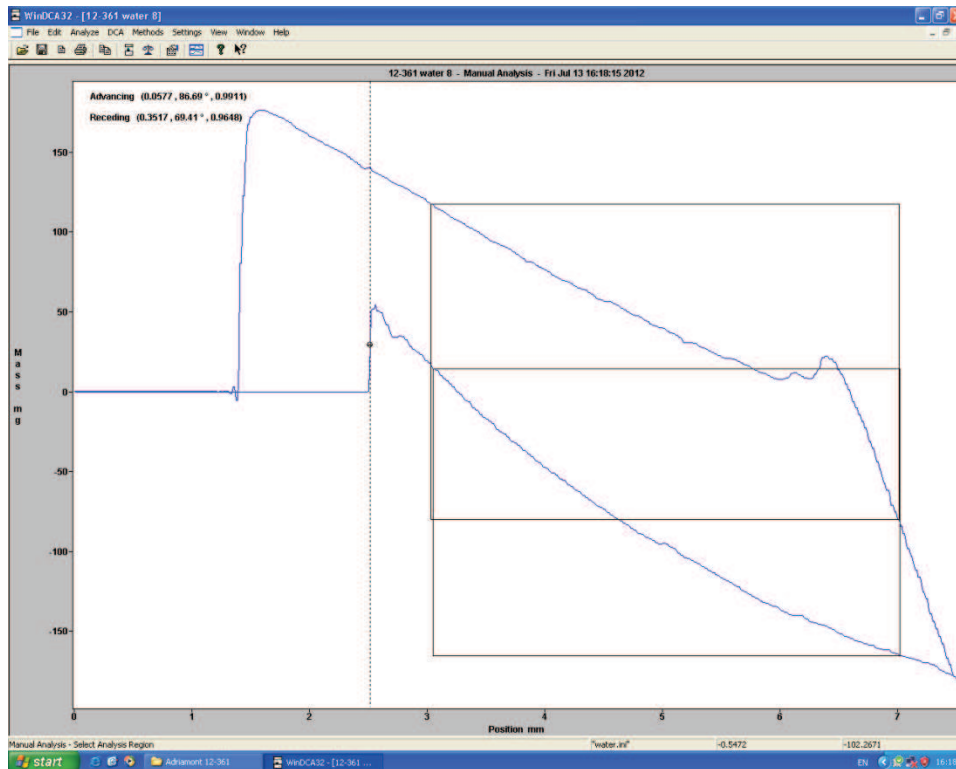


Figure 5.3 Advancing – Receding plot for Water

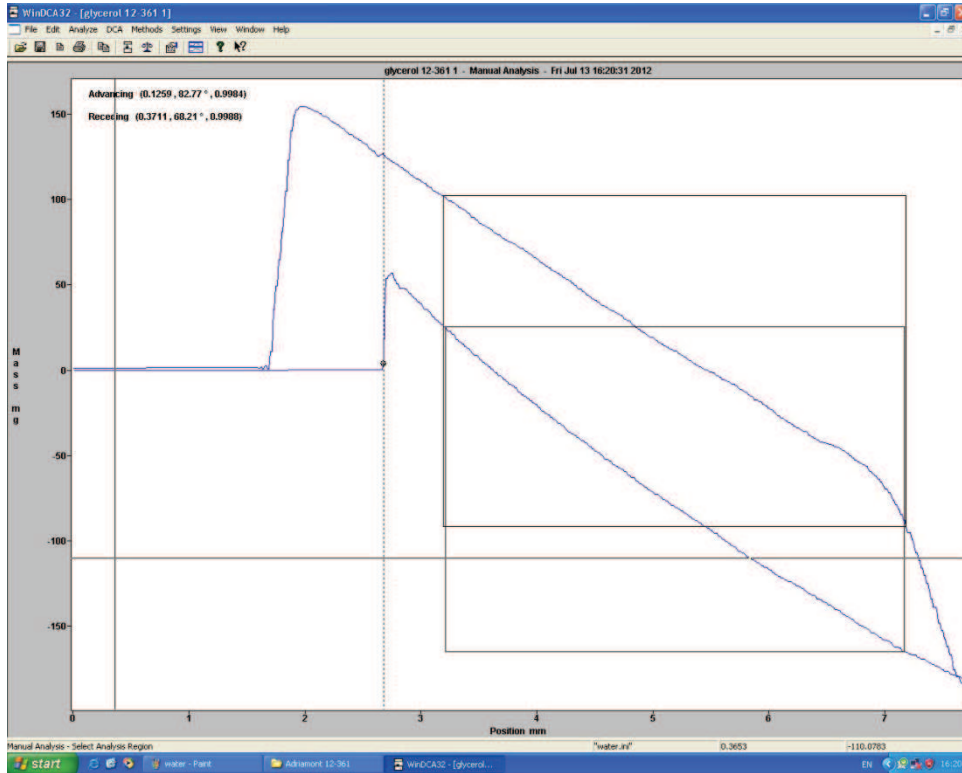


Figure 5.4 Advancing – Receding plot for Glycerol

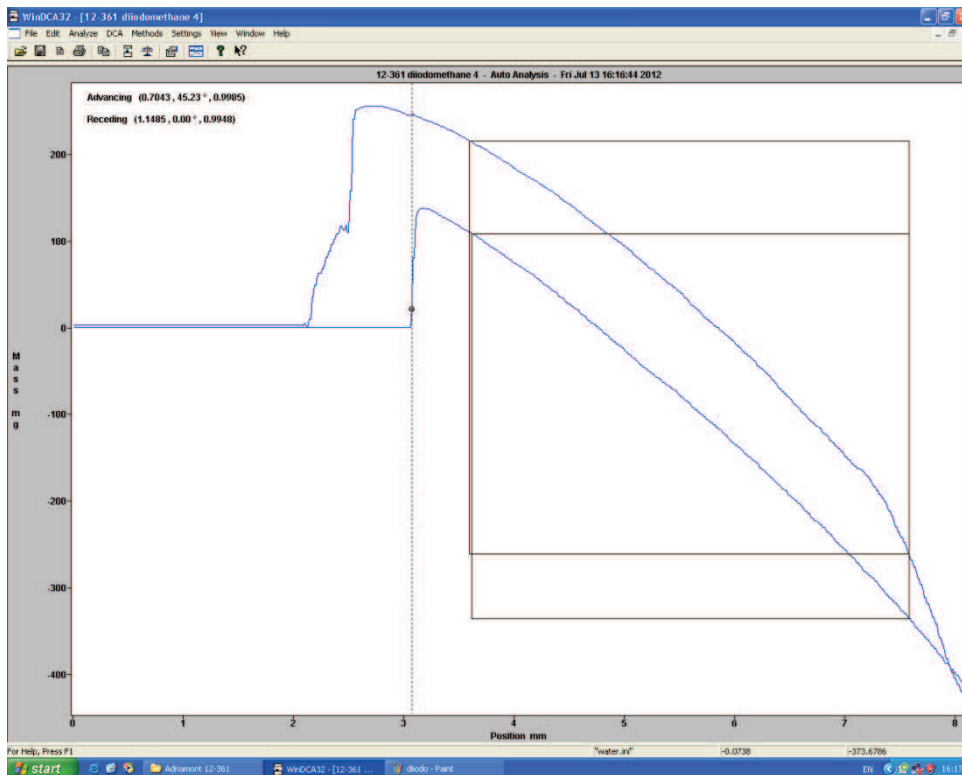


Figure 5.5 Advancing – Receding plot for Diiodomethane

The software allows you to choose between automatic and manual analysis. In this way you can choose what depths the software must calculate the contact angle. Automatic analysis has been chosen and the advancing contact angle as representative. Several tests have been carried out for each bitumen and each probe liquid, in order to obtain reliable angles. This has been possible by statistically analysing the test results. An average contact angle, the arithmetic mean, has been calculated, representing a measure of central tendency:

$$\theta_{average} = \frac{1}{N} \sum_{i=1}^N \theta_i \quad (5.2)$$

Therefore, considering all the values obtained from the tests as the population, the population standard deviation has been calculated:

$$\sigma = \sqrt{\frac{1}{N} \sum_{i=1}^N (\theta_i - \theta_{average})^2} \quad (5.3)$$

representing a measure of dispersion from the average.

The probability density function, which describes the relative probability for the contact angle to take on a given value, has been plotted for each probe liquid and each bitumen.

The data were gradually given in a table and plotted in order to check the values and for any abnormalities. For each test, the advancing and the receding angle have been marked, with the relative slide thickness and width.

The following table summarize all the tests that have been carried out for each bitumens, while the pictures shows the probability density functions . The water is represented by a blue line, the glycerol by the red line and the diiodomethane by the green line.

DCA Test 12-360 Base Binder

SAMPLE	WATER Surface energy 72.8 dynes/cm		GLYCEROL Surface energy 64 dynes/cm		DIODOMETHANE Surface energy 50.8 dynes/cm	
	<i>Advancing Angle</i>	<i>Receding Angle</i>	<i>Advancing Angle</i>	<i>Receding Angle</i>	<i>Advancing Angle</i>	<i>Receding Angle</i>
#	Width [mm]	Thickness [mm]	Width [mm]	Thickness [mm]	Width [mm]	Thickness [mm]
1	85,90	64,56	84,38	66,70	67,67	19,27
	23,86	1,10	23,89	1,30	23,85	1,10
2	86,54	64,89	85,81	68,83	60,23	0,00
	23,86	1,10	23,95	1,15	23,83	1,20
3	85,25	64,14	83,65	62,15	62,57	21,80
	23,90	1,55	23,92	1,15	23,82	1,05
4	86,27	64,93	84,59	62,15	68,72	0,00
	23,83	1,15	23,95	1,40	23,81	1,20
5	87,53	64,93	83,78	64,40	62,14	9,76
	23,89	1,10	23,95	1,45	23,88	1,10
6	86,76	62,26	84,98	62,38	64,38	0,00
	23,84	1,25	23,90	1,40	23,87	1,20
7	89,08	67,24			65,38	21,30
	23,88	1,00			23,84	1,15
8	85,70	63,93			67,13	0,00
	23,83	1,10			23,81	1,05
9					63,02	21,29
					23,86	1,15
10						
11						
12						
Average contact angle	86,63		84,53		64,58	
Standard deviation	1,13		0,73		2,69	

Table 5.1 Contact angles data of 12-360 Neat Bitumen

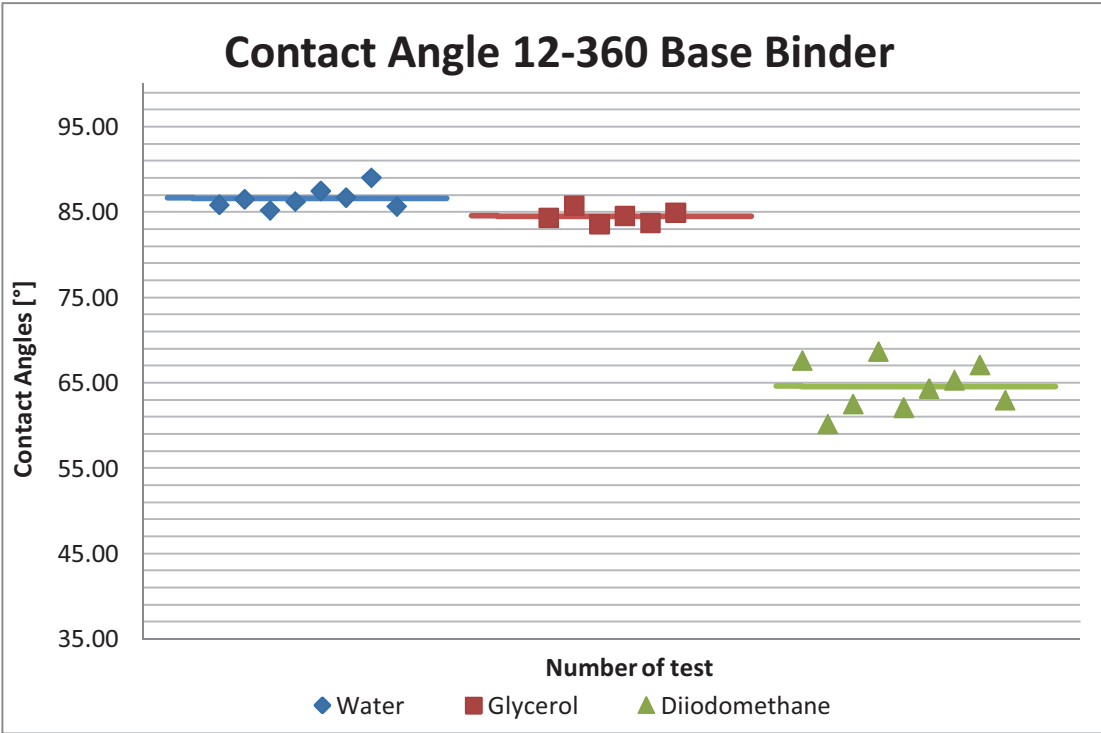


Figure 5.6 Contact angle values of Base Binder

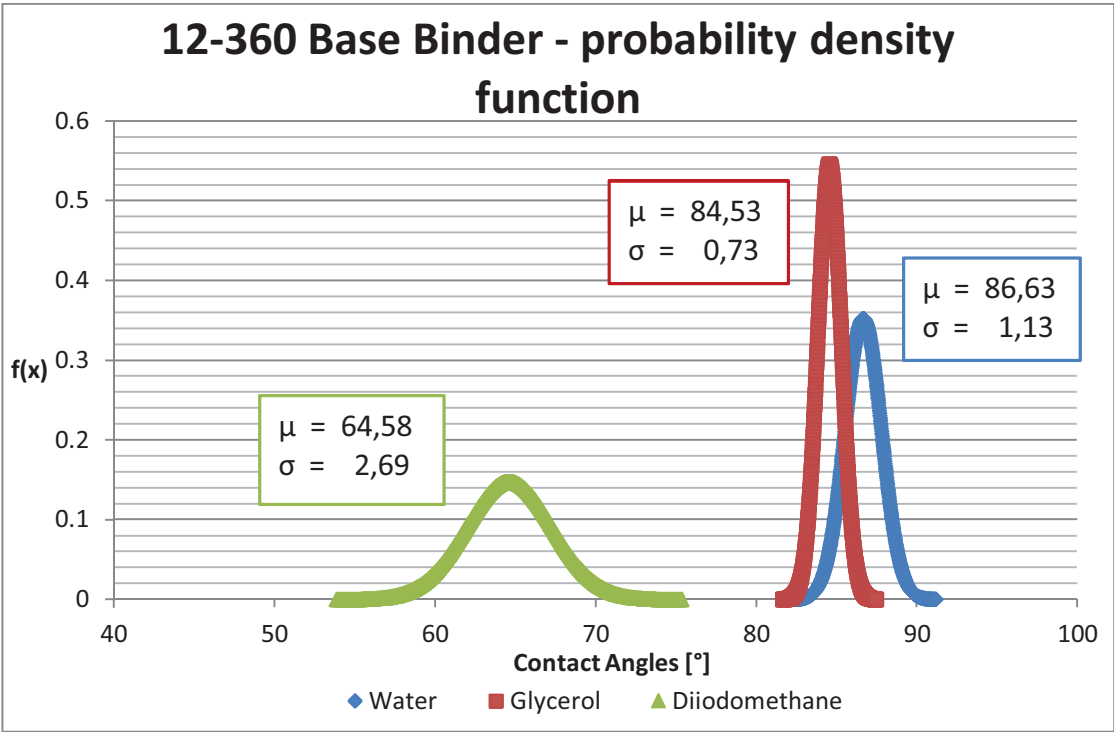


Figure 5.7 Probability density function of Base Binder

DCA Test 12-361 Adriamont

SAMPLE	WATER Surface energy 72.8 dynes/cm		GLYCEROL WATER Surface energy 64 dynes/cm		DIODOMETHANE Surface energy 50.8 dynes/cm	
	<i>Advancing Angle</i>	<i>Receding Angle</i>	<i>Advancing Angle</i>	<i>Receding Angle</i>	<i>Advancing Angle</i>	<i>Receding Angle</i>
#	Width [mm]	Thickness [mm]	Width [mm]	Thickness [mm]	Width [mm]	Thickness [mm]
1	90,26	80,06	82,77	68,21	68,04	47,58
	23,95	1,30	23,95	1,45	23,80	0,90
2	91,33	83,95	81,61	64,24	68,13	45,35
	23,88	1,50	23,92	1,50	23,81	0,95
3	91,83	81,47	82,15	66,87	69,31	58,75
	23,91	1,00	23,93	1,00	23,80	0,85
4	89,09	76,66	84,29	66,83	70,64	50,62
	23,91	1,15	23,94	1,15	23,84	0,85
5	87,54	74,44	82,26	65,68	69,70	0,00
	23,94	1,25	23,96	1,50	23,86	1,00
6	85,49	70,98			64,16	40,51
	23,95	1,30			23,84	1,00
7	90,17	78,68			68,46	47,78
	23,95	1,20			23,83	0,95
8	86,69	69,41				
	23,96	1,35				
9	91,29	81,30				
	23,94	1,10				
10						
11						
12						
Average contact angle	89,30		82,62		68,35	
Standard deviation	2,12		0,91		1,92	

Table 5.2 Contact angles data of 12-361 Adriamont modified

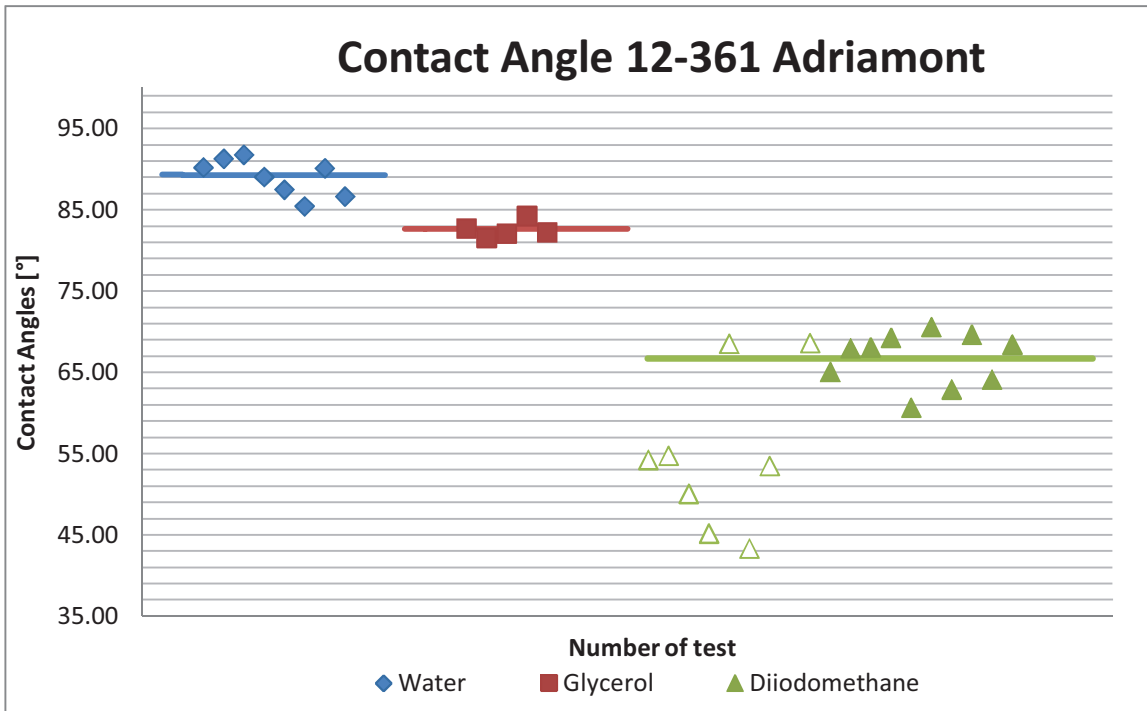


Figure 5.8 Contact angle values of Adriamont

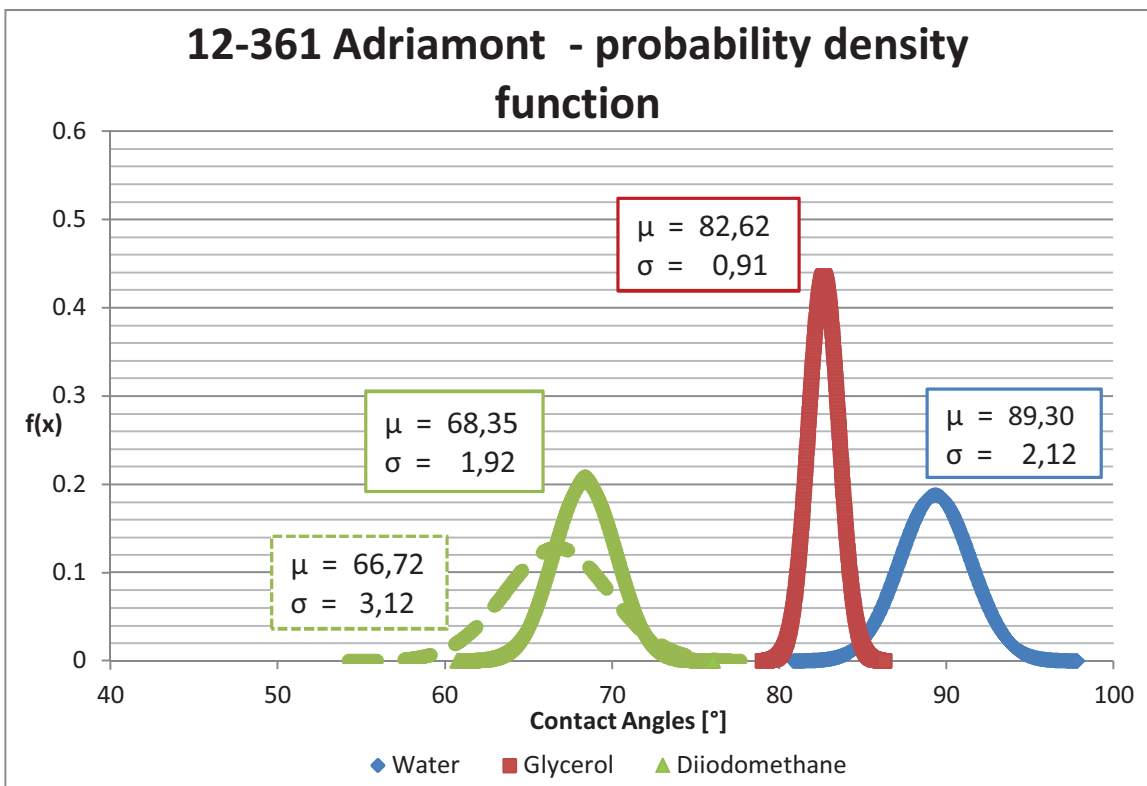


Figure 5.9 Probability density function of Adriamont

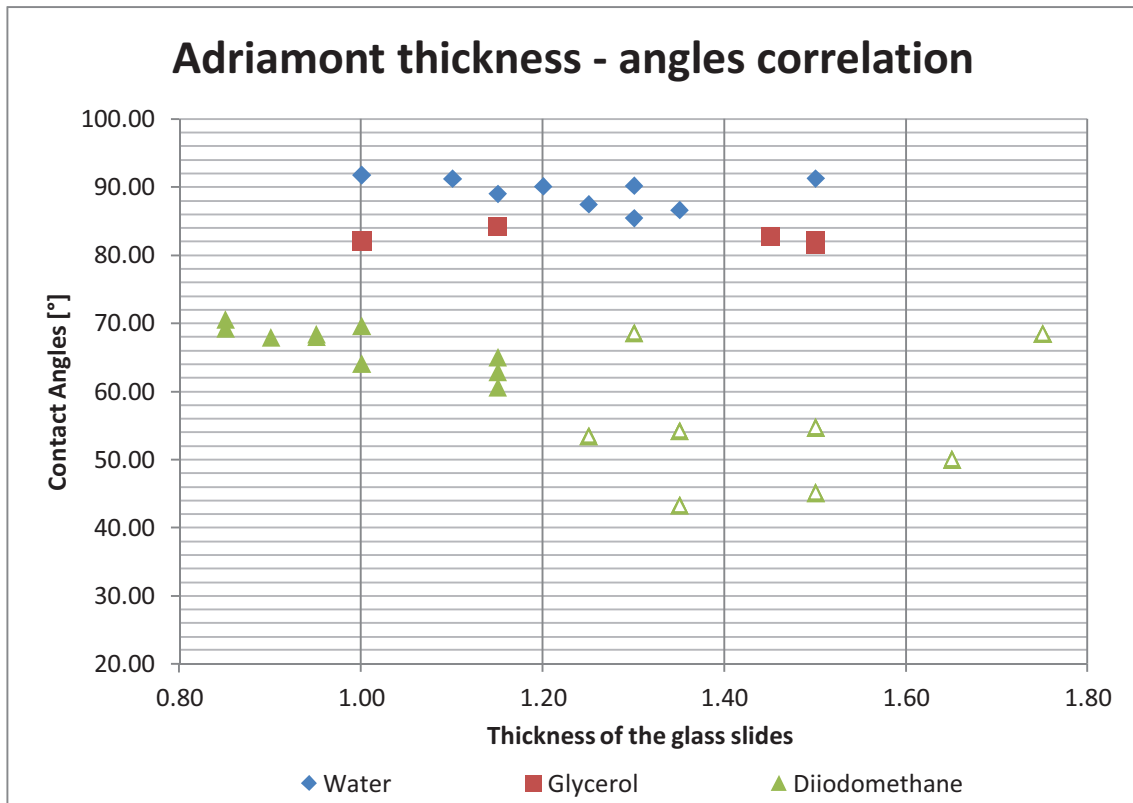


Figure 5.10 Thickness-angles correlation of Adriamont

In all cases glycerol has shown the smallest standard deviation, followed by water. Unlike the first two liquids, for diiodomethane a thickness- contact angle correlation arose from the tests. It can be observed that, by maintaining the thickness of the glass slides below 1.00 mm, the contact angles are uniform. By exceeding the above limit, the contact angles obtained are confusing. For this reason, these values are deemed not reliable. In figure 5.9, two different probability density function for diiodomethane are present. The dashed line indicates the distribution calculated by using all the obtained value and, hence, is to consider not reliable. The solid line, instead, indicates the probability density function by considering only the values under 1.00 mm thickness. The latter approach was used in order to calculate the contact angles from the diiodomethane.

DCA Test 12-362 Sasobit

SAMPLE	WATER Surface energy 72.8 dynes/cm		GLYCEROL WATER Surface energy 64 dynes/cm		DIIDOMETHANE Surface energy 50.8 dynes/cm	
	<i>Advancing Angle</i>	<i>Receding Angle</i>	<i>Advancing Angle</i>	<i>Receding Angle</i>	<i>Advancing Angle</i>	<i>Receding Angle</i>
#	Width [mm]	Thickness [mm]	Width [mm]	Thickness [mm]	Width [mm]	Thickness [mm]
1	90,22	75,22	81,44	65,31	63,26	29,58
	23,88	0,90	23,93	1,35	23,81	1,00
2	86,25	60,80	84,14	70,88	61,25	30,95
	23,93	1,05	23,95	1,30	23,85	1,00
3	88,57	74,88	82,21	69,29	62,23	35,33
	23,81	1,15	23,88	0,95	23,84	1,00
4	86,00	71,67	81,48	61,39	62,15	31,29
	23,80	1,20	23,95	1,55	23,82	1,00
5	87,40	77,73	80,90	69,66	59,09	37,82
	23,96	1,25	23,91	1,25	23,81	1,00
6	90,28	73,34	82,50	66,83	59,19	33,05
	23,90	1,05	23,92	1,15	23,80	1,00
7	86,67	71,03				
	23,93	1,15				
8	89,95	73,18				
	23,94	1,30				
9	90,26	66,20				
	23,90	1,10				
10						
11						
12						
Average contact angle	88,40		82,11		61,20	
Standard deviation	1,74		1,05		1,57	

Table 5.3 Contact angles data of 12-362 Sasobit modified

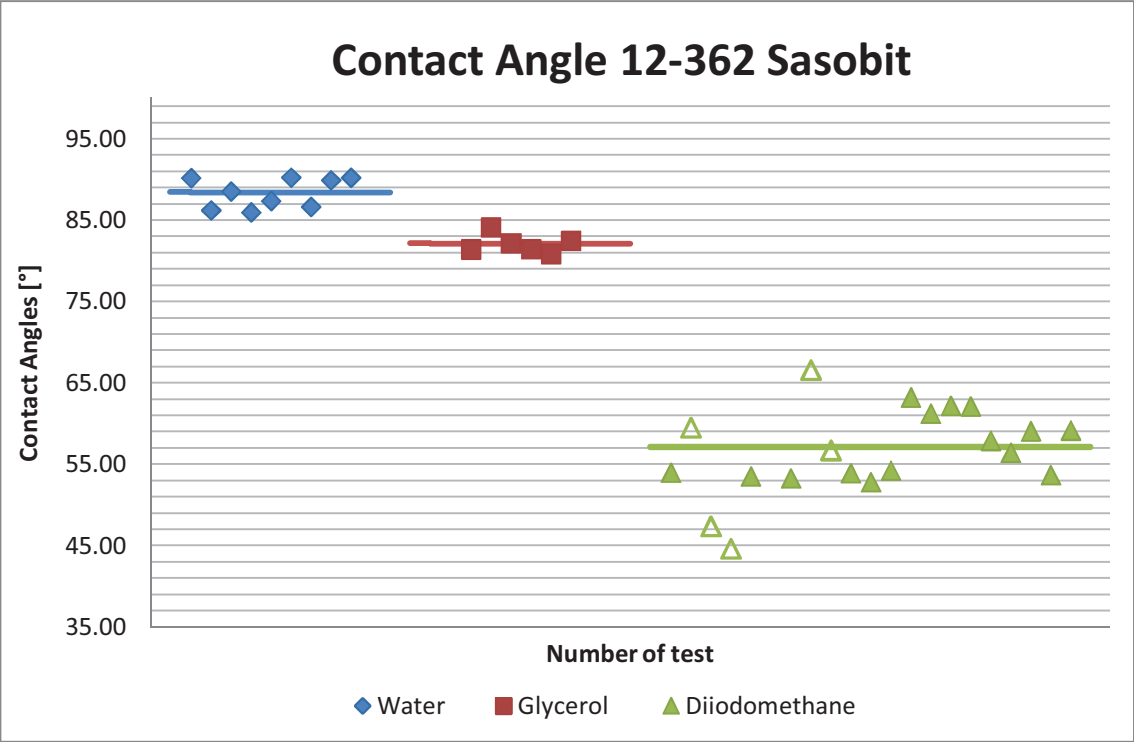


Figure 5.11 Contact angle values of Sasobit

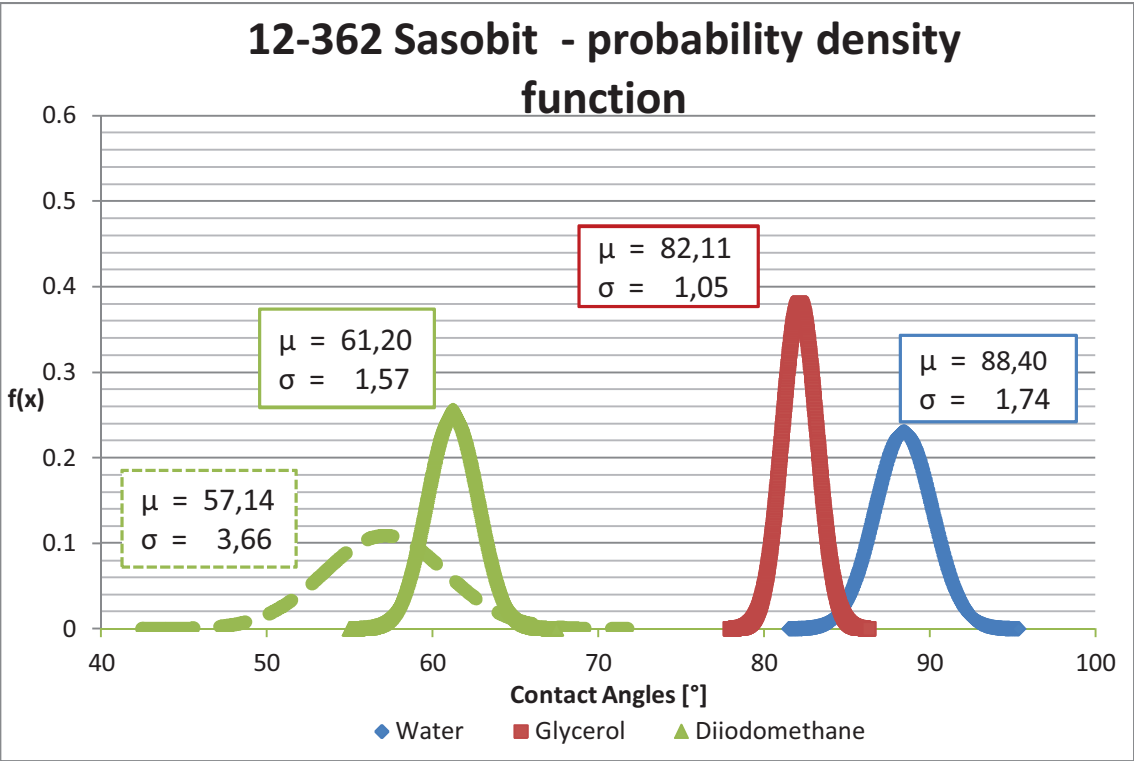


Figure 5.12 Probability density function of Sasobit

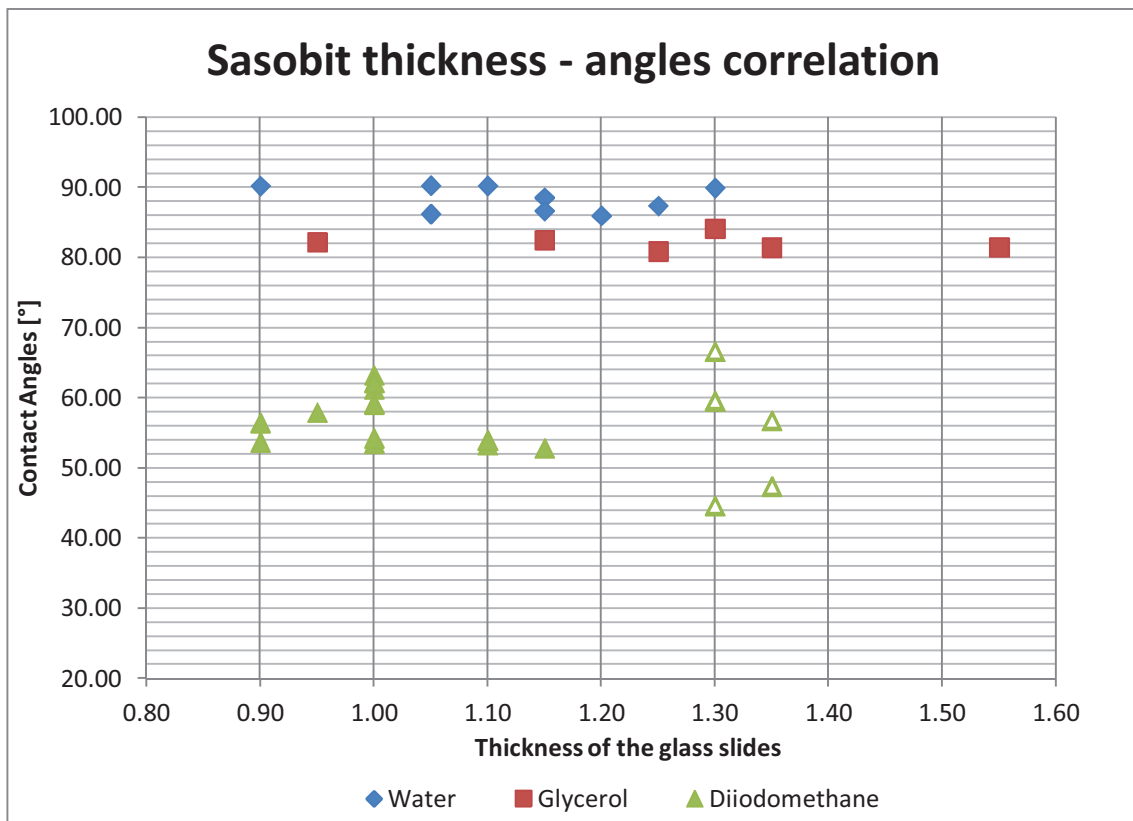


Figure 5.13 Thickness-angles correlation of Sasobit

For Sasobit, the same considerations can be done. For the thickness of the glass slide up to 1.20 mm the contact angles obtained from the tests are uniform; on the contrary, an high thickness result in confusing value.

Sample	Probe liquid		
	Water	Glycerol	Diiodomethane
12-360 Base Binder	86,63	84,53	64,58
12-361 Adriamont	89,30	82,62	68,35
12-362 Sasobit	88,40	82,11	61,20

Table 5.4 Comparison of the Contact angles data for the three bitumens

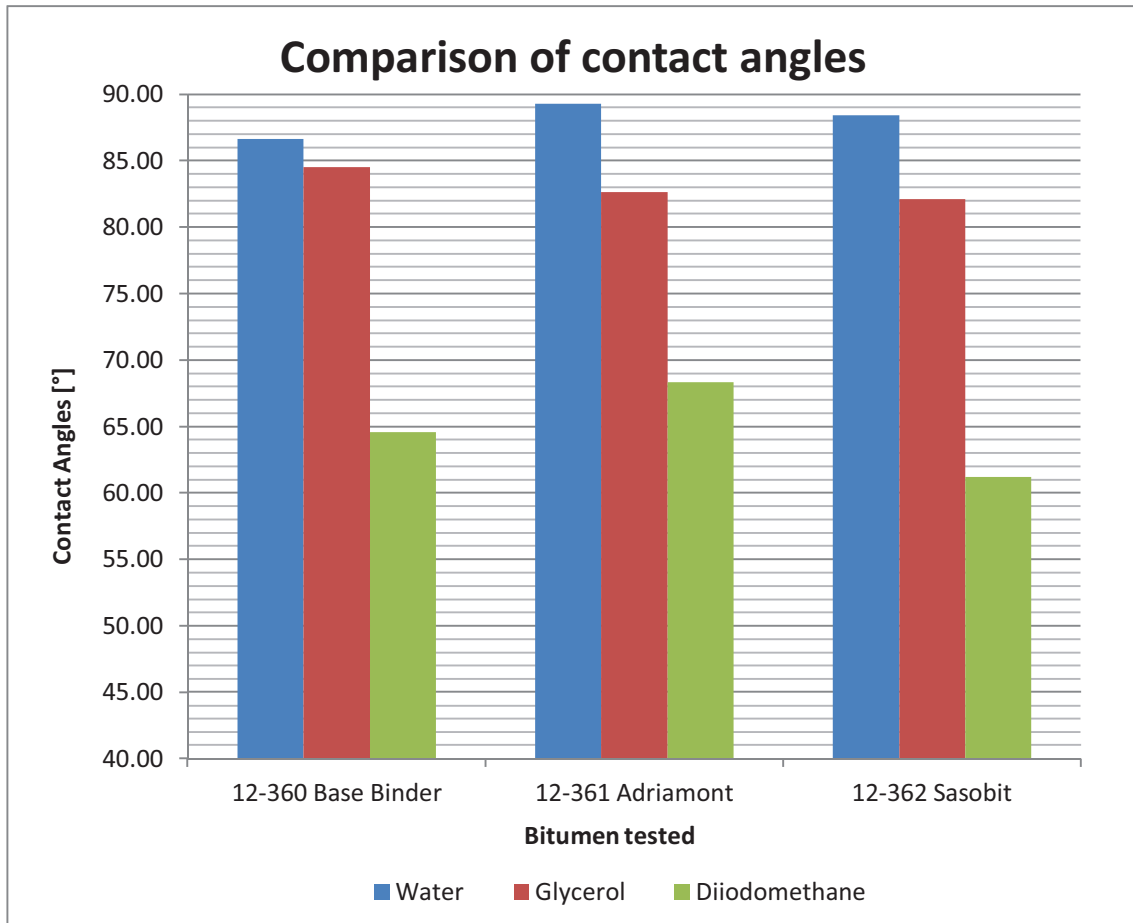


Figure 5.14 Comparison of the Contact angles data for the three bitumens

No large differences can be noted in the comparison. Adriamont has demonstrated the greater contact angles with water and diiodomethane while Base Binder showed the higher contact angle with glycerol. However, these values have poor significance and energy parameters need to be calculated in order to give an affinity opinion.

5.2.2 Surface energy of bitumens

After obtaining the contact angle data, these data have been used to calculate the surface energy of the bitumens. By combining equations 2.8, the Young-Dupré equation, and equation 2.17, the adhesive bond strength in dry condition (considering the two phases “liquid” and “bitumen” instead of the subscripts “bitumen” and “aggregate”) we have:

$$\gamma_L(1 + \cos \theta) = 2\sqrt{\gamma_B^{LW}\gamma_L^{LW}} + 2\sqrt{\gamma_B^+\gamma_L^-} + 2\sqrt{\gamma_B^-\gamma_L^+} \quad (5.3)$$

By dividing all terms for γ_L it is then possible rearrange the equation into known and unknown components as follows:

Known components:

$$A_{1i} = \frac{\sqrt{\gamma_L^{LW}}}{\gamma_L} ; A_{2i} = \frac{\sqrt{\gamma_L^+}}{\gamma_L} ; A_{3i} = \frac{\sqrt{\gamma_L^-}}{\gamma_L} \quad (5.4)$$

Where the subscripts “i” represents the values obtained for probe liquid 1,2,3 (which in our case are water, glycerol, diiodomethane). These values can be written in a three-by-three matrix, coefficient matrix.

Constant terms (for $i = 1,2,3$):

$$Y_i = 1 + \cos\theta \quad (5.5)$$

Unknown components:

$$X_1 = \sqrt{\gamma_B^{LW}} ; X_2 = \sqrt{\gamma_B^+} ; X_3 = \sqrt{\gamma_B^-} \quad (5.6)$$

We now have a system of three linear equations with three unknown terms that can be written in a compact form:

$$A \cdot X = Y \quad (5.7)$$

As well in the matrix form:

$$\begin{bmatrix} A_{11} & A_{21} & A_{31} \\ A_{12} & A_{22} & A_{32} \\ A_{13} & A_{23} & A_{33} \end{bmatrix} \begin{bmatrix} X_1 \\ X_2 \\ X_3 \end{bmatrix} = \begin{bmatrix} Y_1 \\ Y_2 \\ Y_3 \end{bmatrix} \quad (5.8)$$

Therefore the surface energy components of the three bitumens can be easily calculated one by one. The selection of suitable probe liquids is very important for the determination of reliable surface energy characteristics of a material. Combinations of polar and non-polar probe liquids are used for this purpose. For this reason, water has been used as base liquid, glycerol as an acid and diiodomethane as a non-polar probe liquid. A table with probe liquids used with their surface energy components is shown below (table 5.5).

Surface energy components of probe liquids

Probe liquid	γ^{LW}	γ^+	γ^-	γ^T	$\sqrt{\gamma^{LW}}$	$\sqrt{\gamma^+}$	$\sqrt{\gamma^-}$
Water	21.80	25.50	25.50	72.80	4.67	5.05	5.05
Glycerol	34.00	3.92	57.40	64.00	5.83	1.98	7.58
Diiodomethane	50.80	0.00	0.00	50.80	7.13	0.00	0.00

Table 5.5 Surface energy components of probe liquids used for DCA tests

Using the contact angles obtained from DCA tests, the surface energy components of the three binders have been calculated:

Surface energy components of bitumens

Bitumens	γ^{LW}	γ^+	γ^-	γ^T
12-360 Base Binder	25,94	0,01	9,00	26,41
12-361 Adriamont	23,80	0,15	5,77	25,65
12-362 Sasobit	27,89	0,01	5,86	28,40

Table 5.6 Comparison of the surface energy components for the three bitumens

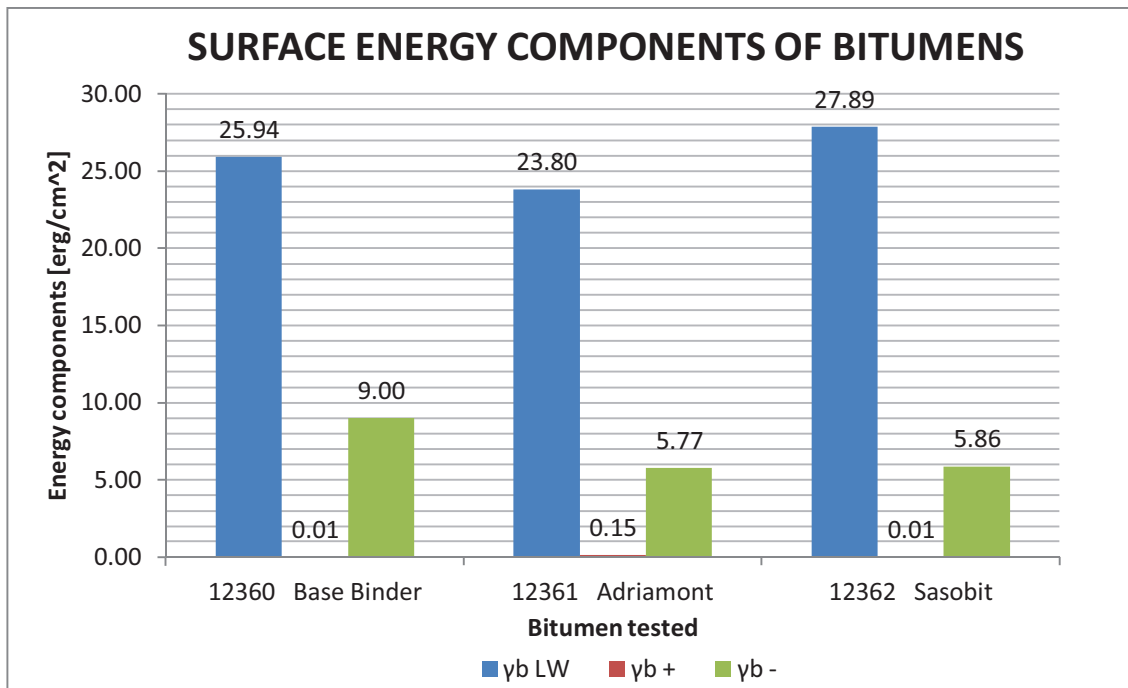


Figure 5.15 Comparison of the surface energy components for the three bitumens

Where the total surface energy is obtained as:

$$\gamma^T = \gamma^{LW} + 2\sqrt{\gamma^-\gamma^+} \quad (5.9)$$

Sasobit-modified bitumen has the greatest total surface energy, while Adriamont has the smallest. As we will see by calculating the affinity parameters, what we have stated above does not mean that the Sasobit modified binder has a greater affinity with aggregates rather than the other bitumens. This depends on the combination of the single components with that of aggregates. After calculating the surface energy components of bitumens we want to study the aggregates.

5.3 Dynamic Sorption Device tests

Aggregates are high surface energy materials. The contact angle technique cannot be used in case of aggregates as the liquids readily spread on a high energy surface and the contact angles approach zero. Equation 5.3 is used for the calculation of surface energy components of solids whose surface energies are not particularly high (less than the surface tension of probes); the spreading pressure, π_e , of the probes in this case is very small and is ignored in the calculations.

In case of high energy surfaces, the contact angle approaches zero while the spreading pressure has a high value. Therefore the work of adhesion is related to the spreading pressure of the probe vapour on the solid, rather than the contact angle of the probe liquid [15].

The DVS Advantage is designed to accurately measure a sample's change in mass as it precisely sorbs controlled concentrations of water or organic vapours in an air carrier gas. The sample is hung from a microbalance in a sample pan (a pan with a counter weight is hung on the other side of the balance as a 'reference'). Air carrying the test vapours is then passed over the sample at a well-defined flow rate and temperature. The sample mass readings from the microbalance then reveal the vapour adsorption/desorption behaviour of the sample [23].

5.3.1 Setting of the test and specimen preparation

Firstly aggregate samples are thoroughly washed and then dried in an oven before testing with DVS; samples are then stored in glass vials.

The DVS system is provided with two glass bottles. The first one has to be half filled with the probe liquid and the second one should either be empty or half-filled with deionised water.



Figure 5.16 Probe Liquid Bottles

The bottles should be cleaned and they should be free of any solvents from the previous experiments and should be used for one solvent only. The bottles are then placed in the Bottle A and Bottle B position in the Advantage manifold.

The sample and reference side pans are hung with the balance with the help of hanging wires. The DVS manifold is levelled with the help of thumb screws provided at the bottom of the manifold to make sure that the hang wires do not touch the walls of the sample or reference chamber.

In order to run the test the pressure regulator on the gas cylinder is set to a pressure of 1.5bar and is adjusted if required. The regulator should always be set for a pressure of 1.5bar.

The temperature of the environmental chamber containing the DVS manifold should always be set at 25°C.

The reference pans as well as the counter weights are then washed with deionised water followed by ethanol. The pans should not be handled directly by hands at any stage so

they are washed by with the help of forceps over a beaker and by spraying the liquid with the help of a wash bottle (figure 5.18).



Figure 5.17 Cleaning of the stir balls with water and ethanol

Regarding the software, it is important to check that the clean mirror value (CMV) should read about 120. If greater, the dew point analyser (DPA) sensor must be cleaned. The solvent which is being used for the test is selected by 'clicking select solvent' from the solvent drop-down menu.

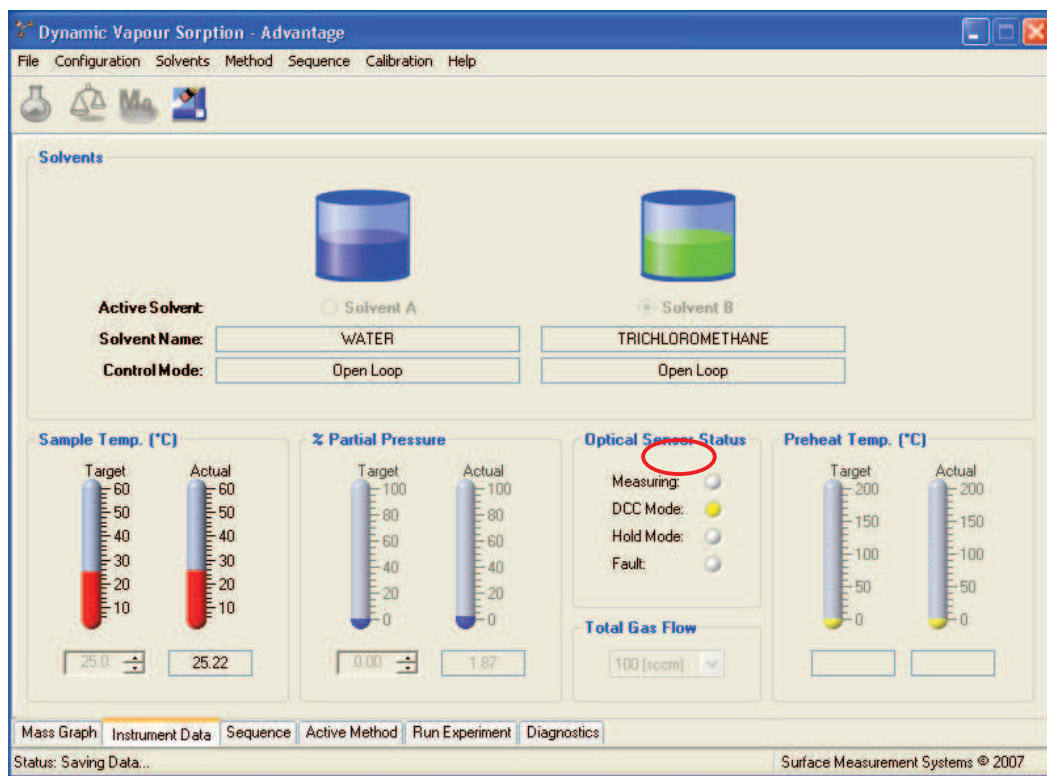


Figure 5.18 DVS Control panel

The sequence editor allows for sequencing of the methods that are to be run and also for the configuration of which solvent is to be used for each particular method. The control mode is set to open loop, the sampling rate at 1 second and the save data rate at 1 minute. A gas flow rate of 200cc/min is used for water and is dropped to half i.e. 100cc/min for probe liquids (solvent B).

The cleaned sample and reference pans are carefully hanged in the respective chambers with the help of a forceps. As the pans settle the chamber is closed. Once the balance has stabilised the tare balance is calibrated by clicking on a button.

After the balance has been calibrated the pans are taken out and the required amount of aggregate sample (normally 2 to 3 grams of sample is used) and counter weight/steel ball bearings are added into their respective pans. Then they are carefully hung back on the stirrups/hang wires and the chamber is closed.

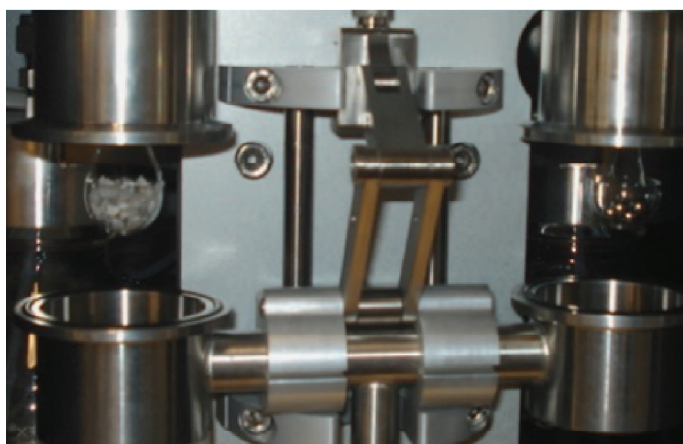


Figure 5.19 Placing the Sample in the Manifold

In the last two steps, the weight of the counter weight is added to the required field and the initial mass of the samples is set. The mass graph window plots the actual and target partial pressure along with the change in mass of the sample. An image of the mass graph window during a typical desorption cycle is shown in Figure 5.20.

When a Sequence is running, the Instrument Data panel serves only as a display of the system's parameters, and none of the parameters it indicates may be altered. However, if there is no Sequence running, then the Instrument Data panel may be used to input set-points for almost all of the system parameters displayed.

Once the experiment is in progress, the change in mass, humidity, Stage time, etc. can be monitored using the Mass Graph and Instrument Data panels. At any time during an experiment it is possible to gain an overall view of the data.

The Import DVS Data function provided in the DVS Analysis Suite is used to analyse the data in Microsoft Excel. Once the Run Sequence and Save Data switch of the Run Experiment panel has returned to the OFF state, the experiment has finished.

However, after removing the sample pan for cleaning, the sample should be inspected visually for any change in colour or state. Once the experiment is complete the results may be analysed using the DVS Analysis Suite software [15].

By way of example, some of the graphs automatically plotted by the Software are shown below:

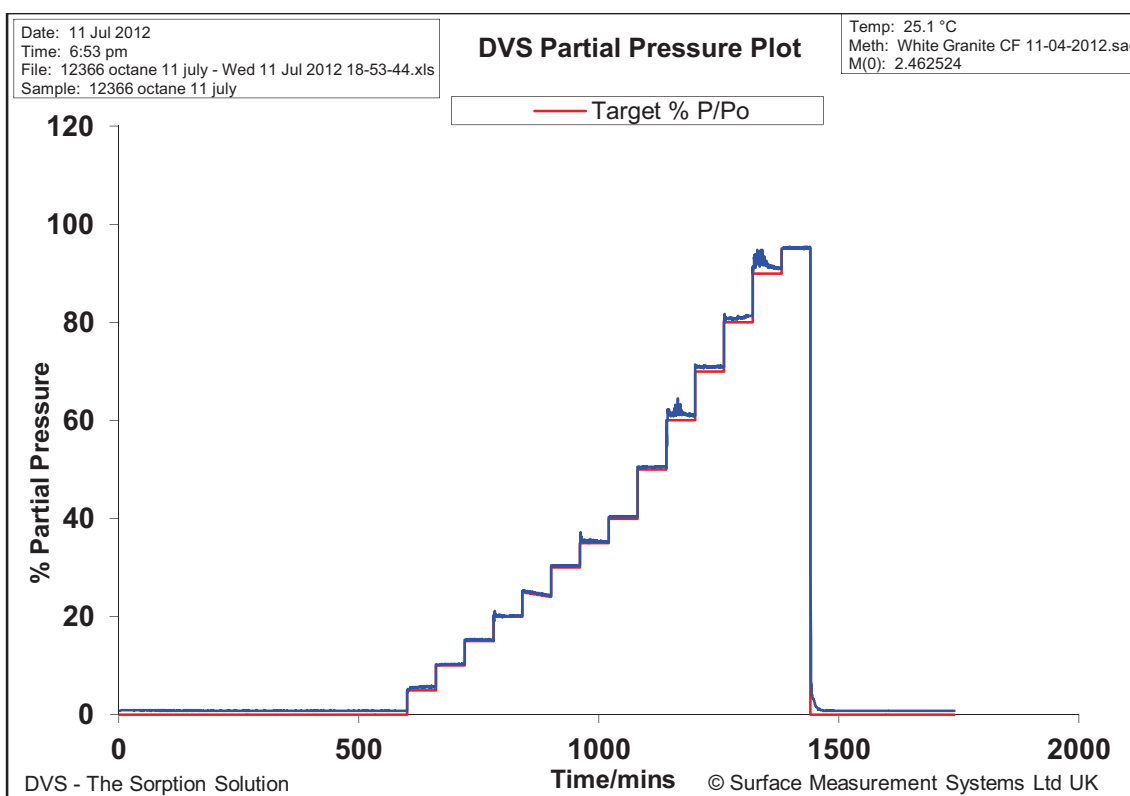


Figure 5.20 Percentage of partial pressure plotted versus time

This graph indicates the percentage of partial pressure at which the sample is subject to versus time. Each pressure level is maintained for 60 minutes and then is raised to a

upper value. A half cycle (as shown in figure 5.21) is usually carried out; it is sufficient to obtain the spreading pressure. In a full cycle the pressure is reduced until it returns to zero.

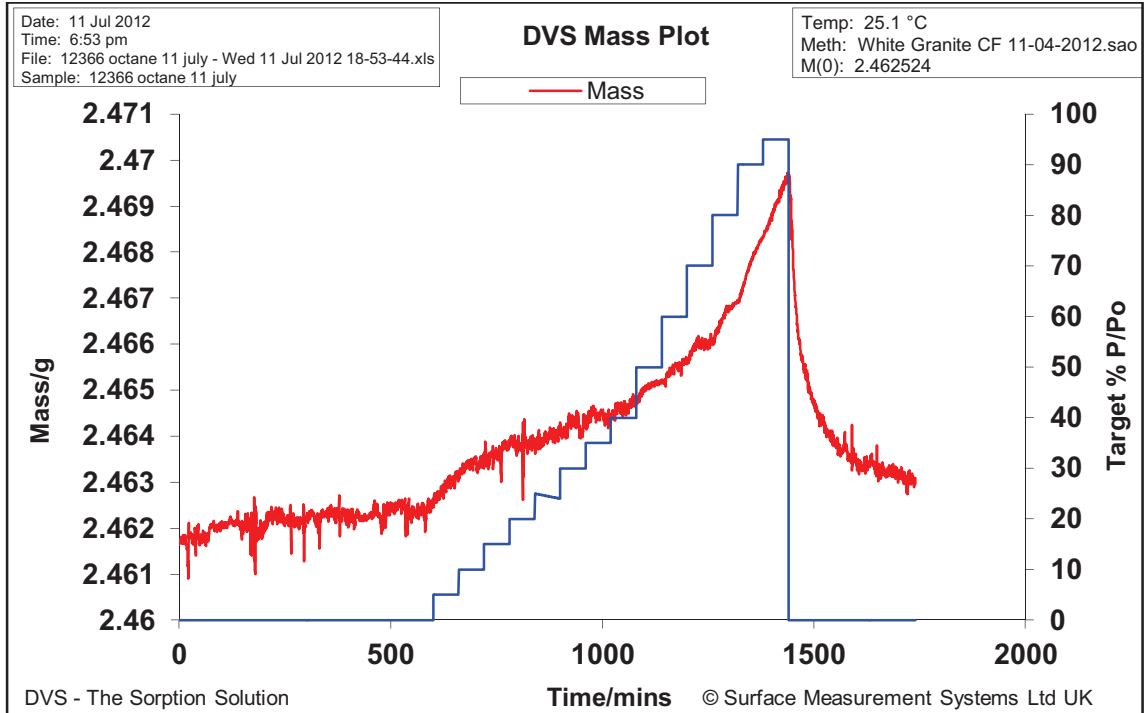


Figure 5.21 Mass of the sample plotted versus time

This graph shows the increase of mass of the sample versus the time. In the background, the partial pressure ratio is still appreciable, offering an idea of cause-and-effect of the pressure on the mass. In the case shown on picture 5.22 it is possible to observe that the mass undergoes a significant rise as the pressure ratio reaches approximately 40 P/P₀.

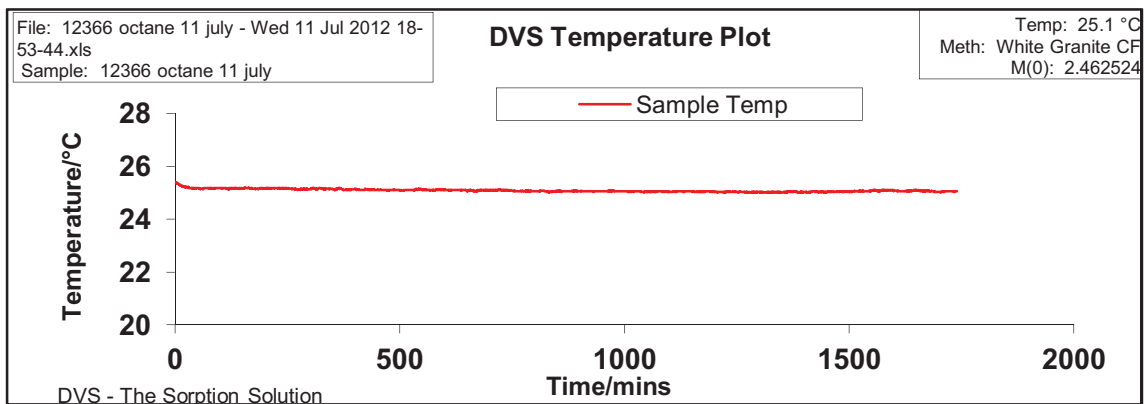


Figure 5.22 Temperature of the chamber plotted versus time

The temperature of the chamber is continuously under control to ensure it is constant and equal to 25°C.

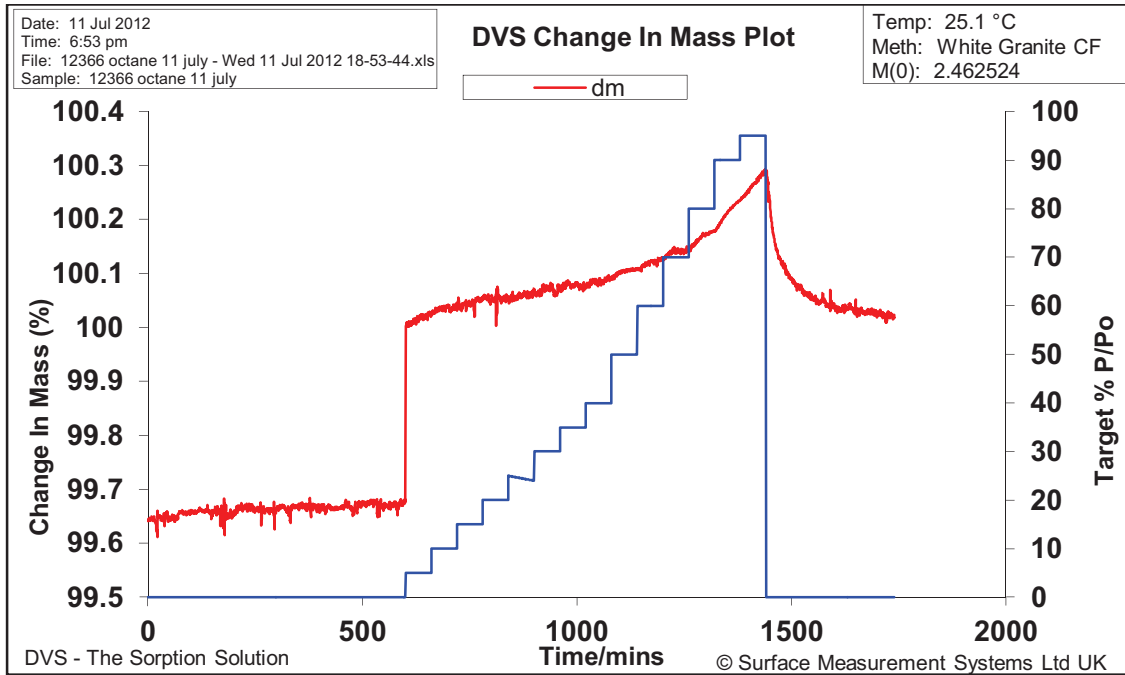


Figure 5.23 Change in mass % of the sample plotted versus time

Alternatively to figure 5.22, change in percentage mass can be plotted instead of the absolute value of the mass.

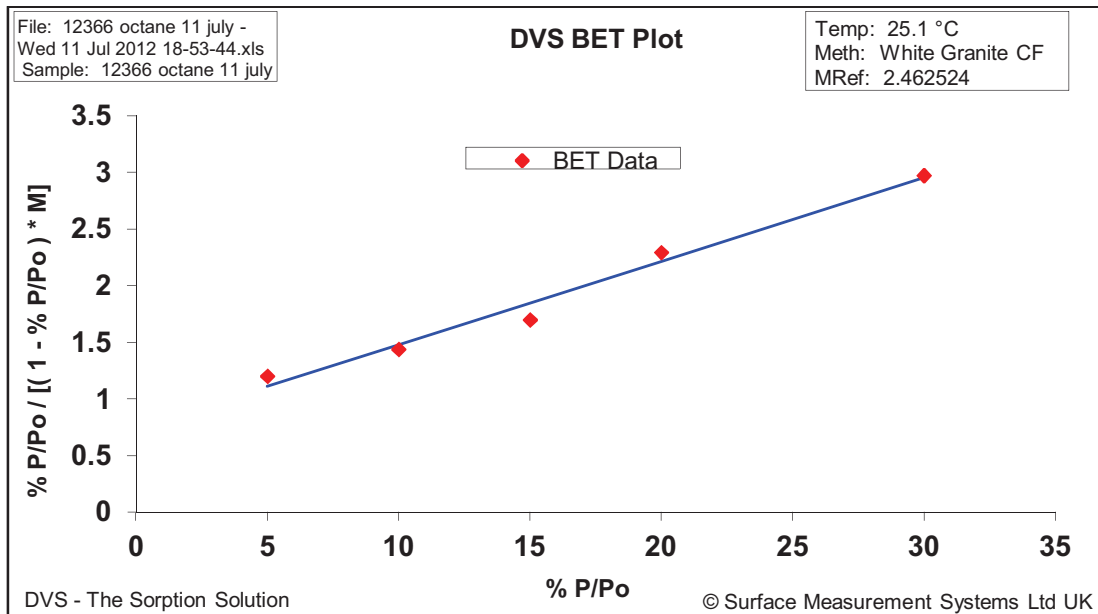


Figure 5.24 Brunauer – Emmett - Teller approach

Figure shows the Brunauer – Emmett - Teller approach (BET), useful for calculating the specific surface area of the solid. This value, as we will see, is used to calculate an affinity parameter.

DVS π_e Analysis Report

Date: 11 Jul 2012
 Time: 6.53 PM
 File: C:\DVS-Advantage\data\12366 octane 11 july - Wed 11 Jul 2012 18-53-44.xls
 Meth: C:\DVS-Advantage\method\White Granite CF 11-04-2012.sao
 Sample: 12366 octane 11 july
 Temp: 25.1 °C
 MRef: 2.462524

Experimental Parameters

Specific surface area:	2.0875 m ² /g
Molecular weight:	114.23 g/mol
Surface tension of vapour:	21.13 mN/m
Temperature read from file	

Calculation Options

% P/Po type:	Target
Half cycle:	Sorption
Isotherm cycle 1	

Analysis Results

Calculated π_e :	26.96 mN/m
Work of adhesion (W_{S-L}):	69.22 mN/m
Calculated γ_s :	56.69 mN/m

Figure 5.25 DVS report

In the end, a DVS report is provided, with all the details of the test performed. From this report, the work of adhesion, spreading pressure and specific surface energy are recorded for further calculations.

The following pictures show a comparison of the percentage of change in mass versus the percentage of the ratio $\frac{m - m_0}{m_0}$, where:

P = partial vapour pressure [Pa]

P_0 = saturated vapour pressure of solvent [Pa]

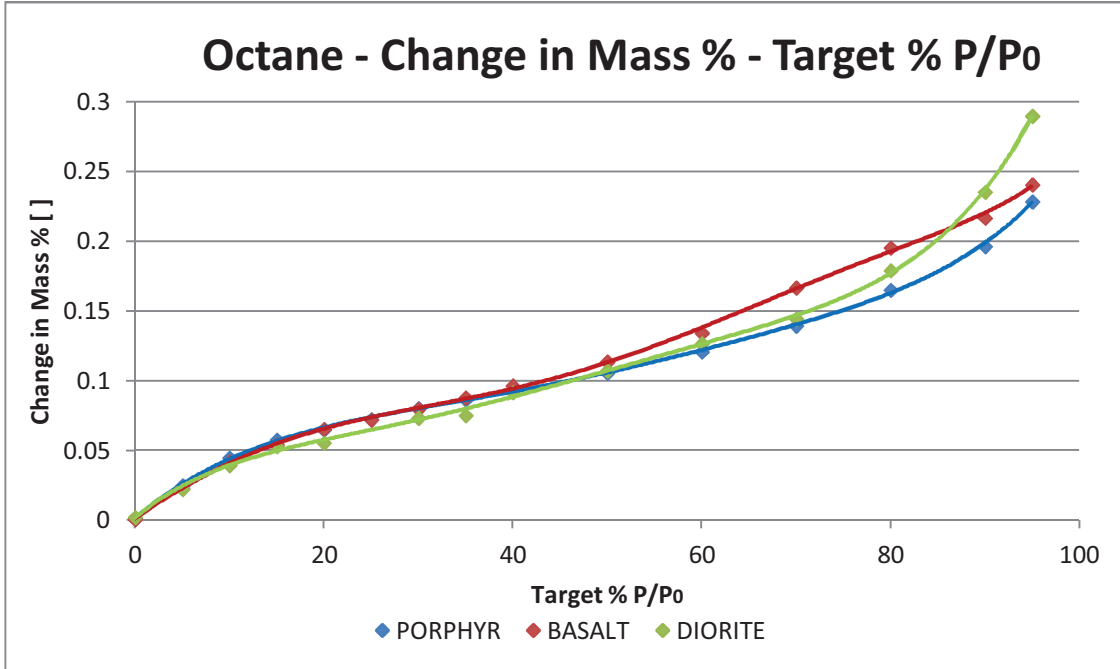


Figure 5.26 Change in mass versus the percentage of the ratio P/P_0 with Octane

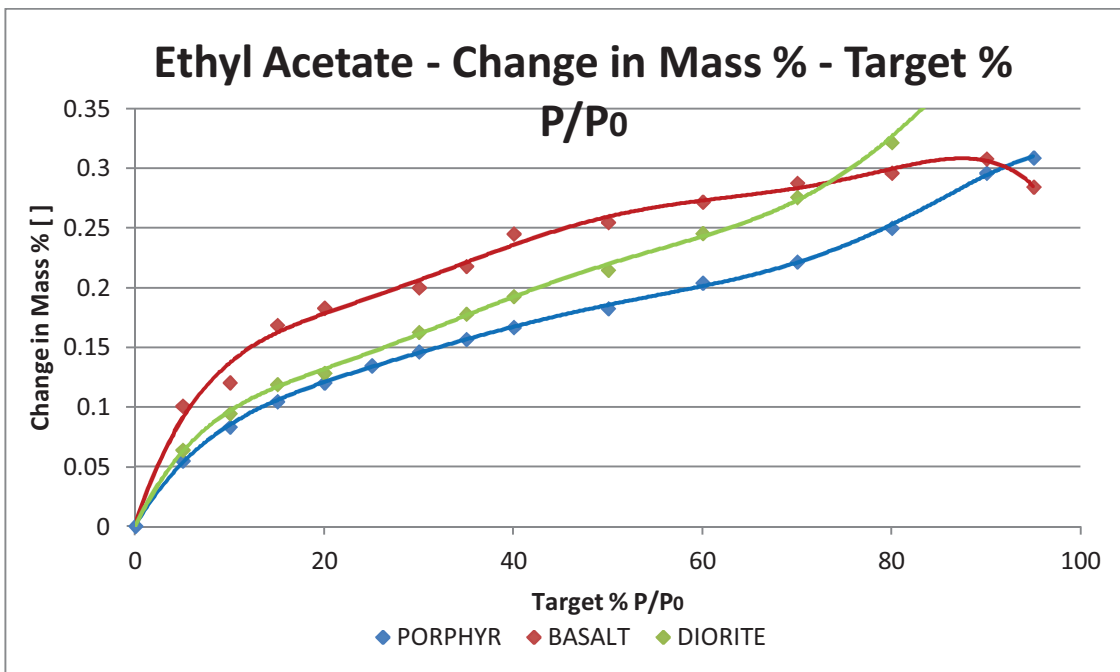


Figure 5.27 Change in mass versus the percentage of the ratio P/P_0 Ethyl Acetate

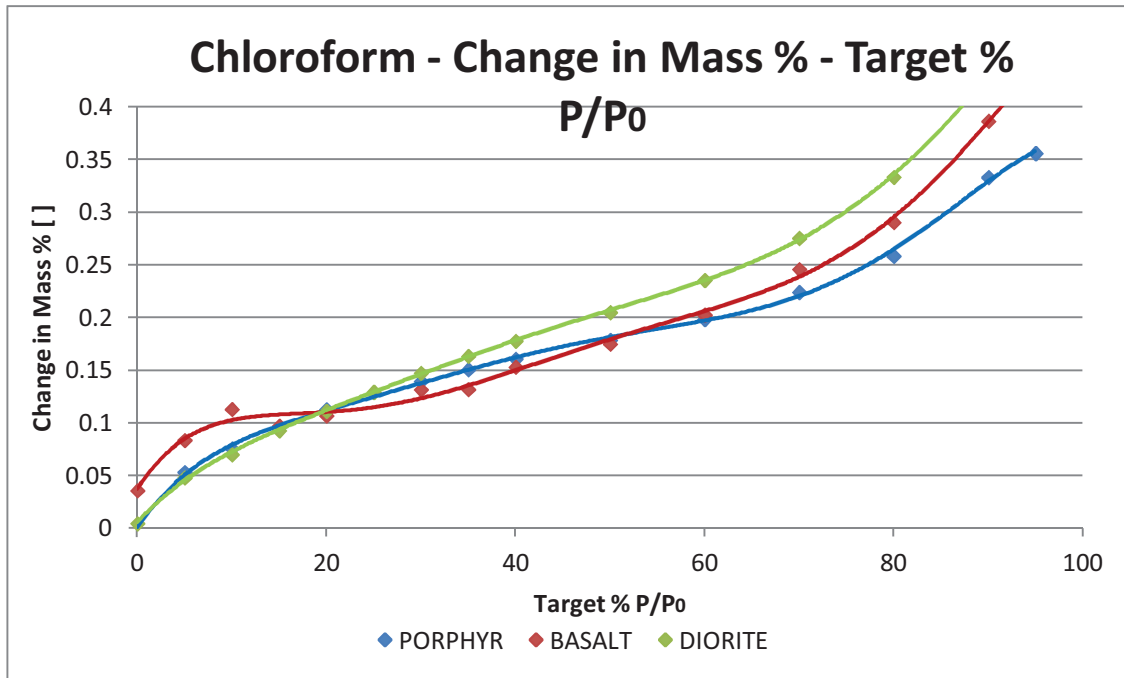


Figure 5.28 Change in mass versus the percentage of the ratio P/P_0 with Chloroform

The tendency of the change in mass is essentially the same for the three aggregates. Only with Ethyl Acetate are the curves slightly different ; we can note that the diorite seems to increase the mass even after an high P/P_0 ratio, and in both three cases it has got the upper percentage of change in mass.

5.3.2 Surface energy calculation of Aggregates

The provided DVS Advantage Analysis Software is used to calculate the surface area and spreading pressure properties of the sample from the obtained mass change/sorption results, when tested with different vapour probes. The surface energy parameters are then calculated from the obtained surface area and spreading pressure values.

An aggregate sample, as well as a bitumen sample, is tested by using a combination of three probe liquids. A table with probe liquids used with their surface energy components is show below (table 5.5).

Surface energy components of probe liquids [mJ/m^2]

Probe liquid	γ^{LW}	γ^+	γ^-	γ^T	$\sqrt{\gamma^{LW}}$	$\sqrt{\gamma^+}$	$\sqrt{\gamma^-}$
Octane	21.62	0.00	0.00	21.62	4.65	0.00	0.00
Ethyl Acetate	23.90	0.00	19.20	23.90	4.89	0.00	4.38
Chloroform	27.15	3.80	0.00	27.15	5.21	1.95	0.00

Table 5.6 Surface energy components of probe liquids used for DVS tests

The output of the DVS tests are the values of spreading pressures of the probes on the aggregate (from DCA tests we obtained contact angles). These values are then substituted into equation 2.17. The obtained equations for three probe liquids are then solved by using the usual matrix solution.

$$\begin{bmatrix} A_{11} & A_{21} & A_{31} \\ A_{12} & A_{22} & A_{32} \\ A_{13} & A_{23} & A_{33} \end{bmatrix} \begin{bmatrix} X_1 \\ X_2 \\ X_3 \end{bmatrix} = \begin{bmatrix} Y_1 \\ Y_2 \\ Y_3 \end{bmatrix} \quad (5.8)$$

As for bitumens, a three by three matrix is used in order to obtain the three unknown surface energy parameters of the aggregate material. The obtained spreading pressure values are provided in Table 5.6 below.

Spreading pressures [mJ/m^2]	Octane	Ethyl A.	Chloroform
12-364	24.72	56.85	41.32
12-365	24.66	79.01	45.96
12-366	26.96	74.08	49.53

Table 5.7 Obtained Spreading Pressures (DVS Test Results)

Equation 3.18 can be then be separated as usual into the known and unknown components as three separate matrices:

$$2 \cdot \gamma_L + \pi_e = 2 \sqrt{\gamma_S^{LW} \gamma_L^{LW}} + 2 \sqrt{\gamma_S^+ \gamma_L^-} + 2 \sqrt{\gamma_S^- \gamma_L^+} \quad (3.18)$$

Known components:

$$A_{1i} = \sqrt{\gamma_L^{LW}} ; A_{2i} = \sqrt{\gamma_L^+} ; A_{3i} = \sqrt{\gamma_L^-} \quad (5.10)$$

where the subscripts “i” represent the values obtained for probe liquid 1,2,3 (which in our case are octane, ethyl acetate, chloroform). These values can be written in a three-by-three coefficient matrix.

Constant terms (for $i = 1,2,3$):

$$Y_i = 2 \cdot \gamma_i + \pi_e \quad (5.11)$$

Unknown components:

$$X_1 = \sqrt{\gamma_A^{LW}} ; X_2 = \sqrt{\gamma_A^+} ; X_3 = \sqrt{\gamma_A^-} \quad (5.12)$$

By solving the matrix the following surface Energy components have been obtained:

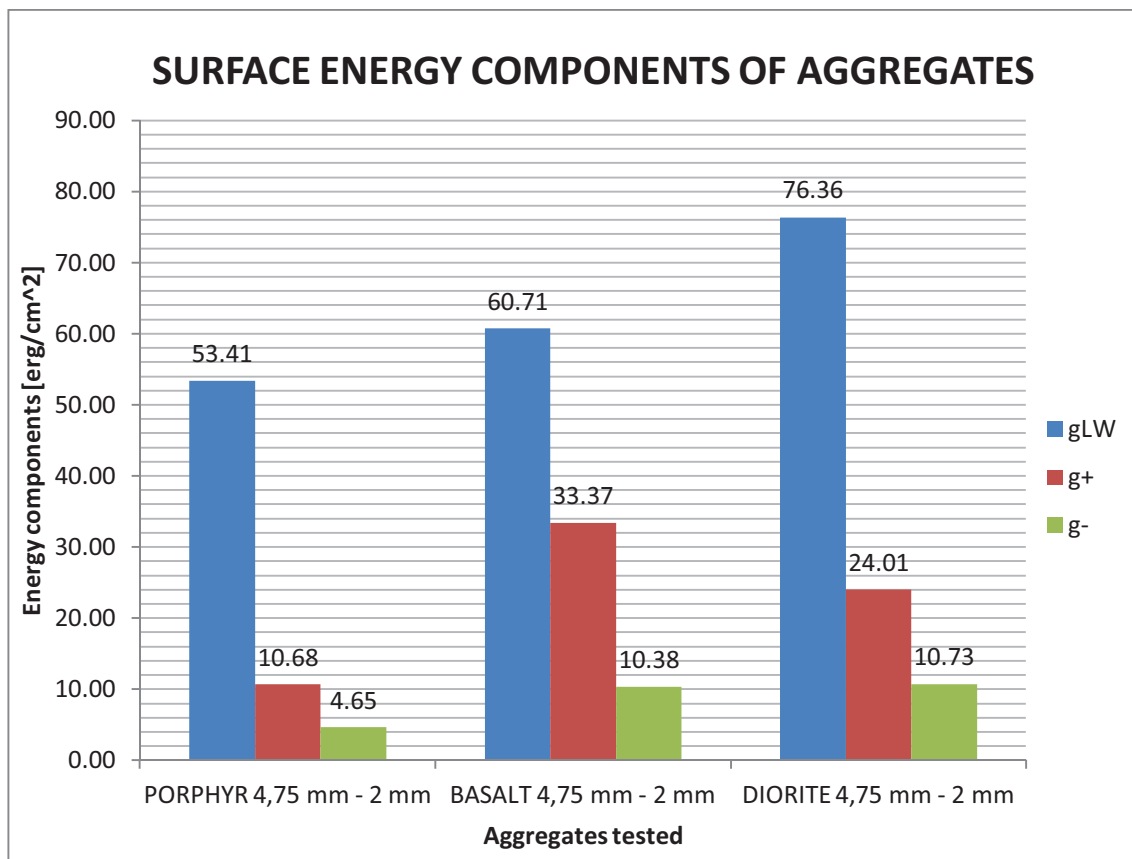


Figure 5.29 Surface energy components of aggregates

Surface energy components of aggregates

Aggregates	γ^{LW}	γ^+	γ^-	γ^T
Porphy 4,75 mm - 2 mm	53.41	10.68	4.65	67.5
Basalt 4,75 mm - 2 mm	60.71	33.37	10.38	97.9
Diorite 4,75 mm - 2 mm	76.36	24.01	10.73	108.5

Table 5.8 Surface energy components of aggregates [mJ/m^2]

Diorite, followed by basalt, shows the higher total surface energy while the porphyry has a significantly lower energy compared to them. Wetting is favored by high surface energies of aggregates and low interfacial energies: hence, porphyry seems to bind to the bitumen less well than the others.

With the intent to provide an affinity opinion, the work of adhesion and cohesion need to be calculated. Bhasin, in 2006, proposed some parameters to facilitate a quick understanding of the bond relationship between a defined combination of bitumen and aggregates.

5.4 Moisture damage parameters

The most evident form of moisture damage is stripping of asphalt binder from the aggregate surface due to exposure to moisture. The correlation between the surface properties of these materials and their tendency to strip in the presence of water is relatively well established in the literature. The three quantities based on the surface energies of asphalt binders and aggregate that are related to the moisture sensitivity of an asphalt mixture are:

- work of adhesion between the asphalt binder and aggregate ΔG_{BA}^a (figure 5.30)
- work of debonding or reduction in free energy of the system when water displaces asphalt binder from a binder-aggregate interface ΔG_{BWA}^a (figure 5.31)
- work of cohesion of the asphalt binder or mastic ΔG_{BB} .

The above three quantities are computed using the surface free energy components of the individual materials. For an asphalt mixture to be durable and have a relatively low sensitivity to moisture, it is desirable that the work of adhesion, ΔG_{BA}^a , between the asphalt binder and the aggregate be as high as possible [17].

Diorite appears as the aggregate with the upper adhesive bond strength value, followed by basalt, and finally by porphyry. No big differences are notable between the bitumens even though the base binder seems to have the greater bond strength (figure 5.30).

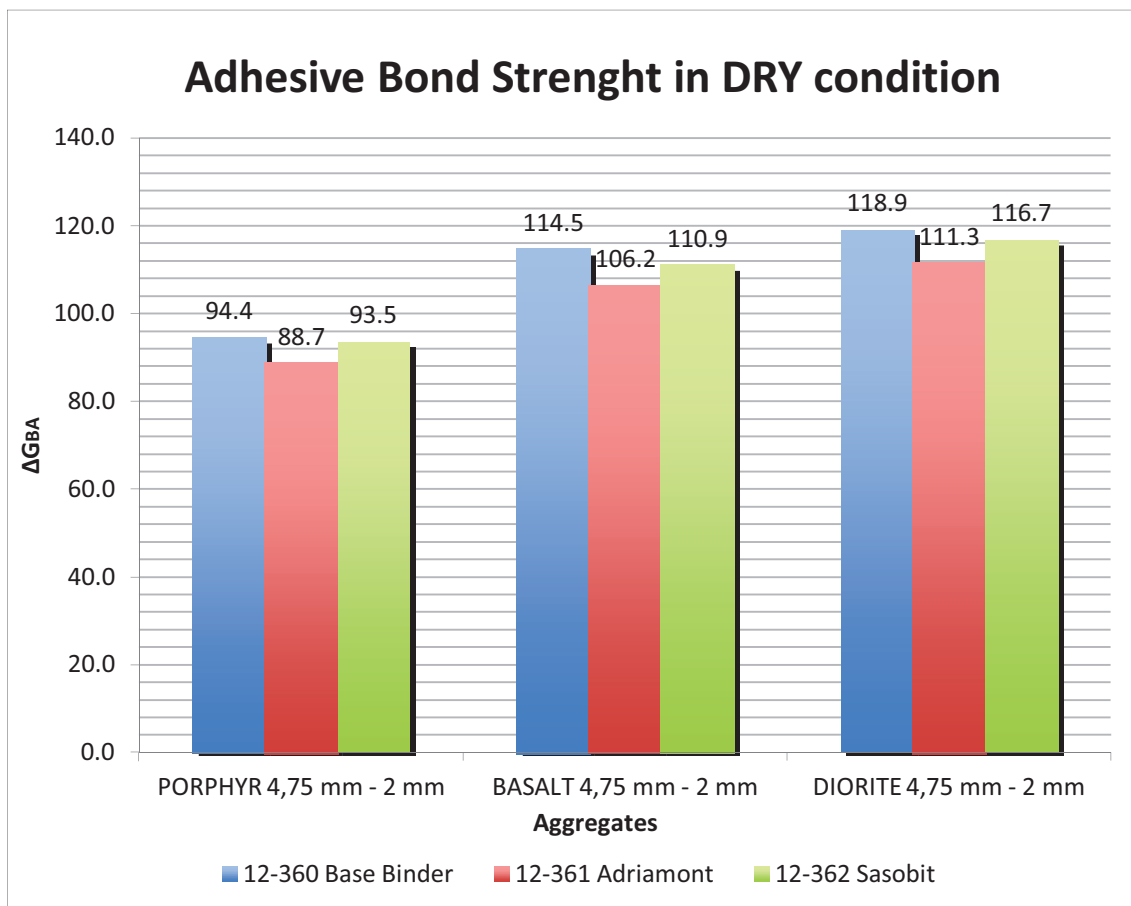


Figure 5.30 Adhesive Bond strength in dry condition

Furthermore, the greater the magnitude of work of debonding when water displaces the asphalt binder from the binder-aggregate interface, ΔG_{BWA}^a , the greater the thermodynamic potential that drives moisture damage. Therefore, it is desirable that this quantity be as small as possible.

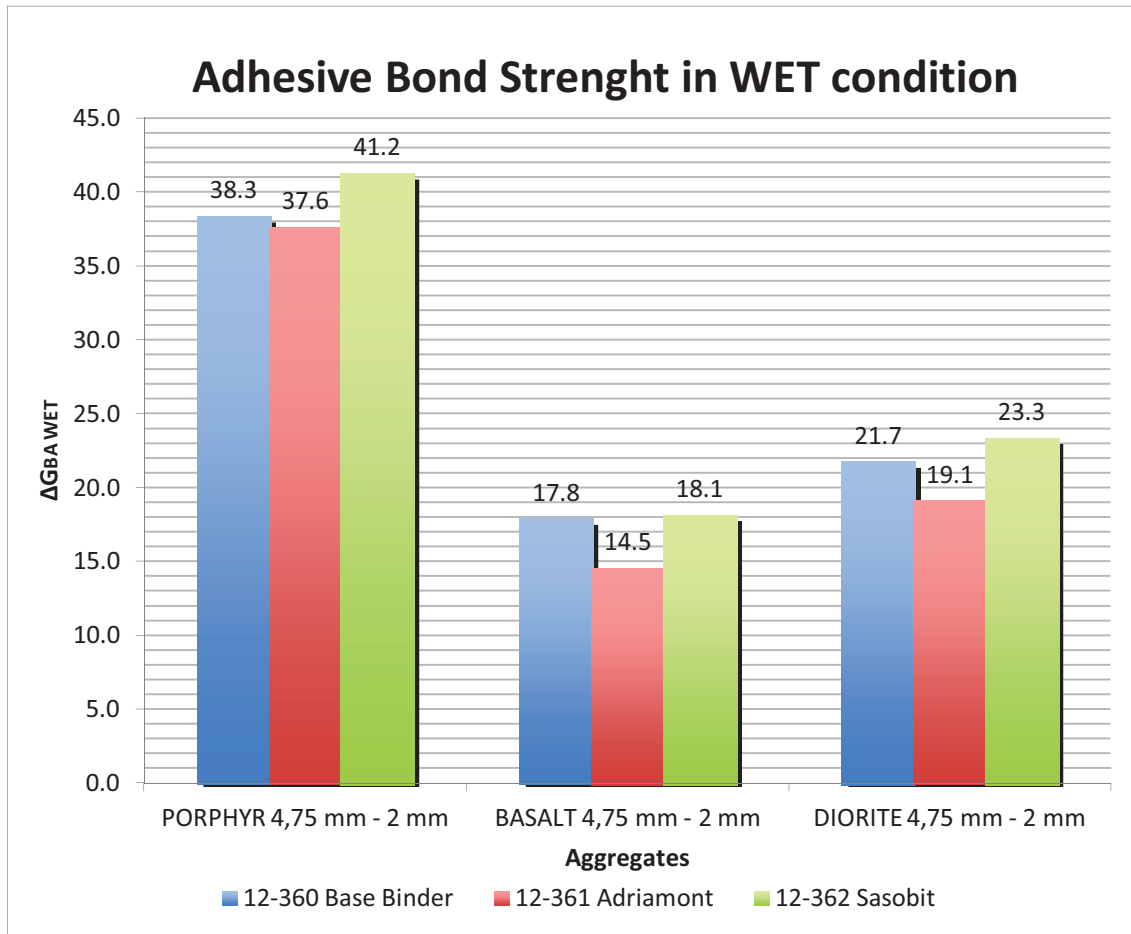


Figure 5.31 Adhesive Bond strength in wet condition

Figure 5.31 points out that the porphyry values are approximately twice the others. This is detrimental to the performance of the mixture and will affect the bond strength of the porphyry with the bitumen. The basalt has the lower values hence the thermodynamic potential that drives moisture damage must be greater.

The ratio between the adhesive bond energy values in dry condition (ΔG_{BA}^a) and in the presence of water (ΔG_{BWA}^a) is used to predict the moisture sensitivity of asphalt mixtures. In order to represent the moisture damage by a single value, Bhasin et al. (2006) combined the two bond energy parameters as a dimensionless energy ratio.

$$R^{Total} = R_1 = \left| \frac{\Delta G_{BA}^a}{\Delta G_{BWA}^a} \right| \quad (5.9)$$

CONCLUSIONS

The aim of this research is to figure out the effect on an asphalt binder behaviour of the waxes Adriamont and Sasobit. As well known, the modification of bitumen with waxes has the objective of reduce the viscosity of bitumen, permitting to lower the workability temperature. We discussed about all the resulting benefits like reduction in emissions, healthier work environment, fuel production cost savings and so on.

The main query deal with the effect of the waxes on the performance of the asphalt binders, because the WMA, a global term that includes also the wax modification, has still been not confirmed on the fields since it is a relatively recent technique.

The rheological investigation showed that the three asphalt binder have a rheologically similar behaviour. Initially, the waxes confer to the asphalt binder a greater complex modulus. The base binder seems to undergo the higher long term aging.. No big differences have been found neither in the absolute values of complex modulus nor in the phase angle.

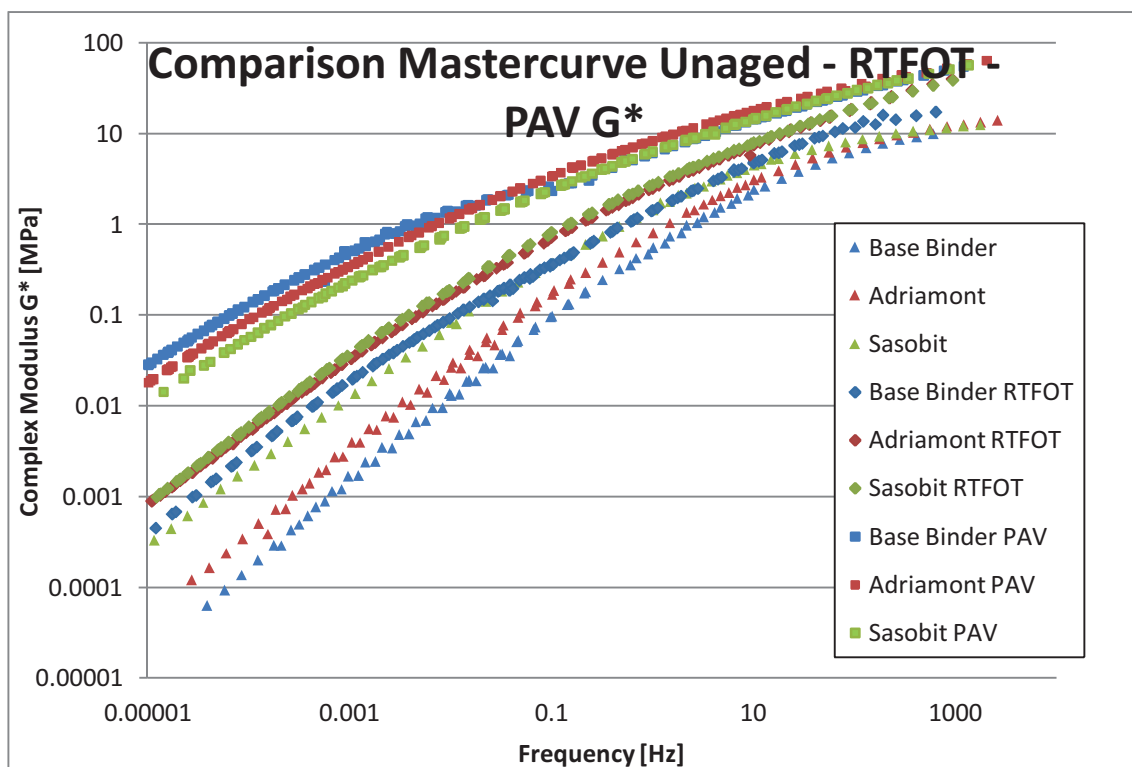


Figure 6.1 Comparison of master curves related to the three aged stages

This statement can be confirmed for instance, by the comparison of the master curves of the complex modulus in the three aged stages of the life of an asphalt binder, especially in the PAV.

It was interesting to observe the differences in the black diagrams of the Base Binder and the modified binders. It resulted that, as the bitumen loses his consistency (at low values of complex modulus, recorded at high temperatures) the wax forms a sort of grid which causes a greater springback. The Aging also affects the wax, whose lattice weakens after PAV. The base binder instead shows the general tendency of a non-modified bitumen: as the complex modulus decreases, the phase angle tends to the upper values (viscous behaviour).

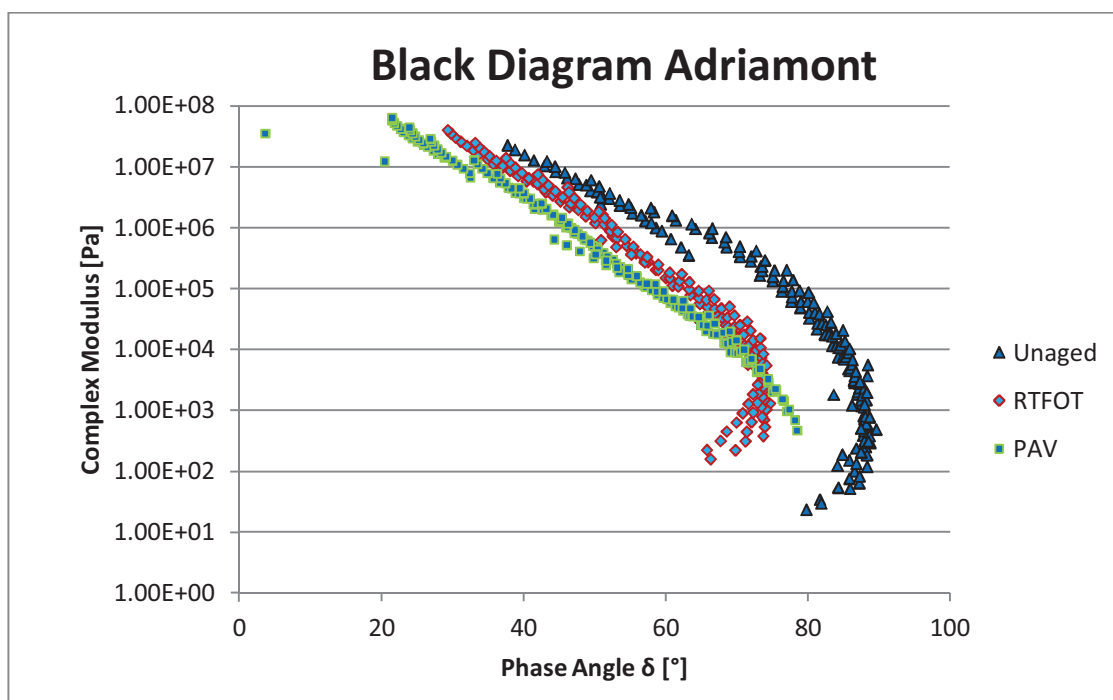


Figure 6.2 Black Diagram for Adriamont wax-modified asphalt binder

By analyzing the Superpave specifications, it has been found that the wax-modified bitumens satisfies the criterions at a 6° higher temperature. Therefore, the effect of Adriamont and Sasobit bring a benefit to the performance at intermediate-high temperatures.

Nevertheless, the main result is obtained from the tests with Bending Beam Rheometer. In this case, the base binder showed a superior ability to relax the stresses applied. Adriamont and Sasobit waxes do not affect the stiffness of the binder, but influence in a considerable manner the relaxation properties of the binder. Therefore, as the surrounding temperatures drop, both the wax modified bitumens are less able than the Base Binder to relax the internal stresses that they contract and build up.

The base binder is consequently 54-18 while both modified asphalt binders are PG 60-12.

Regarding the energetic characterization, the porphyry, compared to the other aggregates tested, shows the worse affinity with the bitumens. This is something well known among road operators, and is due to the surface charge of the porphyry. In fact, bitumen has a tendency to be negatively charged: consequently adhesion issues arises when acid aggregates, like porphyry are used. Basalt and Diorite instead, indicate a good affinity with the bitumens, with high value of the energy parameters.

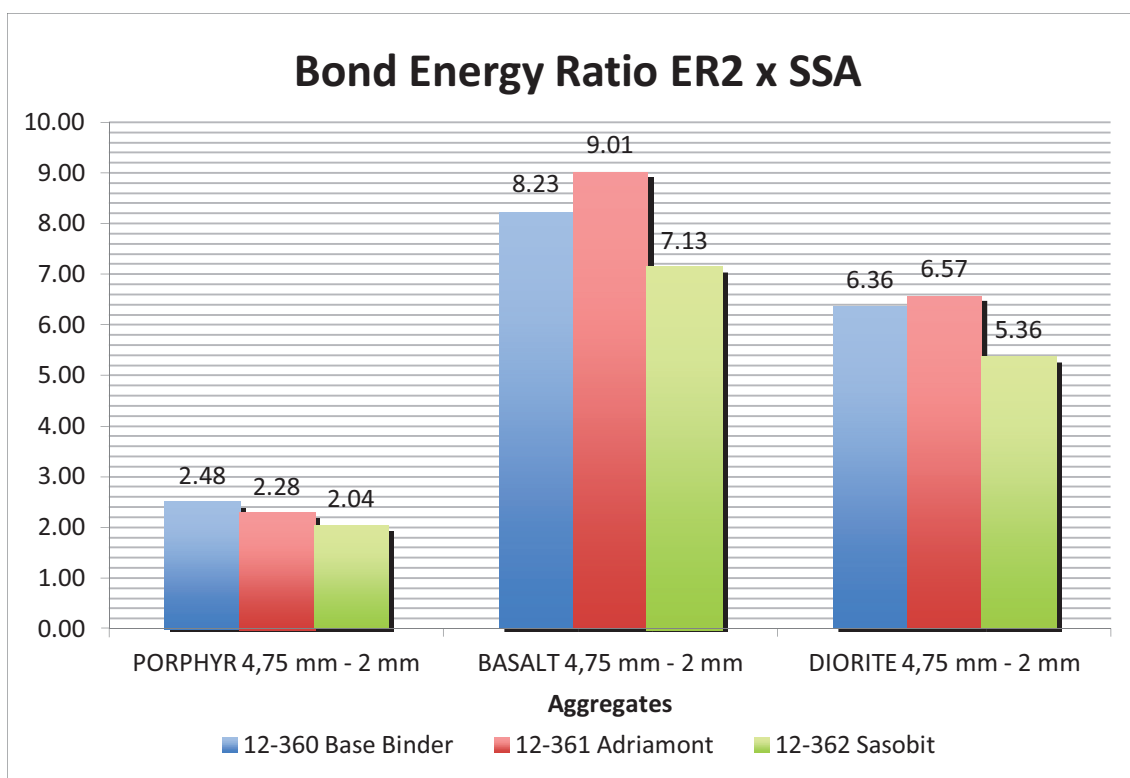


Figure 6.3 Bond energy ratio ER2XxSSA for different mixtures

A finally remark is for underline the ambiguous effect of the wax on the mechanism of adhesion. In fact, the Adriamont wax seems to increase the affinity of the mixture, up to a value of 15 % of the energy bond ratio.

Sasobit wax, instead, has a negative effect on the bond strength of the mixture, by lowering the bond energy ratio by a value up to 10% compared to base bitumen. Hence, more tests need to be carried out, maybe using different fractions of aggregates or changing different base binder, in order to resolve this doubt.

BIBLIOGRAPHY

- [1] <http://en.wikipedia.org/wiki/Asphalt>
- [2] Lo Presti Davide, Rheology and curing of tyre rubber modified bitumen, 2011
- [3] The Shell Bitumen Handbook, John Read, David Whiteoak, 2003
- [4] <http://www.bitumenengineering.com/technology/asphalt-production>
- [5] [http://www.bp.com/sectiongenericarticle.do?categoryId=9027521
&contentId=7050109](http://www.bp.com/sectiongenericarticle.do?categoryId=9027521&contentId=7050109)
- [6] <http://en.wikipedia.org/wiki/Rheology>
- [7] E. C. Bingham, Fluidity and Plasticity, New York 1922
- [8] Mezger, T. G. (2002). In Ulrich Zorll (Ed.), The rheology handbook: for users of rotational and oscillatory rheometers, 2002
- [9] Strategic Highway Research Program, Binder Characterization and Evaluation, Volume 4: Test Methods, Report 370, 1994
- [10] ASTM D907 - 12a Standard Terminology of Adhesives
- [11] Adhesive in bitumen-aggregate systems and quantification of the effects of water on the adhesive bond, Arno Hefer and Dallas Little. Texas Transportation Institute. 2005
- [12] Thomas Young, Philosophical transactions of the Royal Society of London, 1805
- [13] Eustathopoulos, Nicholas and Drevet, Wettability at high temperatures. Oxford 1999
- [14] Schrader, M.E; Loeb, G.I. Modern Approaches to Wettability. Theory and Applications. New York, 1992
- [15] Naveed Ahmad, Asphalt Mixture Moisture Sensitivity Evaluation using Surface Energy Parameters, PhD thesis 2011

- [16] Shafrin, E.G., and W.A. Zisman, "Constitutive relations in the wetting of low energy surfaces and the theory of the retraction method of preparing monolayers,"
- [17] Dalla Little, Amit Bhasin, Using Surface Energy Measurements to Select Materials for Asphalt Pavement, NCHRP Report, 2006
- [18] <http://www.pavementinteractive.org/article/rolling-thin-film-oven/>
- [19] <http://www.pavementinteractive.org/article/pressure-aging-vessel/>
- [20] Airey G.D., Rheological performance of aged polymer modified bitumens, 1997
- [21] <http://www.pavementinteractive.org/article/bending-beam-rheometer/>
- [22] Mihai O. Marasteanu, Xue Li, Timothy R. Cly, Low temperature cracking of asphalt concrete pavements.
- [23] DVS Advantage, operation manual, Surface measurement system LTD, UK
- [24] Airey G.D. ,Use of Black Diagrams to Identify Inconsistencies in Rheological Data, 2002

*Ringrazio di cuore tutti coloro che mi vogliono
davvero bene*